INHIBITION, STRUCTURE, AND FUNCTION OF GHRELIN-O-ACYLTRANSFERASE

by
Martin Samuel Taylor

A dissertation submitted to Johns Hopkins University in conformity with the requirements for the degree of Doctor of Philosophy

Baltimore, Maryland
March, 2015

ABSTRACT

Ghrelin-O-Acyltransferase (GOAT) is an 11-transmembrane integral membrane protein that octanoylates Ser3 of the metabolism-regulating gastric peptide hormone ghrelin, producing the active form of this hormone. Protein octanoylation is unique to ghrelin in humans, and GOAT may represent an attractive target for the treatment of type II diabetes and the metabolic syndrome. Ghrelin physiology is complex; it has often been called a "hunger hormone," but a growing body of literature suggests that this is incorrect. Rather, ghrelin seems to have evolved to help vertebrates survive extreme starvation by controlling metabolism to maintain blood sugar, minimize energy expenditure, and maximize energy storage. Ghrelin is potently pro-kinetic in the enteric nervous system, and this combined with pro-storage metabolic effects has led to a number of promising agonists in clinical trials for cachexia. Additionally, ghrelin has been implicated in a variety of other physiologic processes, including cardiovascular function, learning, memory, reward behavior, and addiction. This work outlines the development of the first *in vivo* inhibitors of ghrelin octanoylation and their effects in mice, the determination of the topology of GOAT, and studies on the structure, mechanism, and enzymology of GOAT.

Chapter 1 provides an introduction, reviewing the history of the ghrelin field, recent progress in the development of cell and *in vitro* assays to measure GOAT action, and the identification of several synthetic GOAT inhibitors. In Chapter 2, we describe the design, synthesis, and characterization of GO-CoA-Tat, a peptide-based bisubstrate analog that

antagonizes GOAT. GO-CoA-Tat potently inhibits GOAT in vitro, in cultured cells, and in mice. Intraperitoneal administration of GO-CoA-Tat improves glucose tolerance and reduces weight gain in wild-type mice but not in ghrelin-deficient mice, supporting the concept that its beneficial metabolic effects are due specifically to GOAT inhibition. In addition to serving as a research tool for mapping ghrelin actions, GO-CoA-Tat may help pave the way for clinical targeting of GOAT in metabolic diseases.

In Chapter 3, we use phylogeny and a variety of bioinformatic tools to predict the topology of GOAT, which was previously unknown. Using selective permeabilization indirect immunofluorescence microscopy in combination with glycosylation-shift immunoblotting, we demonstrate that GOAT contains 11 transmembrane helices and one reentrant loop. We report the development of the V5Glyc tag, a novel, small, and sensitive dual topology reporter, which facilitated these experiments. The MBOAT family invariant residue His338 is in the ER lumen, consistent with other family members, but conserved Asn307 is cytosolic, making it unlikely that both are involved in catalysis. Photocrosslinking of synthetic ghrelin analogs and inhibitors demonstrates binding to the C-terminal region of GOAT, consistent with a role of His338 in the active site. This knowledge of GOAT architecture is important for a deeper understanding of the mechanism of GOAT and other MBOATs and could ultimately enhance the discovery of selective inhibitors of these enzymes.

In Chapter 4, we develop explore an *in vitro* microsomal ghrelin octanoylation assay to analyze its enzymologic features. Measurement of K_m for 10-mer, 27-mer, and synthetic

Tat-peptide-containing ghrelin substrates provide evidence for a role of charge interactions in substrate binding. Ghrelin substrates with amino-alanine in place of Ser3 demonstrate that GOAT can catalyze the formation of an octanoyl-amide bond at a similar rate compared with the natural reaction. A pH-rate comparison of these substrates reveals minimal differences in acyltransferase activity across pH 6.0-9.0. These data support a GOAT catalytic mechanism which is insensitive to substrate nucleophilicity. Limitations of the microsomal assay then led us to attempt to find conditions where solubilized GOAT retained activity; we report failure in this effort with 35 detergents and no activity of GOAT successfully packaged into phospholipid bilayer membrane scaffolds (nanodiscs).

Thesis Advisors: Philip A. Cole, M.D., Ph.D.

Jef D. Boeke, Ph.D., D.Sc.

Thesis Readers: Philip A. Cole, M.D., Ph.D. and Carolyn E. Machamer, Ph.D.

PREFACE

This dissertation is dedicated my wife Cristin,

for her love and unwavering support of my intellectual meanderings.

The work in this dissertation would have never come to fruition without the support of my family, friends, colleagues, and advisors. To Phil Cole and Jef Boeke, who have been both great mentors and friends, I owe whatever scientific acumen I have gained over the past 8 years. Their uncommon brilliance and passion for discovery is underscored by intellectual rigor, creativity, love for teaching, patience, and unwavering support of their trainees. I would have been very fortunate to learn from one such mentor, and I consider it the greatest privilege of my education to have worked with two. Likewise, the Boeke and Cole labs are wonderful places, and I am indebted to too many members of both groups to name who made the lab a stimulating and supportive place to work and play.

I've had the opportunity to take advantage of the rich collaborative scientific community at Johns Hopkins in a way in which I could never have imagined. In addition to the labs of my mentors, I have performed experiments in the labs of Drs. Dan Leahy, Carolyn Machamer, Sin Urban, Joshua Mendell, Jun Liu, Sol Snyder, Geraldine Seydoux, Cynthia Wolberger, Herschel Wade, Ann Hubbard, Dan Raben, Ron Schnaar, Wade

Gibson, Jim Stivers, and Kathy Burns, and I have benefitted immensely from their generosity, advice, and scientific expertise, as well as that of too many others to name here. I still have keys to the Leahy and Machamer labs, both of whom have provided me a home-away-from-home and knowledge, techniques, and resources that would have otherwise been unavailable. In particular, I thank Yousang Hwang and Anutosh Chakraborty for training me, and I thank Jennifer Kavran for her generosity with her time and knowledge of all things protein. I have also had the honor to mentor and learn from a number of brilliant young scientists and am indebted to Robert Hsiao and Emily Adney for their hard work, dedication, and patience with my multiple competing interests. Likewise, my friends in graduate school and in particular the MD-PhD program have supported my wild ideas and helped sculpt my career.

Most of my work at Hopkins has been extremely collaborative, and I thank in particular Travis Ruch, whose unforgettable response to my request for a protocol was, "That sounds really interesting, I'll teach you and let's work on this together." This combined with the generosity of Carolyn Machamer blossomed into our entire topology project. I also thank the Pharmacology and Medical Scientist Training Programs for financial, scientific, and administrative support, Bob Siliciano for his mentorship, friendship, staunch advocacy, and support, and Lixin Dai and John LaCava, with whom I worked hand-in-hand for three years on an exciting excursion into LINE-1 biology.

As I near the end of a 10-year meandering training in medicine and science, I am grateful to my friends and family for understanding my commitment to my work and that

often my time was not my own. My parents have made this endeavor possible with their love and support, but moreover in instilling in me values of academic study, hard work, intellectual curiosity, and creativity. They have also provided me with endless opportunities, for which I am forever indebted. I am also very fortunate that my grandmother is still alive and will read and cherish this dissertation. In addition to reinforcing the aforementioned values, she instilled a love of science in me from an early age and left an indelible mark that has in part led me down this path.

Cristin, when you and I met in 2007, I had just begun in the Cole Lab, the project was sailing along, and I was sure I would be back to the wards in three years. I think you believed me; all that mattered to me was that you believed in me. Our daughter Evelyn Rose, now almost 6 months old, was at the time no more than a thought or a dream. Now, although it's been a few years longer than promised, I feel that the time has been well spent and I'm excited to take these next steps together. We've grown immensely together over the last 8 years, or perhaps mostly I've grown under your constant tutelage, and words cannot express what you mean to me.

TABLE OF CONTENTS

LIST OF TABLES

LIST OF FIGURES

CHAPTER 1 - INTRODUCTION

A Brief History of This Project

In the summer of 2007, I took with great enthusiasm the opportunity to work on a joint project between the Cole and Boeke labs to identify the then-unknown acyltransferase that octanoylates ghrelin, which at the time was widely called a hunger hormone. A collaboration quickly took shape. At an initial meeting, the design of our biotinylated inhibitor/probe, GO-CoA-Tat, was drawn out on the whiteboard in Dr. Cole's office by Dr. Cole and Dr. Yousang Hwang. When I joined the project shortly thereafter, the drawing was on still on the wall, and we began fishing, together. In January 2008, the identity of Ghrelin-O-Acyltransferase (GOAT) was published by the Brown & Goldstein group (Yang et al., 2008a), and within the month, Gutierrez and coworkers from Eli Lilly published the identity of GOAT as well, noting also GOAT knockout mice produced no acylated ghrelin (Gutierrez et al., 2008). We realized that we had the inhibitor in hand, and were therefore uniquely positioned to study GOAT function.

Our study on GOAT inhibition was published in 2010. Having learned at the time to purify milligram quantities of GOAT, I focused for some time on improving protein preparations and crystallography. These efforts were paralleled by ongoing work in enzymology. When our constructs failed to crystallize, we sought to engineer new GOAT

constructs for crystallography but realized we lacked even the most basic understanding of its organization. I therefore turned my efforts to determining GOAT topology, both experimentally and computationally. This work paralleled ongoing enzymology.

GOAT and Ghrelin Physiology

Ghrelin-O-Acyltransferase (GOAT) is an 11-transmembrane integral membrane protein that activates metabolism-regulating hormone ghrelin by octanoylation, attaching the 8-carbon fatty acid octanoate to Ser3 (Gutierrez et al., 2008; Kojima et al., 1999; Taylor et al., 2013; Yang et al., 2008a). Only this active form of the hormone (also called acyl ghrelin; hereafter referred to as ghrelin) can activate ghrelin's receptor, the growth hormone secretagogue receptor (GHSR), a broadly-expressed G-protein coupled receptor that is concentrated in the hypothalamus (Cowley et al., 2003; Cruz and Smith, 2008; Lau et al., 2000). Ghrelin is predominantly produced in the stomach, and ghrelin signaling through GOAT modulates energy balance through hypothalamic neuropeptide Y and agouti-related protein-expressing (NPY/AgRP) neurons in response to nutrient status, tipping metabolism in favor of storage (Chen et al., 2004a; Kamegai et al., 2001; Kirchner et al., 2009; Kojima et al., 1999). Therefore, GOAT signaling provides a link between the gut and the brain, and because Ghrelin is the only octanoylated protein in humans, this unique modification may represent an attractive target for the treatment of type II diabetes and the metabolic syndrome (Barnett et al., 2010; Gualillo et al., 2008).

Blood ghrelin levels in humans peak before meals and are suppressed by food intake, and exogenous ghrelin at supraphysiologic levels confers a feeling of intense hunger in human volunteers and induces adiposity in rodents. These observations led to the belief that ghrelin might be a "hunger hormone" (Cummings et al., 2001; Tschöp et al., 2000; Tschöp et al., 2001; Wren et al., 2001a). However, a growing body of literature suggests that this is incorrect; indeed, ghrelin, GHSR, and GOAT-deficient mice generally have only mild reductions in body mass under specific conditions (Sun et al., 2003; Sun et al., 2004; Wortley et al., 2004; Wortley et al., 2005; Zhao et al., 2010a).

Rather than controlling appetite, GOAT directly conjugates dietary fats to ghrelin, modulating energy expenditure and fat storage, and local fatty acid metabolism modulates neuronal ghrelin signaling (Kirchner et al., 2009; Lopez et al., 2008; Nishi et al., 2005). Supporting this role, acute pharmacologic inhibition of GOAT reduces weight gain and provides tighter blood glucose control without altering food intake in mice on a high-fat diet enriched for medium-chain triglycerides (Barnett et al., 2010). A number of redundant pathways control appetite and metabolism, and the need for acute ablation of signaling to dissect function was similarly seen NPY/AgRP-neuron mediated control of appetite (Granata et al., 2010). GOAT may still play a role in hunger under some circumstances(Teubner et al., 2013).

The metabolic consequences of GOAT activity are best understood in the context of surviving starvation, supporting fat storage and glucagon signaling while antagonizing insulin. It is in this context that ghrelin likely evolved, and GOAT-signaling deficient mice

generated in two different ways fail to maintain blood glucose in conditions of calorie restriction, becoming moribund; this phenotype can be rescused by growth hormone (GH) infusion (Li et al., 2012; Zhang et al., 2015; Zhao et al., 2010a).

The link provided by GOAT between the gut and the brain extends to roles in learning and memory, reward behaviors for food and drugs of addiction (Carlini et al., 2002; Diano et al., 2006; Egecioglu et al., 2010; Murray et al., 2014), as well as modulation of neural development in areas affecting metabolism (Steculorum et al., 2015). Ghrelin also has potential cardioprotective (Baldanzi et al., 2002; Okumura et al., 2002; Schwenke et al., 2008; Tokudome et al., 2014), neuroprotective (Ku et al., 2015; Spencer et al., 2013), and anti-apoptotic effects (Li et al., 2015); some of these may be mediated through inhibition of inflammation (Cao et al., 2013). Ghrelin is potently pro-kinetic in the enteric nervous system, and this combined with pro-storage metabolic effects has led to a number of promising agonists in clinical trials for cachexia, improving weight gain and quality of life (Ali et al., 2013; Dornonville de la Cour et al., 2004; Trudel et al., 2002). Most of these effects require signaling through the GHSR-1a and are therefore GOAT-dependent, but a number of studies suggest the possibility of GHSR-independent ghrelin signaling in the control of vascular tone and in antiapoptotic effects (Baldanzi et al., 2002; Ku et al., 2015; Porporato et al., 2013).

A number of controversies remain in of ghrelin physiology. Proper measurement of blood ghrelin levels requires inconvenient and often-skipped practices at the time of collection, and failing to follow best practices produces conflicting results and continues to

be common (Liu et al., 2008); this is discussed below and reviewed in (Taylor et al., 2012b). A recent genetic study induced ablation of ghrelin-producing cells in adult mice using a diptheria toxin/receptor system in ghrelin-promoter expressing cells (McFarlane et al., 2014). This system recapitulates the moribund phenotype seen in GOAT-deficient mice under starvation conditions but challenges the effects of inhibition of ghrelin signaling on glucose metabolism and energy balance in the context of a high-fat diet (Barnett et al., 2010). However, the mice were handled differently in these two studies and fed different high-fat diets. Additionally, the moribund phenotype of GOAT-deficient mice may be context-dependent (Yi et al., 2012).

Ghrelin, GOAT, and GHSR Structure and Signaling[1]

The biosynthesis of ghrelin is outlined in Figure 1.1. The 117-amino-acid preprohormone contains a signal peptide and is co-translationally cleaved, releasing the 94 amino acid proghrelin into the lumen of the endoplasmic reticulum (ER). Attachment of the octanoate group to Ser3 of proghrelin by GOAT occurs in the ER. Prohormone convertase 1/3 (PC1/3) then cleaves at the C-terminus of acyl proghrelin to produce mature 28-amino acid ghrelin; this occurs in secretory granules or perhaps as early as the trans-Golgi (Zhou et al., 1999; Zhu et al., 2006).

[1] *This introductory section contains pieces updated from Taylor et. al, 2012, with permission*

Figure 1.1. Ghrelin biosynthetic pathway.

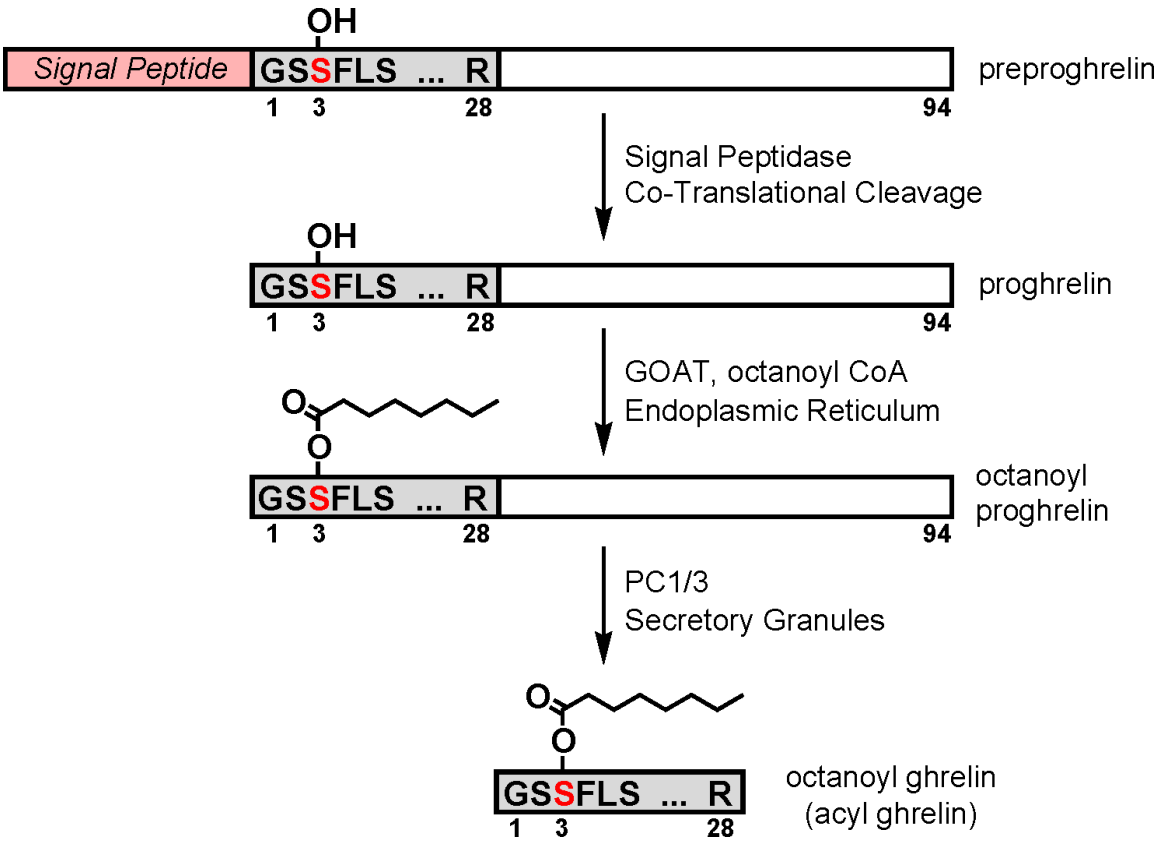

Legend, Figure 1.1. Ghrelin is synthesized as a 117-amino-acid precursor, preproghrelin, containing a signal peptide, the 28 amino-acid ghrelin sequence, and a 66 amino-acid C-terminal peptide. The signal peptide is cotranslationally cleaved, releasing the 94 amino acid proghrelin into the lumen of the endoplasmic reticulum (ER). Attachment of the octanoate group to Serine-3 of proghrelin occurs in the ER and is catalyzed by GOAT. In secretory granules, prohormone convertase 1/3 (PC1/3) then cleaves at the C-terminus of acyl proghrelin to give the mature acyl ghrelin.

The amino acid sequence of ghrelin is highly conserved among mammals, differing only at two residues between human and rodent. Ghrelin homologs have also been identified in all vertebrates examined including bullfrogs, green anole, chicken, and zebrafish; some species including bullfrogs have octanoyl-Thr3 in place of octanoyl-Ser3 (Kaiya et al., 2001; Kojima and Kangawa, 2005; Taylor et al., 2013). Ghrelin was discovered in 1999 by reverse pharmacology as the endogenous ligand of the GHSR, which at the time was an orphan receptor (Kojima et al., 1999). Upon ghrelin binding to the GHSR, cellular phospholipase C is activated to generate inositol triphosphate (IP3) and diacylglycerol, which in turn increases intracellular levels of Ca2+, resulting in GH release (Korbonits et al., 1999). This pathway is distinct from that of the growth hormone-releasing hormone (GHRH) where binding to the GHRH receptor results in increase in cAMP levels, and ghrelin signaling through the GHSR releases significantly more GH than can be achieved through GHRH signaling (Cruz and Smith, 2008).

The GHSR is predominantly expressed in the arcuate nucleus of the hypothalamus, but is also found in the pituitary, the ventromedial nuclei, the hippocampus, and vagal afferent neurons, with lower levels of expression seen non-neuronal cell types in the periphery, including the pancreas (Chen et al., 2004a; Cowley et al., 2003; Guan et al., 1997; Howard et al., 1996). Specialized ghrelin-producing cells in the stomach are the major source of circulating ghrelin; lower levels are also produced in the pancreas and hypothalamus. (Date et al., 2000; Heller et al., 2005; Kojima et al., 1999; Prado et al., 2004; Wierup et al., 2002). Acyl ghrelin may modulate metabolism via a variety of mechanisms

(Chen et al., 2004a; Morton and Schwartz, 2001; Willesen et al., 1999); its action is mediated at least in part by the uncoupling protein UCP2 (Andrews et al., 2008).

GOAT is a member of the family of membrane-bound O-acyltransferases (MBOAT), which includes hedgehog acyltransferase (HHAT) and porcupine (PORC), the substrates of which are the secretory proteins Sonic Hedgehog and Wnt, respectively. Ghrelin and Wnt3a are the only proteins known to contain acylated serine residues. MBOAT family members been also shown to acylate sterols, phospholipids, and GPI-anchored proteins, but as integral membrane proteins, the enzymatic properties of these proteins are poorly understood (Bosson et al., 2006; Buglino and Resh, 2008; Chamoun et al., 2001; Chen et al., 2004b; Hofmann, 2000; Kadowaki et al., 1996; Petrova et al., 2013; Takada et al., 2006) . To date, ghrelin is the only established substrate for GOAT (Darling et al., 2015).

The potential therapeutic benefits of exploiting the ghrelin-GOAT system in managing obesity and diabetes are attractive but not yet fully explored. Much drug discovery work has been focused on GHS-R1a receptor modulators, but the discovery of GOAT offers new potential for the generation of GOAT-selective inhibitors; the potential scope of pharmacologic actions of such modulators is not yet known.

The remainder of this chapter is reproduced from (Taylor et al., 2012b), with permission.

Analysis of Acyl Ghrelin Levels and GOAT Activity

Assays measuring acyl and desacyl ghrelin from blood and cells

In order to develop effective GOAT inhibitors, an important technical hurdle to overcome is reliable measurement of acyl and desacyl ghrelin. A challenge in designing assays to measure ghrelin acylation is the instability of acyl ghrelin in biological systems, predominantly due to hydrolysis of the acyl group by esterases in plasma, cell culture medium, and cell extracts. Any assay must measure typically dilute concentrations of hormone, preserve acylation through isolation, and then detect the acylation in the context of what is usually a larger amount of desacyl ghrelin. A comparison of literature reports suggest wide ranges (10-100-fold or more) in concentrations of acyl ghrelin hormone in studies on normal humans and rodents, underscoring the complexity of the measurements (Groschl et al., 2004; Liu et al., 2008).

Early acyl ghrelin assays used the functionality of the hormone on the GHS-R1a receptor. While useful, these assays are rather complex and lack precision. Combinations of reversed phase HPLC and immunoassays have proved increasingly reliable. Acyl ghrelin measurements relying on mass spectrometry have also been reported although our lab has had limited success with this approach (Gutierrez et al., 2008; Satou et al., 2010). The

current state-of-the art for ease of use and reproducibility seems to be sandwich ELISA assays.

Two-site immunoassays are generally more sensitive and specific than single-antibody assays and also do not cross-react with peptide fragments (Nussbaum et al., 1987). Some early publications use a 2-site sandwich ELISA developed in house (Barkan et al., 2003), but this was not widely adopted. Liu et al. (Liu et al., 2008) developed two novel sandwich ELISAs specific for acyl and desacyl full-length ghrelin. Capture is achieved using N-terminal acyl- and desacyl-specific antibodies and detection for both assays uses an affinity-purified antibody to ghrelin's C-terminal amino acids 21-27. They also detailed an improved collection protocol in which blood is collected directly into chilled tubes preloaded with the protease inhibitor AEBSF (4-(2-aminoethyl)benzenesulfonyl fluoride), are maintained on ice until prompt centrifugation, and then immediately acidified with 20% (v/v) 1N HCL to protect the ghrelin ester from hydrolysis. These combined improvements represent the current state of the field, although the esterase inhibitor PHMB (p-hydroxymercuribenzoic acid) can be substituted for AEBSF, and adding 1 M NaCl improves plasma separation.

Commercial 2-site sandwich ELISA kits by Spi-Bio (now Bertin Pharma) are now available sold through Cayman Chemical and Alpco Diagnostics. These kits have been used in contemporary studies (Barnett et al., 2010; Zhao et al., 2010b). The kits include wells coated with a C-terminal capture antibody and a modification-specific N-terminal antibody conjugated to acetylcholinesterase. The kits from the two companies are

apparently identical except for the color of their packaging. We have validated their modification-specificity and sensitivity against both house-made standards and those supplied by the manufacturer. We also tested kits from Millipore with similar results. Other 2-site kits are available from Mitsubishi Kagaku Iatron (Tokyo, Japan), using N-terminal modification-specific antibody and C-terminal capture antibody, although we have not tested them.

Measuring acyl and desacyl ghrelin levels in cell-based model systems

To establish a model system for ghrelin acylation, the field first turned to cell lines. The first cell line established was the TT Cell, a medullary thyroid carcinoma line (Kanamoto et al., 2001) Ghrelin production from these cells was similar to that in rat intestinal production, and approximately 20% of the ghrelin produced was found to be acylated. Ghrelin was secreted into the culture medium as well; the vast majority of secreted material was found to be desacyl and the different ratio between intracellular and secreted pools was attributed to degradation. This cell line was used to discover GOAT by Gutierrez et al. (Gutierrez et al., 2008) (see below). They demonstrated that the amount of acyl ghrelin in the medium can be increased by addition of octanoic acid or protection of the acyl group with a modification-specific antibody and that octanoylation occurs only at Ser3.

The human erythroleukemia (HEL) cell line (De Vriese et al., 2005) also produces acyl ghrelin, which was shown to be part of an autocrine loop leading to cell proliferation. Interestingly, they also demonstrate that the half-life of acyl ghrelin in culture medium is

approximately 1 hour. However, these cells are of limited utility as a model because the amount of acyl ghrelin produced is very low and ghrelin production is unstable (Takahashi et al., 2009).

Yang et al. (Yang et al., 2008a) tested a number of cell lines for the ability to process proghrelin to ghrelin, measuring retained intracellular ghrelin in cell lysates. HEK-293 and CHO-7 lysates contained only proghrelin, but the endocrine cell lines AtT-20, INS-1, and MIN-6 all contain mixtures of proghrelin and mature, processed ghrelin. Transfection of candidate acyltransferases into the INS-1 cell line was then used to independently discover GOAT, and all three cell lines were able to produce mature, octanoyl ghrelin when GOAT was transfected in.

Gutierrez et al. have transiently transfected plasmids expressing ghrelin and GOAT into Griptite HEK-293 MSR cells and, combined with addition of fatty acids in the medium, showed production of mature acyl ghrelin at much higher levels than seen in TT cells (Gutierrez et al., 2008). Interestingly, they detect mature, processed ghrelin in the medium of the precise expected mass. This demonstrates that HEK-293 cells can in fact process proghrelin to ghrelin, but the cleaved form may be promptly secreted. Enhanced production of acyl ghrelin was subsequently reported in 3 cell lines, TT, AtT20, and COS-7 by co-transfecting a plasmid expressing ghrelin with either or both plasmids expressing GOAT and one of five proteases (Takahashi et al., 2009).

Three improved cell lines were recently isolated from ghrelinomas in ghrelin-promoter SV40-T-antigen transgenic mice: MGN3-1, PG-1, and SG-1 cells. These cell

lines all express ghrelin, GOAT, and PC1/3, and have been shown to recapitulate physiologic ghrelin signaling to some extent, so they should be useful model systems going forward. MGN3-1 (Mouse Ghrelinoma 3-1) cells produce 5000 times more ghrelin than TT cells (Iwakura et al., 2010). Approximately 6-14% of the ghrelin produced in this cell line is acylated when octanoic acid is added to the medium, depending on the experiment, and acyl ghrelin is secreted into the culture medium in mature, cleaved form. siRNA knockdown of GOAT slightly depressed the ratio of acyl:desacyl ghrelin produced.

The similar cell lines PG-1 and SG-1 were derived from pancreatic and stomach ghrelinomas, respectively (Zhao et al., 2010b). These lines produce comparably high levels of ghrelin to MGN3-1, although direct comparison is difficult because of different measurement techniques (single-site RIA vs 2-site ELISA) and distinct normalizations (per cell vs per μg cellular protein). In PG-1 and SG-1 cells, up to 30% of secreted ghrelin is octanoylated when sodium octanoate-albumin is added to culture medium.

We recently established the vector phPPG-mGOAT for stable expression of ghrelin and GOAT in the widely available 293T and HeLa cell lines (Barnett et al., 2010). This episomally maintained vector has a CMV promoter, ghrelin, internal ribosome entry site (IRES), and then GOAT, in that order, providing substantial production and a high substrate:enzyme ratio. Measuring intracellular ghrelin by ELISA, we then used this system to test structure:activity relationships for GOAT inhibitors. Note that this approach does not explicitly distinguish proghrelin from mature ghrelin forms and avoids the issues of ester hydrolysis that appear to accompany secretion into the medium. We have also found

it most advantageous to consistently measure acyl and desacyl ghrelin from the same samples and express the percentage of acyl ghrelin as a key parameter to circumvent the fluctuations of total ghrelin that may be related to cellular conditions or isolation procedures.

In vitro direct GOAT activity assays using microsomes

Yang et al. established an in vitro GOAT acyl transfer assay using membranes enriched for ER (microsomes) from insect cells infected with baculovirus encoding mouse GOAT to transfer 3H-labeled octanoate onto proghrelin-His8 (Yang, Zhao et al. 2008). Mouse GOAT microsomes were prepared as follows: GOAT was cloned into pFastBac HT-A, giving it an N-terminal His10-TEV tag and the baculovirus infected SF9 cells from which microsomes were harvested. As a negative control, the MBOAT fingerprint residue H338 was mutated to alanine and control virus was also employed. Proghrelin-His8 and mutant proghrelins were produced in bacteria using an N-terminal GST-TEV tag, such that TEV cleavage produced the authentic N-terminal sequence of proghrelin.

The in vitro octanoylation assay of Yang et al. was performed using 1 μM 3H-octanoyl-CoA (high specific activity) and 5 μg proghrelin-His8 (8.6 μM) and 50 μg GOAT-containing microsomes. Reactions were quenched with buffer containing 0.1% SDS and labeled proghrelin separated from the reaction mixture using nickel-affinity chromatography and 3H-octanoyl-proghrelin was quantified using liquid scintillation counting. Yang et al found that addition of long-chain fatty CoA conjugates stimulate the

reaction up to 3.5-fold by preventing hydrolysis of octanoyl-CoA to octanoate and 50 μM palmitoyl-CoA was present in all further reactions.

The enzyme kinetics observed in these studies was complex and non-linear, probably because of the presence of esterases, palmitoyl-CoA, and product inhibition. Apparent K_m values for octanoyl-CoA and proghrelin were found by Yang et al. to be 0.6 and 6 μM, respectively. As a control, it was shown that S3A mutant ghrelin could not be octanoylated by GOAT. Octanoylation of ghrelin mutants G1S, G1A, and F4A was dramatically reduced, indicating the importance of residues G1, S3, and F4 in this recognition. L5A and S6A ghrelin mutations had smaller effects, indicating a lesser contribution of these side-chains to recognition, and there was no effect of S2A or P7A mutations. Also, the addition of the two N-terminal residues Ser-Ala, which would be present were the signal peptide not cleaved, markedly reduced octanoylation. Together with the finding of acylated proghrelin in transfected INS-1 cells, this evidence suggests that the natural substrate for GOAT is proghrelin after signal peptide cleavage (Yang et al., 2008a). Yang et al also demonstrated that truncated ghrelin pentapeptides could be acylated by microsomal GOAT, although they showed weaker apparent affinity for the enzyme.

Our group has developed a related assay studying recombinant microsomal GOAT, but prepared from human cells rather than insect cells (Barnett et al., 2010). HEK293T GnTI- cells were transfected with mouse GOAT containing a C-terminal 3xFlag tag cloned into a mammalian expression vector (CAG promoter). Microsomes were prepared in a similar manner to that reported by Yang et al. and GOAT assays were performed using

a synthetic ghrelin tagged with a C-terminal biotin (Ghrelin27-Biotin), taking advantage of the robustness of streptavidin-biotin affinity. Assays were carried out with 3H-octanoyl-CoA with streptavidin beads used to isolate radiolabeled octanoyl ghrelin. Although signal was detected in this human cell expression system, there appears to be significantly greater signal using the insect cell expression system.

Garner and Janda (Garner and Janda, 2010) have developed an elegant non-radioactive GOAT assay exploiting click chemistry. Replacing octanoyl-CoA with octynoyl-CoA which contains a carbon-carbon triple bond at the 7-8 position, Garner and Janda then react this with microsomal GOAT and bead-immobilized ghrelin pentapeptide affording octynoyl ghrelin. This immobilized octynoyl ghrelin is then conjugated using copper-catalyzed cycloaddition to azido-HRP (horseradish peroxidase) and then detection is achieved using amplex red fluorogenic substrate. A strong signal:noise ratio was achieved and the apparent K_m's measured for n-octynoyl-CoA and immobilized ghrelin(1–5) pentapeptide were 68 nM and 100 nM, respectively. The fact that the peptide is immobilized on a solid surface while the enzyme is still membrane-bound may explain the 1000-fold lower apparent KM for peptide and 10-fold lower apparent KM for octynoyl-CoA in these conditions. The triple bond in the octynoyl-CoA may also affect its interaction with GOAT. This click assay appears to be potentially more amenable to high throughput screening compared to the radioactive assay (Garner and Janda, 2010, 2011).

Figure 1.2. GOAT inhibitors.

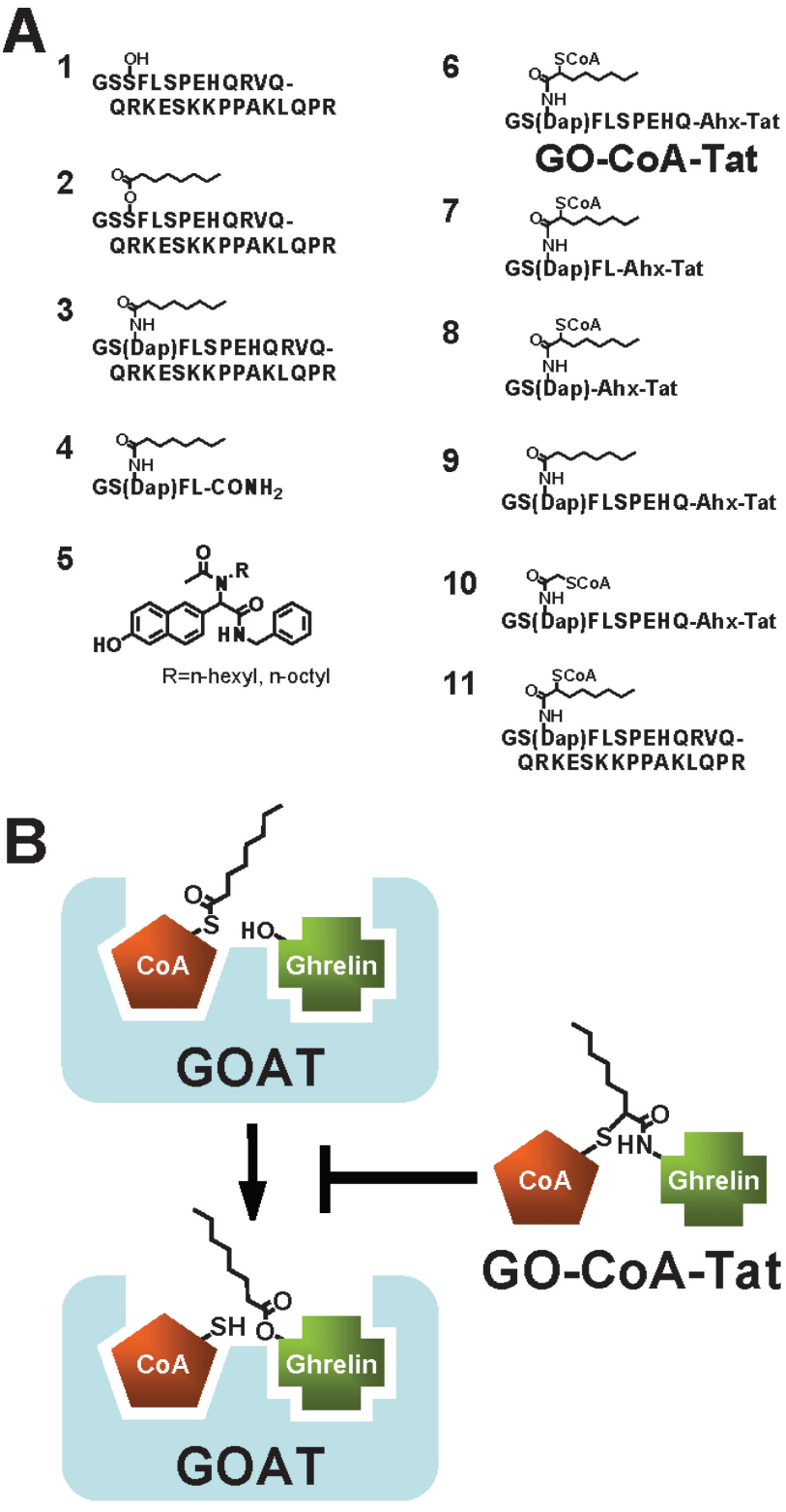

Legend, Figure 1.2. (A) Chemical structures of ghrelin and GOAT inhibitors. 1: Desacyl ghrelin. 2: Acyl ghrelin. 3: Amide-linked octanoyl ghrelin. 4: Amide-linked 5-mer octanoyl ghrelin with C-terminus amidated. 5: Inhibitors discovered by Garner and Janda (2011). 6: GO-CoA-Tat. 7,8: Bisubstrate compounds with 5- and 3-amino-acids of ghrelin. 9: GO-Tat: an octanoyl-amide Tat-tagged product analog. 10: Bisubstrate inhibitor with 2-carbon acyl group. 11: Ghrelin28-Oct-CoA, a bisubstrate compound. (B) Mechanism-based design strategy of GO-CoA-Tat. The lipid-enzyme interaction is not shown but may be important. Also, the form of ghrelin acylated by GOAT is likely proghrelin; the smaller version is shown for clarity.

GOAT Inhibitor Discovery

Three classes of GOAT inhibitors have been described so far: product acyl-peptide analogs, a small molecule detected in a high throughput screen, and a rationally designed bisubstrate analog.

When Ser3 in ghrelin (Figure 1.2, compound 2) was replaced with dap ((S)-2,3-diaminopropionic acid) creating an octanoyl-amide in place of ester (Figure 1.2, compounds 3 and 4), both the 28-mer and 5-mer acyl ghrelins were potent GOAT inhibitors with IC50 values of 0.2 μM and 1 μM, respectively. It is likely that these compounds correspond with strong product inhibition of GOAT, but the lack of hydrolytic sensitivity of the amide linkage confers greater stability.

While showing high potency, product analogs have pharmacologic challenges for in vivo applications. As peptide compounds, their ability to penetrate cell membranes may be limiting. Perhaps more importantly, they are likely to be potent agonists of GHS-R1a. Four residues of ghrelin functionally activates GHS-R1a about as efficiently as full length ghrelin (Bednarek et al., 2000). We have also found that a Tat-conjugated 10mer-amide is also a potent GHS-R1a agonist (see below).

Garner and Janda (Garner and Janda, 2011) carried out compound screening using their click assay. The assay's Z' factor was determined at 0.63, indicating high assay quality (Zhang et al., 1999). A small "credit card" library of drug-like small molecules was then screened for inhibition of GOAT and two related small molecule inhibitors were discovered (IC50=7.5 μM and 13 μM respectively, see Figure 1.2, compound 5). Interestingly, these compounds contain 6- and 8- carbon alkyl chains, suggesting that they possibly compete for the octanoic acid binding site on GOAT. Although these compounds have not yet been explored in depth pharmacologically, they appear to represent attractive leads.

Bisubstrate analogs

It is now well-established that mimics of the transition state of an enzyme-catalyzed reaction can serve as high affinity inhibitors based on the premise that most enzymes have evolved to bind tightly to the transition state. For enzymes that use two substrates in a ternary complex mechanism, an attractive approach to rational inhibitor design involves covalent linkage of the two substrates to generate a bisubstrate analog, as shown schematically in Figure 1.2B. Such compounds can show energetically favorable interactions with enzymes since dual occupancy of the substrate binding pockets is facilitated without the entropic penalty incurred with random collision of the individual substrate molecules. To be most effective, it is understood that a tether for the linkage must be able to approximate a mechanistically relevant orientation of the two substrates, ideally capturing elements of the transition state. In the best cases, bisubstrate analogs can show

binding free energies to an enzyme that are equal to or greater than the sum of the binding energies of the individual substrate components to the same protein. Successful examples have been recorded of bisubstrate analogs for protein kinases and protein acetyltransferases inspired by enzyme mechanism considerations. By placing an acetyl bridge between ATP and peptide substrate sequences for kinases, compounds that show low micromolar to sub-nanomolar affinities have been achieved for the insulin receptor kinase, protein kinase A, Csk tyrosine kinase, cyclin-dependent kinase, Abl tyrosine kinase and the epidermal growth factor tyrosine kinase. (Jencks 1981; Medzihradszky, Chen et al. 1994; Parang, Till et al. 2001; Shen and Cole 2003; Hines and Cole 2004; Hines, Parang et al. 2005; Bose, Holbert et al. 2006; Cheng, Noble et al. 2006; Levinson, Kuchment et al. 2006)

A related linker worked effectively for the histone acetyltransferase enzymes PCAF/GCN5 and p300/CBP which contain a coenzyme A (CoA) and peptide substrate fragments bridged by an acetyl spacer (Lau, Kundu et al. 2000; Sagar, Zheng et al. 2004). Several of these bisubstrate analogs have been useful in structural analysis of the enzyme reaction mechanism and substrate binding features (Liu, Wang et al. 2008). On the other hand, these analogs have suffered from limited pharmacologic utility due to their large size, polarity, and the challenges of cell membrane penetration. However, the discovery of cell penetrating peptide sequences derived from the HIV Tat protein have allowed for cell and in vivo applications for the bisubstrate analog HAT inhibitors (Cleary, Sitwala et al. 2005; Guidez, Howell et al. 2005; Zheng, Balasubramanyam et al. 2005; Liu, Dentin et al. 2008;

Oussaief, Hippocrate et al. 2009; Bricambert, Miranda et al. 2010; Cerchietti, Hatzi et al. 2010; Spin, Quertermous et al. 2010 ; Marek, Coelho et al. 2011; Wang, Gural et al. 2011).

Development of GO-CoA-Tat, a potent and selective bisubstrate inhibitor of GOAT[2]

Following the bisubstrate analog approach described above, we reported the development of GO-CoA-Tat (Barnett, Hwang et al. 2010). GO-CoA-Tat (Figure 1.2, compound 6) uses non-hydrolyzable amide and thioether linkages to combine octanoyl-CoA with the first 10 amino-acids of ghrelin, which are 100% conserved in mammals. An HIV Tat-derived peptide sequence was attached to the C-terminus using a flexible linker to allow cell penetration. GO-CoA-Tat and a set of related analogs and control compounds (Figure 1.2, compounds 6-11) were synthesized by a solid-phase strategy.

We then tested these compounds in HEK and HeLa cells expressing ghrelin and GOAT stably transfected with our phPPG-mGOAT vector. Cells were maintained in medium supplemented with octanoic acid and pre-incubated with compound for 24 hours, then lysed and intracellular acyl and desacyl proghrelin were measured by ELISA, with values validated using kits from two manufacturers and standards made in-house. We first tested GO-CoA-Tat in these models and the mean inhibitory concentration was ~5 μM; control compound D4-Tat had no effect. Interestingly, maximal inhibition was achieved only after 24 hours incubation with GO-CoA-Tat. This could be due to atypical behavior

[2] *This section summarizes parts of Chapter 2, with perspective.*

of the enzyme or inhibitor or due to pre-existing intracellular stores of acyl ghrelin. To test this, we used the radioassay described above in Section 2.3 and found substantial inhibition occurred within 5 min with 100 nM GO-CoA-Tat. This too suggests that there are intracellular stores of acyl ghrelin in these cells.

We examined structure-activity relationships required for inhibition with compounds used at 6 μM. Consistent with what was seen in other assays, 5 residues of ghrelin were sufficient for inhibition but 3 residues were not. Inclusion of 10 residues increased potency, with a maximum of ~75% inhibition of acylation seen. CoA was also required for inhibition; this finding is discussed further below in Section 4.3, and a version of the bisubstrate compound with a truncated 2-carbon acyl group still showed some inhibition. Tat was required for inhibition, consistent with its role in entry into the cells and ruling out action on a surface receptor. None of the compounds were toxic to the cells in the low micromolar concentration range. GO-CoA-Tat's specificity is also reflected in its lack of inhibition of three acetyl-CoA utilizing enzymes.

To further analyze GO-CoA-Tat's inhibition of GOAT, we developed a direct binding assay for GOAT, taking advantage of photo-crosslinking technology. We first synthesized two chemically modified versions of our bisubstrate inhibitor: GO-CoA-Tat-F4BP and GO-CoA-Tat-L5BP, in which Phe4 or Leu5, respectively, is replaced with a photoreactive amino acid benzoyl-phenylalanine and each is tagged with a biotin group (Barnett et al., 2010). We showed that this compound can covalently cross-link to recombinant solubilized or microsomal GOAT. This crosslinking could be blocked by an

excess of unlabeled GO-CoA-Tat, providing evidence for specificity and demonstrating direct binding of GO-CoA-Tat to GOAT.

For these experiments, we used GOAT with a C-terminal 3xFlag tag, produced in SF9 cells using baculovirus. Microsomes were prepared as above and the reaction was performed either in the microsome membranes or with GOAT purified to homogeneity using anti-Flag affinity chromatography and the Fos-Choline-16 detergent (Anatrace). This detergent was chosen because of its high ability to solubilize GOAT and because we reasoned that the long alkyl chain might be less likely to interfere with the octanoic-acid binding site on GOAT.

Photo-crosslinking reactions were performed in a small water-jacketed quartz cuvette custom made for this purpose by Quark glass. The cuvette is connected to the water line and is suspended above a magnetic stir plate. A small PTFE stir bar is added, with medium agitation. A mercury UV lamp with ~360nm long wave filter, such as UVP #B-100AP, is positioned with the center of the lamp approximately 2cm from the cuvette, positioning the sample at the position of peak intensity. A time course experiment (not shown) demonstrated that the reaction had neared completion by 30 min. Cross-linked membranes were then solubilized and immunoprecipitated. Biotinylation was visualized using SDS-PAGE and streptavidin-HRP or, for more sensitivity, streptavidin followed by polyclonal anti-streptavidin.

Glucose and weight control in mice with GO-CoA-Tat [3]

Treatment of C57BL6 mice on medium-chain triglyceride (MCT) diets (Kirchner et al., 2009) with GO-CoA-Tat at 40mg/kg dose, but not control compound D4-Tat or vehicle, decreased plasma acyl ghrelin levels without changing desacyl ghrelin levels. Maximum inhibition was seen after 6 hours, but some acyl ghrelin suppression was still detectable 24 hours after GO-CoA-Tat treatment. Due to daily fluctuations between animals and ad lib feeding, we found that the acyl:desacyl ghrelin ratio was a more sensitive and specific measure of inhibition.

We explored the effect on weight gain over a 1 month period in mice placed on a medium chain triglyceride diet. Daily IP injections of GO-CoA-Tat as above reduced the weight gain seen in vehicle-treated mice. As measured by QMR spectroscopy, the difference in weight was due to significantly reduced fat mass in the GO-CoA-Tat treated animals. In contrast, ghrelin knockout mice treated with GO-CoA-Tat vs. vehicle-treated showed no statistically significant difference in weight or body composition. To investigate the potential for GO-CoA-Tat toxicity, we examined the blood chemistries and cell counts in the mice after 1 month of treatment with the agent. There was no apparent untoward effect on normal blood chemistries or cell counts under these conditions. Interestingly, GO-CoA-Tat treated WT mice showed reduced IGF-1 and lower blood glucose, consistent with suppression of ghrelin-mediated somatotroph signaling.

---

[3] *This section summarizes parts of Chapter 2, with perspective.*

To investigate the role of acute pharmacologic inhibition of acyl ghrelin in insulin signaling and glucose homeostasis, we pre-treated with GO-CoA-Tat and then measured response to a glucose challenge, first in isolated pancreatic islets and then in mice. The insulin response is increased in islets and mice, where the response is accompanied by reduced blood glucose. In contrast, there was no effect when the studies were repeated in ghrelin knockout animals, suggesting that GO-CoA-Tat's effects on insulin are due to inhibition of ghrelin acylation. Finally, we show by quantitative PCR that islets isolated from mice pre-treated with GO-CoA-Tat have a 20-fold reduction in expression of uncoupling protein 2 mRNA (UCP2, which suppresses insulin secretion), but there was no change in UCP2 expression in the gastric fundus. Together, these data show a tissue-specific role for GOAT inhibition in augmentation of insulin secretion. Regulation of UCP2 also highlights the importance of ghrelin acylation in obesity and type 2 diabetes, underscoring the need for more drug-like GOAT inhibitors (Andrews et al., 2008; Dezaki et al., 2008; Joseph et al., 2002; Sun et al., 2006; Tong et al., 2010; Zhang et al., 2001).

Challenges and Future Directions

While there has been significant progress in GOAT enzymology and inhibition reported in the past few years, many challenges remain.

Targeting GOAT vs. the GHS-R1a

One hurdle in developing therapeutic agents to target GOAT is extensive overlap in the pharmacophore recognized by GOAT and the GHS-R1a. We have recently tested a number of compounds using a version of the GHS-R1a assay reported by Kojima et al. (Barnett et al., 2010; Kojima et al., 1999). Dose-response traces from individual wells treated with acyl ghrelin are shown in Figure 1.3A. The responses to selected compounds are shown in Figure 1.3B. Acyl ghrelin and amide ghrelin (Ser3 Dap-Octanoyl-Amide, Figure 1.2 compounds 2 and 3, respectively) are indistinguishable at the receptor. In contrast, GO-CoA-Tat does not activate the GHS-R1a at concentrations tested, which include concentrations higher than those used in mice. We also showed that the activity of 1 μM or 100 nM ghrelin at the GHS-R was not inhibited by GO-CoA-Tat at 60nM, 600nM, or 6μM. Surprisingly, a 28-mer bisubstrate compound Ghrelin28-Oct-CoA (compound 11) could activate the receptor with reduced affinity.

Figure 1.3. GHS-R1a assay in stably transfected HEK-293T-GHS-R1a cells.

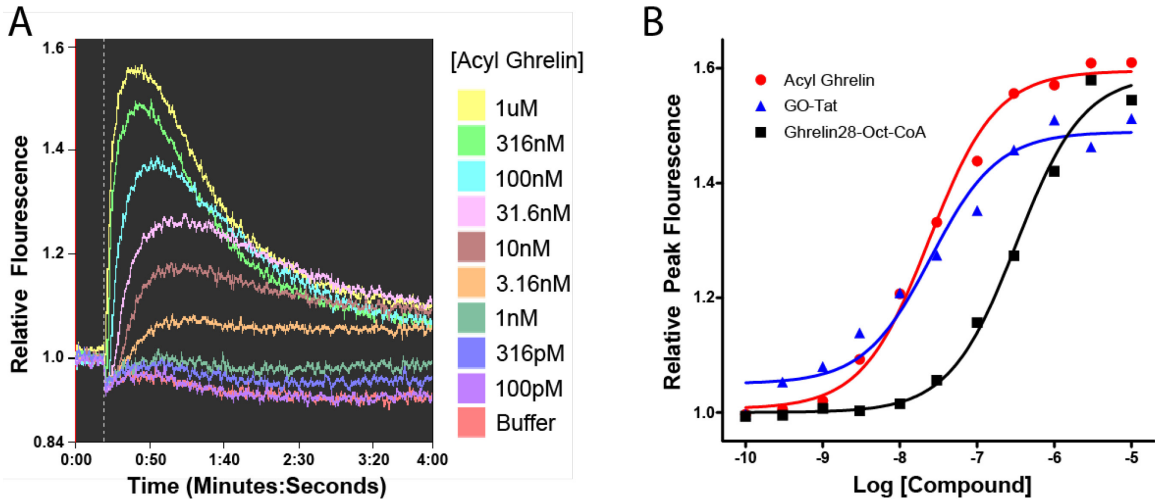

Legend, Figure 1.3. (A) Typical dose-response traces for acyl ghrelin, with concentrations on half-log scale from 1 μM to 100 pM, with buffer-only control. (B) Agonism for acyl ghrelin, GO-Tat (Figure 1.2, Compound 9), and the bisubstrate compound Ghrelin28-Oct-CoA (Figure 1.2, Compound 11). EC50 values are reported in Table 1.1.

Table 1.1. EC50 values in the GHS-R1a assay.

Compound	**EC_{50}**
Acyl Ghrelin	18 ± 6 nM
Desacyl Ghrelin	>10 μM
Amide Ghrelin	19 ± 8 nM
GO-Tat	23 ± 4 nM
GO-CoA-Tat	>10 μM
Ghrelin28-Oct-CoA	270 ± 70 nM
D4-Tat	>10 μM
GO-Tat S_2Oct	>10 μM
GO-Tat S_6Oct	>10 μM

Moving towards studies of purified GOAT

Studying the activity and mechanism of purified GOAT is critical for improved inhibitor development. To date, all reported GOAT assays, with the exception of one example of our photo-crosslinking-based binding assay, have been carried out in complex microsome mixtures containing thousands of other proteins. GOAT is only a small fraction of the total protein in these experiments, and reactions are usually carried out in the presence of relatively high concentrations of palmitoyl-CoA to inhibit esterases and other CoA-utilizing enzymes in these mixtures. Further, only very low conversion percentages are achievable. However, GOAT has not yet been solubilized in an active form. Progress in these areas will be critical to developing better inhibitors and for structural studies of GOAT.

Structural and mechanistic studies of GOAT and GOAT topology

Currently, we know very little about the structure and mechanism of GOAT. The specific and potent binding of the bisubstrate inhibitor GO-CoA-Tat argues for a ternary complex mechanism, but other mechanisms are still formally possible and further studies in this area are needed. We don't know where proghrelin and the octanoyl-donor bind and the identity of the octanoyl donor has not been proven. Also, the identity of the active site has not been confirmed.

A map of the topology of GOAT will be helpful to answer some of these questions. Based on sliding-window Kyte-Doolittle hydropathy plots, mouse GOAT was predicted

to contain 8 transmembrane-helices (TM) (Yang et al., 2008a), however no experiments have yet been reported to further probe GOAT's topology. To acylate ghrelin, GOAT's active site should face the ER lumen where ghrelin is localized; this logic also applies to other MBOATs that acylate secreted and GPI-anchored proteins. The two most conserved residues in the MBOAT fingerprint are N307 and H338 in mouse GOAT, and only H338 is conserved throughout the entire MBOAT family. The homologous histidine in another MBOAT, the human cholesterol acyltransferase ACAT1, was mapped to the lumenal boundary of a TM or perhaps in a short loop in the ER lumen (Guo et al., 2005b). Like GOAT, mutation of this histidine in ACAT1 abolished catalytic activity. The topology of distantly related yeast MBOAT members Ale1p, Are1p, and Gup1p was recently studied in detail (Pagac et al., 2011); these enzymes acylate lipids, cholesterol, and GPI-anchored proteins, respectively, and Are1p is the yeast ortholog of ACAT1. The conserved histidine in all cases was shown to be in the ER lumen, but none of the active sites have yet been mapped.

These conserved residues have been called "catalytic residues," however there is a lack of mechanistic data that firmly establishes this point. Although GOATs with alanine mutants of these conserved His and Asn residues are inactive, the homologous histidine residue was recently shown to be dispensable for palmitoylation of sonic hedgehog (Shh) by HHAT. In this case, the H379A caused reduced binding affinity of Shh as reflected in an increased K_m without changing *Vmax* (Buglino and Resh, 2010). Therefore, at this point the identity of the active site of GOAT and other MBOATs is unclear.

With the active site of GOAT in the ER lumen, one question raised by the success of the microsomal GOAT assays is, how do the ghrelin peptides and octanoyl group reach the active site of GOAT? Microsomes are believed to be sealed bilayer vesicles, so in order to octanoylate ghrelin, some of the microsomes are presumably inside-out, with normally lumenal contents exposed to the assay buffer.

Another unanswered question is, if octanoyl-CoA is the correct acyl donor, how do acyl-CoA's, localized predominantly in the cytoplasm, gain access to the ER lumen? Although it has been hypothesized that GOAT might have a role in transport of the octanoyl group across the membrane, there is no specific evidence yet reported. GO-CoA-Tat appears to rely on Tat-mediated delivery of the agent into the cytoplasm (Potocky et al., 2003; Schwarze et al., 1999), but interestingly GO-Tat does not appear to block cellular GOAT even though it is homologous to potent product inhibitors that block GOAT in vitro. Perhaps the CoA-moiety in GO-CoA-Tat is crucial for ER entry through the proposed transport properties of GOAT. In addition to the possibility of GOAT participating in substrate transport, other enzyme mechanisms are also formally possible. Octanoate may first be transferred from octanoyl-CoA to an intermediate host, either GOAT, another protein, or a lipid. It is even possible that an additional protein collaborates with GOAT to effect acyl transfer.

Exploring other MBOATs

The MBOATs porcupine and HHAT, acylating Wnt and hedgehog proteins, respectively, share many features in common with GOAT. A detailed understanding of these pathways is critical for progress in understanding how these signaling ligands modulate development, stem cell renewal and differentiation, and initiation and maintenance of cancer (Clevers, 2006; Pasca di Magliano and Hebrok, 2003; Reya and Clevers, 2005; Zhao et al., 2009). Techniques learned in studying the enzymology, structure, and function of the GOAT/ghrelin system should be readily translated to these related cases, leading to new inhibitors and insights into structure and function. Porcupine, in particular, is the only other protein known to acylate a serine and should therefore be most mechanistically like GOAT. A family of small molecules targeting porcupine was recently reported (Zhao et al., 2009); analogs of these compounds may also inhibit GOAT or other MBOATs and should be investigated.

Towards potent, small molecule inhibitors of GOAT

With the development of the first small molecule inhibitor of GOAT and a high-throughput-ready screen (ELCCA), the prospect of a potent, specific small molecule inhibitor of GOAT is exciting (Garner and Janda, 2011). Additionally, new in vitro and cell-based assay systems will surely lead to new mechanistic and structural insights and may also be amenable to screening approaches (Barnett et al., 2010; Iwakura et al., 2010; Yang et al., 2008b; Zhao et al., 2010b). With new model systems for GOAT inhibition now established in cells and mice, the efficacy of new compounds can now be evaluated. These

compounds could be very promising leads in the treatment of obesity, diabetes, and other metabolic disorders, and may provide much needed tools to map out a complete understanding of GOAT in biology.

CHAPTER 2 – GLUCOSE AND WEIGHT CONTROL IN MICE WITH A DESIGNED GHRELIN-O-ACYLTRANSFERASE INHIBITOR

This chapter is reproduced from (Barnett et al., 2010), with permission.

Ghrelin is a gastric peptide hormone that stimulates weight gain in vertebrates. The biological activities of ghrelin require octanoylation of the peptide on Ser3, an unusual post-translational modification that is catalyzed by the enzyme ghrelin O-acyltransferase (GOAT). Here we describe the design, synthesis, and characterization of GO-CoA-Tat, a peptide-based bisubstrate analog that antagonizes GOAT. GO-CoA-Tat potently inhibits GOAT in vitro, in cultured cells, and in mice. Intraperitoneal administration of GO-CoA-Tat improves glucose tolerance and reduces weight gain in wild-type mice but not in ghrelin-deficient mice, supporting the concept that its beneficial metabolic effects are due specifically to GOAT inhibition. In addition to serving as a research tool for mapping ghrelin actions, GO-CoA-Tat may help pave the way for clinical targeting of GOAT in metabolic diseases.

Figure 2.1. Press release image accompanying this work.

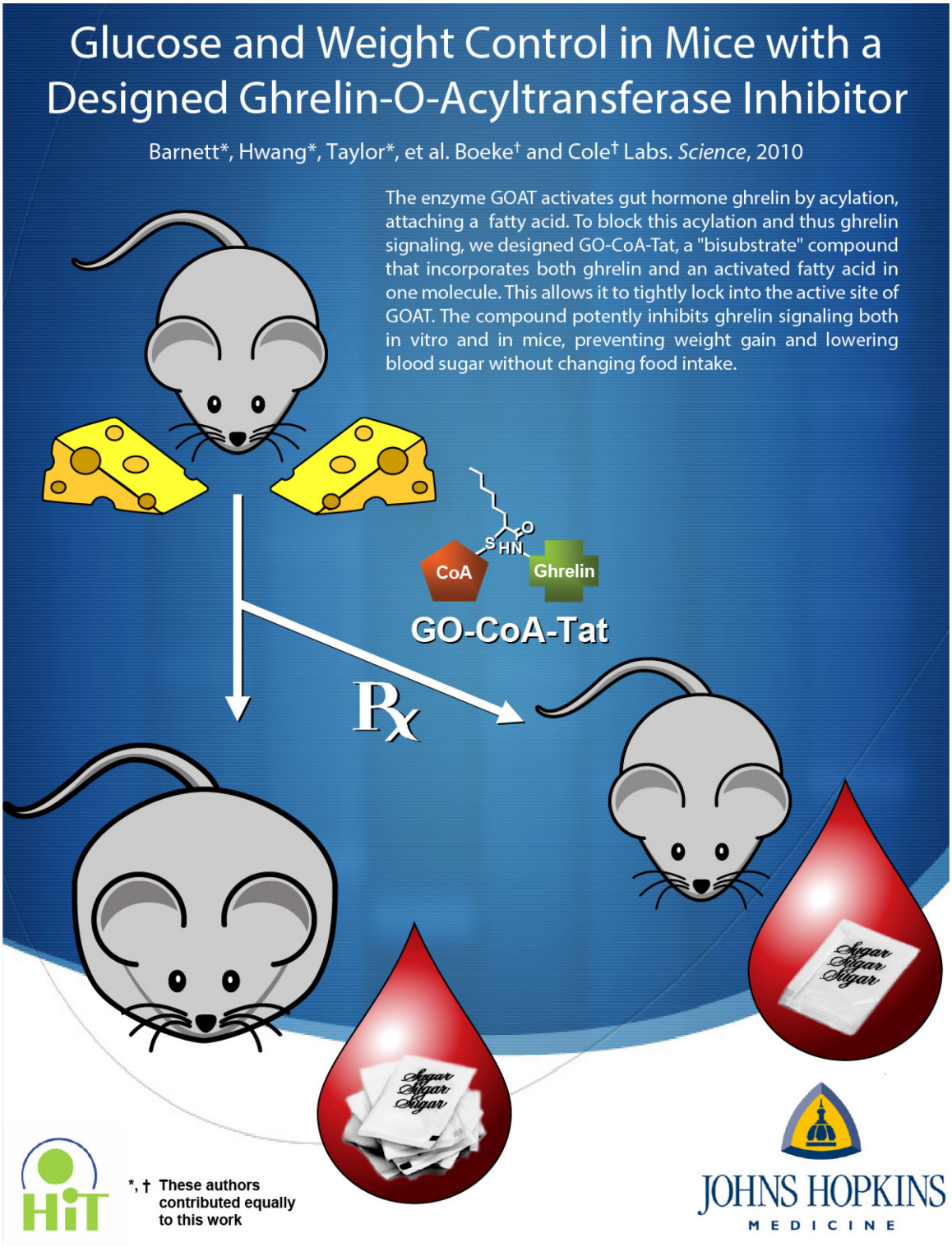

The persistent rise in the proportion of overweight individuals in Western society over the past 30 years has been associated with substantial excess morbidity and is widely recognized as a major public health concern. To address this problem, intensive efforts are underway to clarify nutrient-hormone interactions contributing to weight gain. Starting with the isolation of leptin (Rosenbaum et al., 1996), a series of hormones acting centrally and peripherally to influence body mass have been discovered. Among these, the gastric peptide hormone acyl ghrelin has generated considerable interest as an important stimulus for weight gain (Kojima et al., 1999; Tschöp et al., 2000; Wren et al., 2001b; Zigman et al., 2005) and modulator of glucose homeostasis (Dezaki et al., 2007; Sun et al., 2006; Yada et al., 2008). Various strategies in therapeutic development have been devised to antagonize acyl ghrelin (Gualillo et al., 2008; Lu et al., 2009), although none has yet emerged as clinically beneficial. Acyl ghrelin has an unusual Ser3 octanoylation; only acylated ghrelin can bind and activate the growth hormone secretagogue receptor (GHSR-1a). The cDNA for the enzyme responsible for this esterification, GOAT, has recently been cloned (Gutierrez et al., 2008; Yang et al., 2008a). GOAT has been suggested as a potential therapeutic target for modulating weight gain and glucose control, but this has not yet been directly tested (Gualillo et al., 2008; Kirchner et al., 2009). An acyl ghrelin product analog Dap-ghrelin blocks GOAT activity in a microsomal assay (Yang et al., 2008b).

We designed bisubstrate analog GO-CoA-Tat based on the theory that, if GOAT uses a ternary complex mechanism which templates octanoyl-CoA and ghrelin peptide, then linking the two substrates with a non-cleavable bridge could combine the binding

energies of the individual ligands without the entropic loss associated with forming the ternary complex (Figure 2.2A). A related successful strategy has been used for other peptide modifying enzymes including histone acetyltransferases (HAT) and protein kinases (Lau et al., 2000; Parang et al., 2001). Since we were uncertain about the ghrelin peptide length needed for recognition by GOAT, we selected amino acids 1-10 for coupling to octanoyl-CoA, to maximize inclusion of highly conserved ghrelin residues. An 11-mer HIV Tat-derived peptide sequence was also attached to the C-terminus via an amino-hexanoyl linker to enhance cell penetration. Synthesis of this tripartite compound, GO-CoA-Tat (1), was performed using a solid phase strategy (Figure 2.2). A set of related analogs (2-6) with different peptide lengths and individual deletion of CoA, octyl, and Tat, respectively, were also synthesized (Figure 2.2A).

Figure 2.2. GO-CoA-Tat is a bisubstrate inhibitor that inhibits GOAT, lowering acyl ghrelin levels.

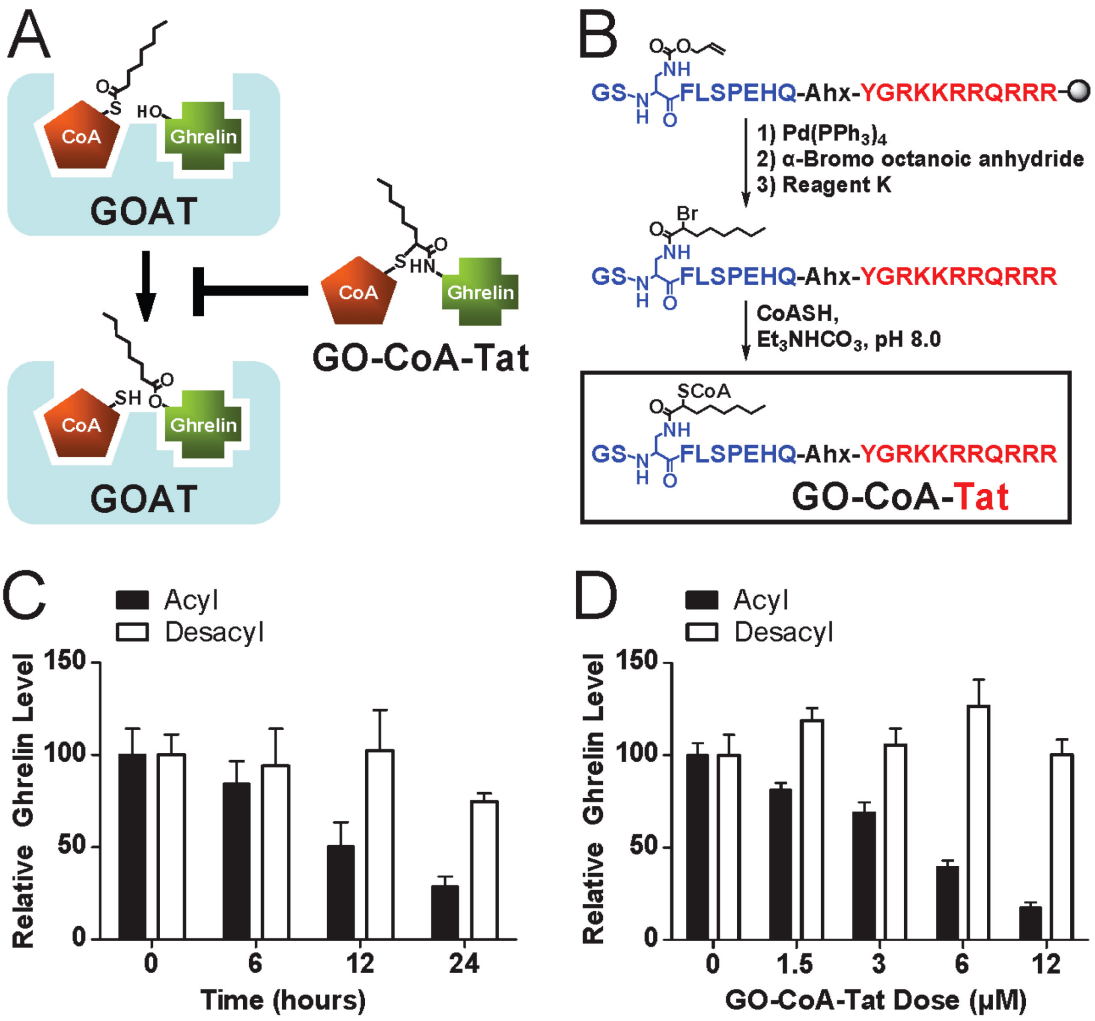

Legend, Figure 2.2. (A) Mechanism-based design strategy. Lipid-enzyme interaction, not shown, may also be important. (B) Structure of GO-CoA-Tat and synthetic scheme for bisubstrate inhibitors that consist of three components: coenzyme A, octanoylated ghrelin peptide and a Tat peptide; Ahx-aminohexanoate. (C) Temporal inhibition of acyl but not desacyl ghrelin production by 6 μM GO-CoA-Tat in GOAT/preproghrelin-transfected HeLa cells. (D) Dose-response reduction of acyl but not desacyl ghrelin levels by GO-CoA-Tat in GOAT/preproghrelin-transfected HeLa cells after 24 h incubation.

Figure 2.3. GO-CoA-Tat targets GOAT directly *in vitro* and in a structure specific manner.

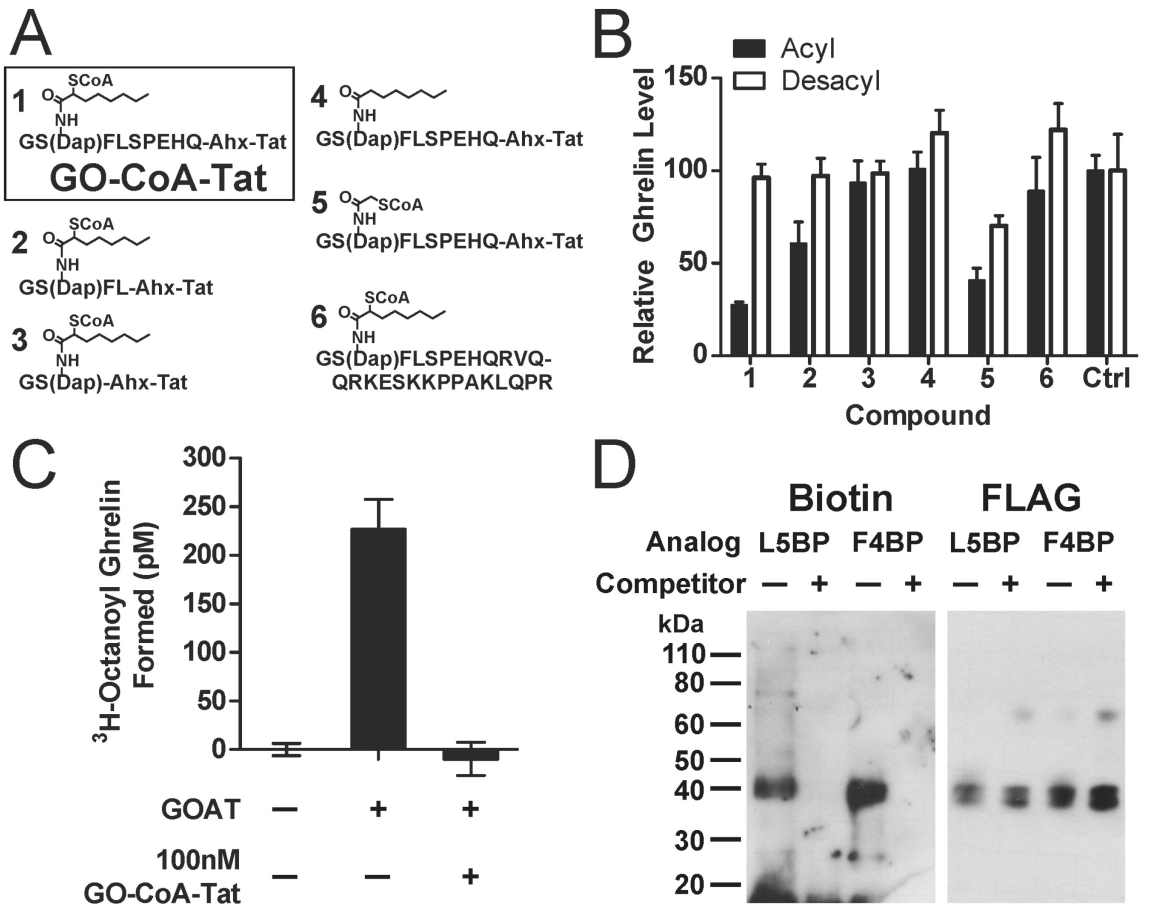

Legend, Figure 2.3. (A) Structure of GO-CoA-Tat analogs (1-6). (B) Acyl and desacyl ghrelin levels after treatment with 6 μM GO-CoA-Tat (1) and analogs (2-6) from GOAT/preproghrelin-transfected HeLa cells after 24 h. (C) In vitro acyltransferase inhibition assay (5 min reaction) with microsomal recombinant GOAT. (D) UV crosslinking of solubilized GOAT by biotin-tagged, benzophenylalanine analogs of GO-CoA-Tat (L5BP, F4BP) (5 μM). Competitor is GO-CoA-Tat at 100 μM. Immunoblots of cross-linked GOAT were visualized with streptavidin, loading was checked with anti-FLAG.

Figure 2.4. Inhibitor effects on acyl and desacyl ghrelin levels in phPPG-mGOAT -transfected HeLa and HEK cells.

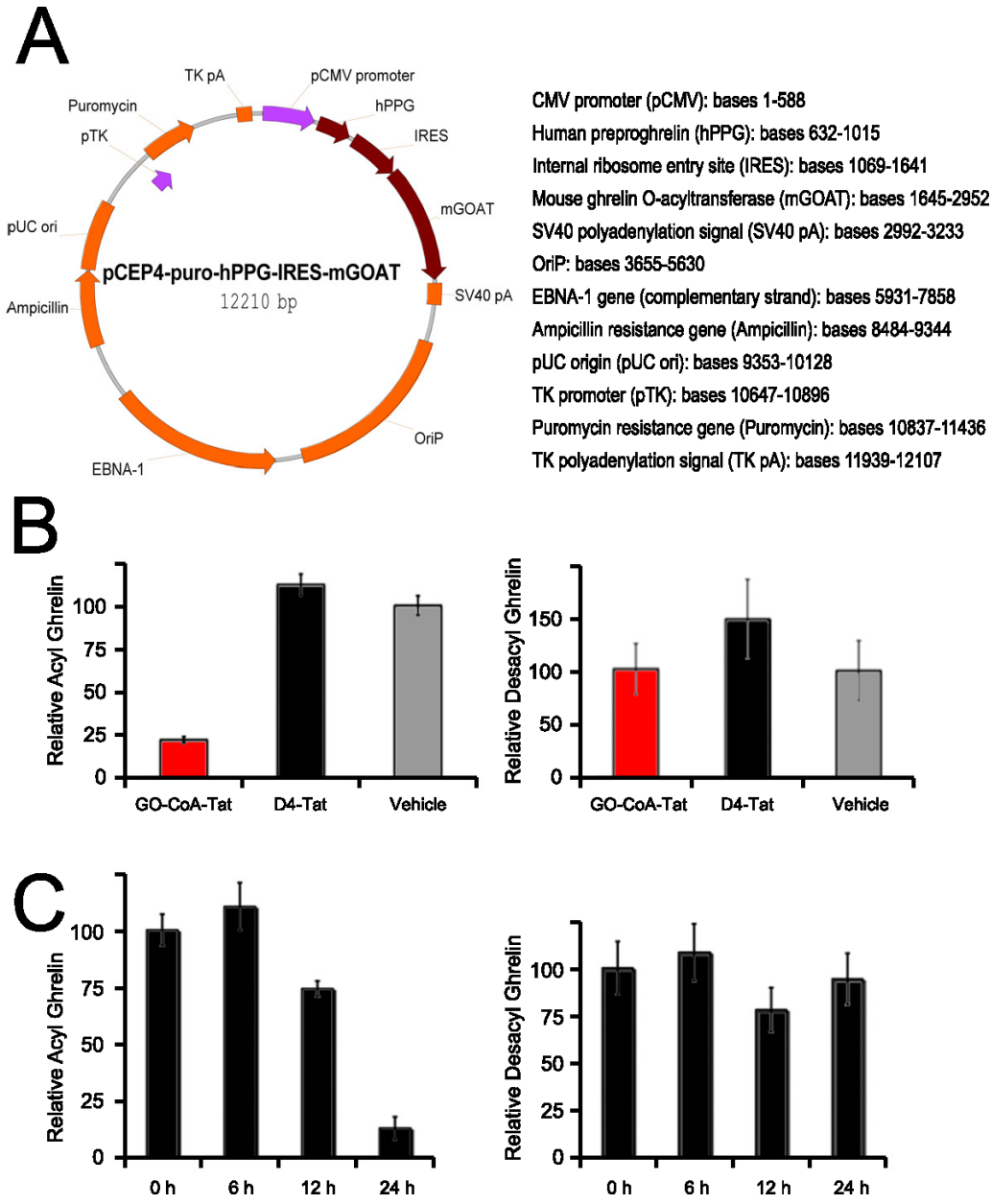

Legend, Figure 2.4. (A) Plasmid used for GOAT/preproghrelin transfection. (B) Acyl and desacyl ghrelin levels measured 24 h after treatment with 6 μM GO-CoA-Tat, D4-Tat or vehicle in transfected HeLa cells. (C) Temporal inhibition of acyl and desacyl ghrelin by 6 μM GO-CoA-Tat in transfected HEK cells. (D) Acyl and desacyl ghrelin levels after treatment with 6 μM Ghr28-Oct-CoA (Tat-free, compound **6**) as in Fig. S1B. For graphs in Fig. S1, standard errors are shown (n=5).

Figure 2.5. Establishment of an *in vitro* assay for GOAT.

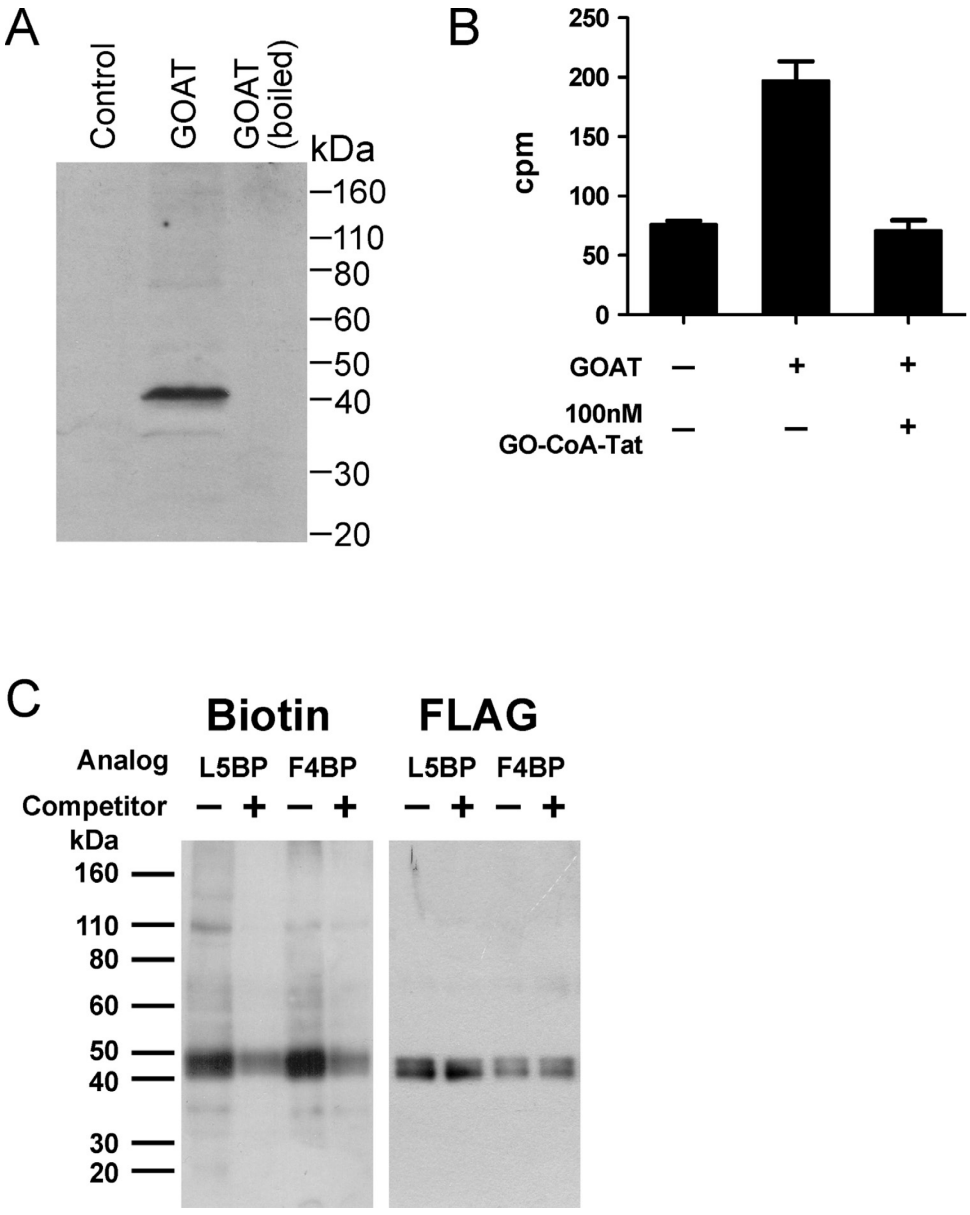

Legend, Figure 2.5. GOAT in microsomes from HEK293T GnTI(-) cells. HEK293T GnTI(-) cells were transfected with GOAT-3xFlag or empty vector (Control) and microsomes were prepared as described in *Materials and Methods*. (A) Immunoblot analysis with 10 μg/mL monoclonal anti-FLAG antibody of microsomes (50 μg of protein) from transfected and untransfected cells. GOAT-transfected microsomes incubated at 50˚C in SDS-Page loading dye for 5 min, but not those boiled at 100˚C for equal time, reveal a band at 42 kDa. (B). GOAT activity is present in microsomes from transfected but not untransfected cells and is virtually completely inhibited by GO-CoA-Tat at 100 nM. Spans of duplicate measurements are shown as error bars.

To analyze the cellular effects of GO-CoA-Tat, we generated two human cell lines (in HeLa [epithelial] and HEK [embryonic kidney]) that stably express GOAT and preproghrelin (Figure 2.4A) and show robust production of ghrelin in both its acyl and desacyl forms when grown in medium supplemented with octanoic acid. GO-CoA-Tat but not control compound D4-Tat (tetra-aspartate, to simulate the negative CoA charge, similarly linked to the Tat peptide) inhibited the production of acyl ghrelin but not desacyl ghrelin with an IC50 ~5μM (Figure 2.2, Figure 2.4). Interestingly, maximal inhibition was achieved only after 24 h of exposure to compound in both preproghrelin/GOAT-transfected HeLa and HEK cells (Figure 2.2, Figure 2.4). The slow kinetics might result from either atypical enzymatic characteristics or pre-formed acyl ghrelin stores. To further investigate this delay, we tested GO-CoA-Tat in vitro with recombinant microsomal GOAT (Figure 2.3C, Figure 2.5) using a radioactive assay (Yang et al., 2008b). Virtually complete GOAT inhibition was achieved with 100 nM GO-CoA-Tat within 5 min (Figure 2.3C, Figure 2.5), suggesting that the delay in reduction of cellular acyl ghrelin levels may reflect a significant preexisting intracellular reservoir. We also showed that two chemically modified versions of the inhibitor, GO-CoA-Tat-F4BP and GO-CoA-Tat-L5BP, in which Phe4 or Leu5, respectively, is replaced with a photoreactive amino acid benzoyl-phenylalanine and each is tagged with a biotin group, can covalently cross-link to recombinant solubilized or microsomal GOAT, providing evidence for direct binding of GO-CoA-Tat (Figure 2.3D, Figure 2.5C). This cross-linking interaction appears to be specific, as it can be blocked by GO-CoA-Tat (Figure 2.3D, Figure 2.5C).

GO-CoA-Tat appears to be a selective GOAT antagonist since at 10 μM, it showed less than 15% inhibition of three acetyl-CoA utilizing enzymes in vitro including p300 HAT, PCAF HAT, and serotonin N-acetyltransferase (Figure 2.6A). Moreover, GO-CoA-Tat appears non-toxic to cell viability in the concentration range studied and does not antagonize the GHSR-1a receptor (Figure 2.6-G). A broader analysis of GO-CoA-Tat (1) and analogs (2-6) reveals a requirement for at least 10 ghrelin residues, as well as the CoA, octanoyl, and Tat components, respectively, for the most potent cellular inhibition of cellular GOAT (Figure 2.3A-B). These results are consistent with GO-CoA-Tat behaving as a bona fide bisubstrate analog in antagonizing GOAT activity. Furthermore, the requirement for the Tat sequence for inhibitory activity (see compound 6, Figure 2.3B) argues that cell penetration is critical, and the compound is not acting on a cell surface receptor.

To examine whether GO-CoA-Tat blocks acyl ghrelin production in mice, we explored the effect of intraperitoneally delivered GO-CoA-Tat at 11 μmol/kg (40 mg/kg) in wild type (wt) C57BL6 animals on a medium chain triglyceride (MCT) diet (Kirchner et al., 2009). Treatment with GO-CoA-Tat, but not D4-Tat control or vehicle, led to decreased serum levels of acyl ghrelin (Figure 2.7A, Figure 2.8C, D), with maximum inhibition 6 h after administration (Figure 2.7A). There was no significant effect on serum levels of desacyl ghrelin (Figure 2.7B). Since the average ghrelin levels were found to vary considerably among mice, the statistical significance was most clear when acyl ghrelin was

expressed as a percent of the total (Figure 2.7C). These results strongly suggest that GO-CoA-Tat targets GOAT in vivo.

Figure 2.6. Assays for non-specific inhibition and toxicity of GO-CoA-Tat.

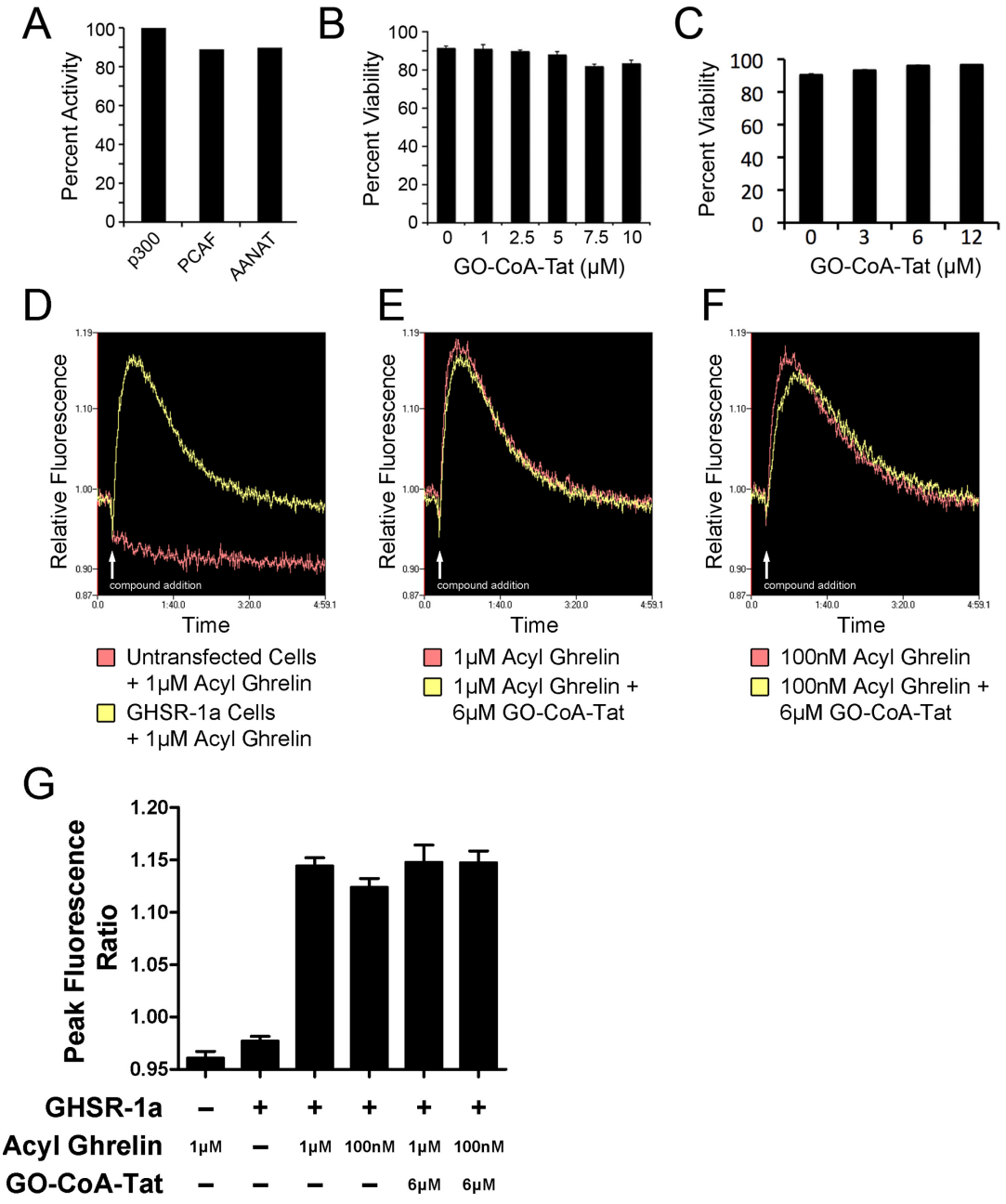

Legend, Figure 2.6. (A) Percent activity in the presence of 10 μM of GO-CoA-Tat with acetyltransferases p300, PCAF and AANAT. (B) Viability of HepG2 cells and (C) HeLa cells after 24 h incubation with varying concentrations of GO-CoA-Tat. (D) Validation of ghrelin receptor function: relative fluorescence change in HEK- 293T-GHSR-1a cells but not untransfected control cells after the addition of 1 μM acyl ghrelin. GO-CoA-Tat at 6 μM concentration does not antagonize this effect vs. either 1 μM (E) or 100 nM (F) acyl ghrelin. These fluorescence changes are quantified in (G). Standard errors are shown.

Figure 2.7. Effects of GO-CoA-Tat on blood ghrelin and body weight in mice.

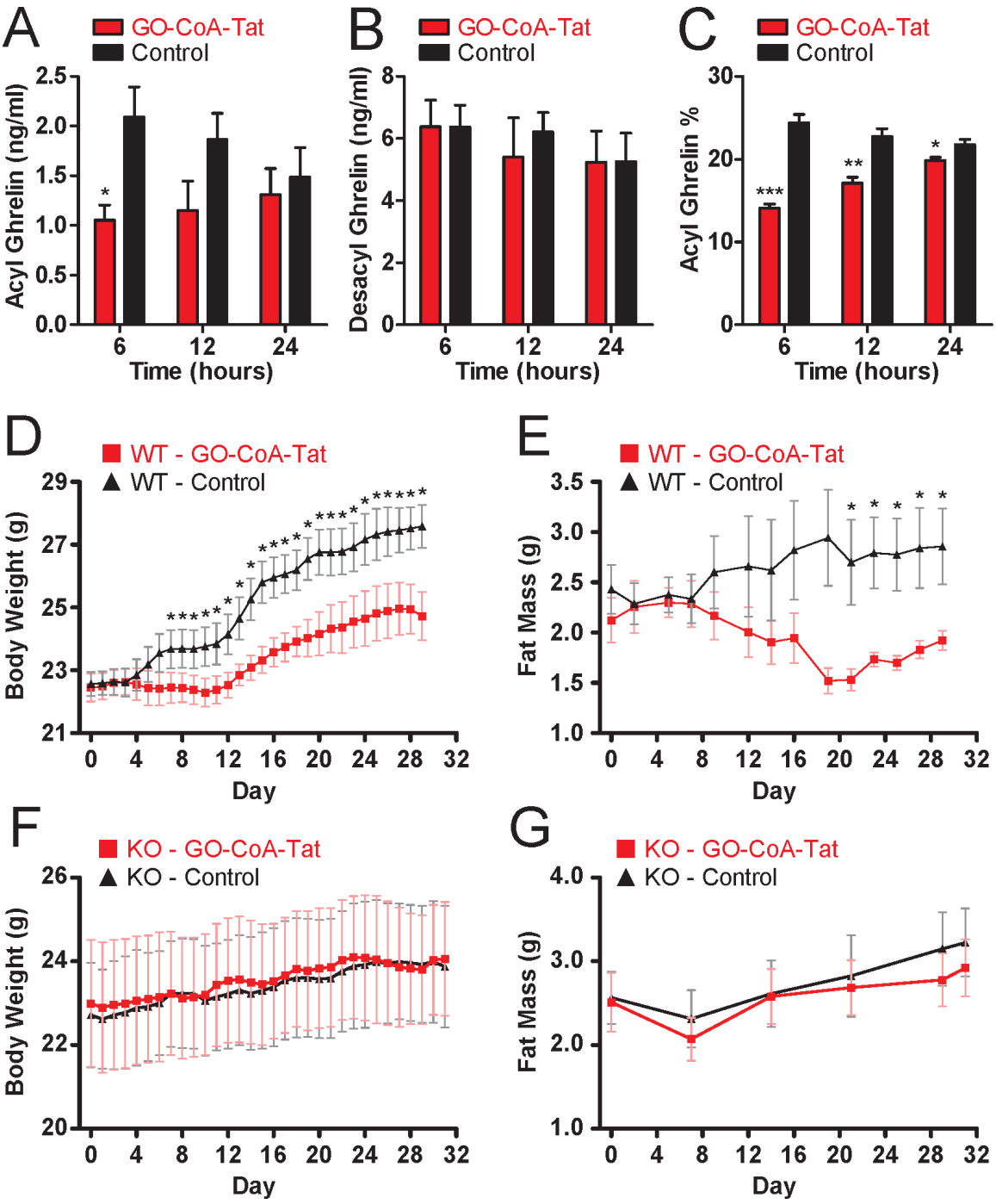

Legend, Figure 2.7. (A) Serum acyl ghrelin levels in WT C57BL6 mice on an MCT diet treated intraperitoneally with 11 μmol/kg GO-CoA-Tat vs. D4-Tat control (n=5) after 6, 12, and 24 h. (*p <0.05, **p<0.01, ***p<0.001, std. errors shown). The changes in acyl ghrelin over 24 h in control animals are neither statistically significant (p>0.2), nor reproducible in other experiments. (B) Serum desacyl ghrelin levels for experiment in Fig. 3A. (C) Percent acyl ghrelin for experiment in Fig. 3A. (D) Body weights in wt C57BL6 mice on an MCT diet treated with 11 μmol/kg GO-CoA-Tat (red, n=5) or vehicle (black, n=6) for 1 mo (*p <0.05; conventional ** and *** omitted for clarity, standard errors shown). (E) Fat mass in wt mice measured by QMR for experiment in 3D. (F) Body weights in ghrelin knockout C57BL6 mice on an MCT diet treated with 11 μmol/kg GO-CoA-Tat (red, n=5) or vehicle (black, n=5) for 1 mo (standard errors shown). The larger error bars compared to data in Fig. 2.7D likely represent the broader distribution of starting weights. Also note that the scales differ in the two panels, contributing to the larger error bars seen here. (G) Fat mass in ghrelin knockout mice measured by QMR for experiment in Fig. 3F.

Figure 2.8. Effect of GO-CoA-Tat on lean mass in mice measured by QMR.

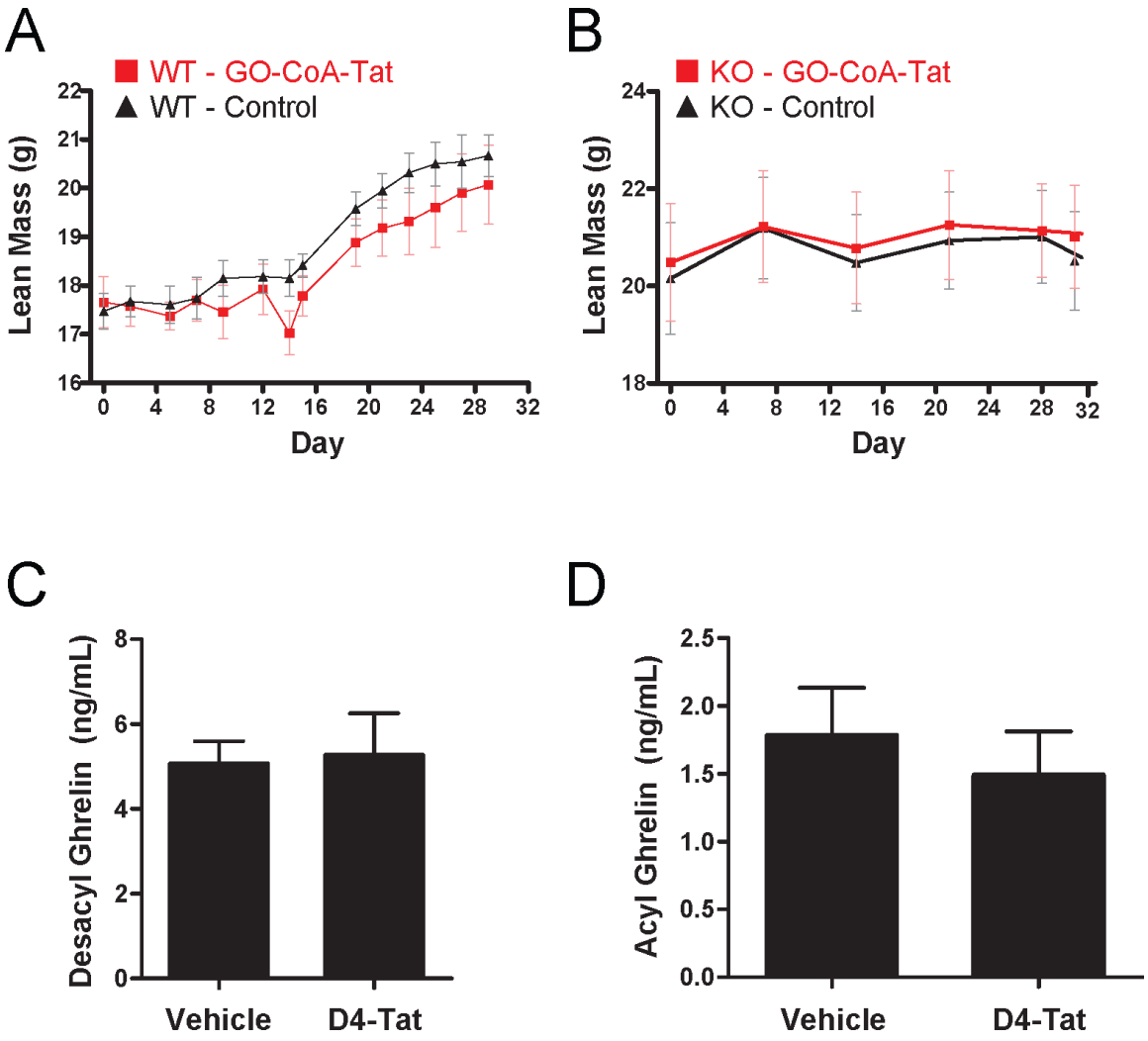

Legend, Figure 2.8. (A) Lean mass in wt mice on an MCT diet treated with GO-CoA-Tat (11 μmol/kg, n=5) or vehicle (n=6). (D) Lean mass in ghrelin knockout mice on an MCT diet treated with GO-CoA-Tat (11 μmol/kg, n=5) or vehicle (n=5). Standard errors shown.

We next examined the effect of GO-CoA-Tat on weight gain. Wt mice were fed an MCT diet over a one month period. These mice were treated every 24 h with GO-CoA-Tat (11 μmol/kg IP) and monitored daily for body mass. In addition, the mice were subjected to quantitative magnetic resonance (QMR) spectroscopy to evaluate the animals' fat and lean mass (Kirchner et al., 2009). These experiments showed that chronic GO-CoA-Tat treatment in mice prevented the significant weight gain observed in vehicle-treated mice on an MCT-rich high fat diet (Figure 2.7D). Moreover, the QMR measurements showed that, relative to controls, the GO-CoA-Tat treated animals displayed significantly lower fat mass, but not lean mass (Figure 2.7E, Figure 2.8A,B)

To investigate the potential for GO-CoA-Tat induced generalized toxicity as a source of weight loss, we assessed the blood chemistries and blood cell counts in the animals after one month of GO-CoA-Tat treatment. These analyses showed no evidence of liver, renal, pancreas, or bone marrow toxicities that could account for weight loss (Figure 2.9). Importantly, GO-CoA-Tat treated mice displayed lower blood glucose as well as lower IGF-1 levels, which is consistent with endogenous acyl ghrelin modulating the somatotropic axis (Figure 2.9).

Figure 2.9. Blood chemistries and cell counts from mice treated with vehicle and GO-CoA-Tat.

A

	Control	GO-CoA-Tat
GLU (mg/dL)	188.40 ± 9.91	117.40 ± 19.78
IGF-1 (ng/mL)	456.00 ± 35.86	317.75 ± 23.72
GH (ng/mL)	29.25 ± 5.01	13.90 ± 2.40
Trig (mg/dL)	45.40 ± 2.92	49.40 ± 5.36
HDL (mg/dL)	35.00 ± 1.88	36.20 ± 3.14
UA (mg/dL)	1.40 ± 0.12	1.20 ± 0.07
CK (U/L)	2467.00 ± 460.12	1719.80 ± 434.47
GGT (U/L)	2.00 ± 0.57	1.00 ± 0.28
ALT (U/L)	78.60 ± 8.18	57.80 ± 13.42
AST (U/L)	343.20 ± 21.93	284.20 ± 56.07
AMYL (U/L)	1382.80 ± 227.12	1108.00 ± 103.13
LDH (U/L)	1048.00 ± 184.09	870.80 ± 215.62
ALP (U/L)	81.80 ± 8.80	84.60 ± 6.23
TBILI (mg/dL)	0.32 ± 0.07	0.16 ± 0.02
TPROT (g/dL)	4.86 ± 0.08	4.48 ± 0.42
CA (mg/dL)	9.02 ± 0.14	7.94 ± 0.73
BUN (mg/dL)	25.40 ± 2.27	24.20 ± 0.87
CREAT (mg/dL)	0.30 ± 0.03	0.28 ± 0.02
ALB (g/dL)	3.08 ± 0.07	3.06 ± 0.07

B

	Control	GO-CoA-Tat
WBC (K/µL)	4.66 ± 0.37	5.36 ± 0.81
NE (K/µL)	2.92 ± 0.28	3.19 ± 0.66
LY (K/µL)	1.43 ± 0.12	1.70 ± 0.20
MO (K/µL)	0.09 ± 0.01	0.18 ± 0.04
EO (K/µL)	0.15 ± 0.02	0.22 ± 0.03
BA (K/µL)	0.07 ± 0.01	0.07 ± 0.01
RBC (M/µL)	8.51 ± 0.15	8.39 ± 0.27
Hb (g/dL)	11.34 ± 0.17	11.16 ± 0.30
HCT (%)	34.24 ± 0.58	33.98 ± 1.17
MCV (fL)	40.28 ± 0.18	40.46 ± 0.21
MCH (pg)	13.34 ± 0.11	13.28 ± 0.10
MCHC (g/dL)	33.10 ± 0.24	32.88 ± 0.29
RDW (%)	17.48 ± 0.16	17.42 ± 0.25
PLT (K/µL)	1071.00 ± 25.92	837.00 ± 77.31
MPV (fL)	5.94 ± 0.05	6.04 ± 0.06
Chol (mg/dL)	97.80 ± 4.94	102.00 ± 3.07

Legend, Figure 2.9. Samples taken from sacrificed mice on an MCT diet for 1 mo. of daily IP GO-CoA-Tat (11 µmol/kg, n=5) or vehicle (n=5) demonstrated a statistically significant decrease in blood glucose and IGF-1 for GO-CoA-Tat mice vs. vehicle treated mice. No other differences were found to be statistically significant between the two groups. Standard errors shown.

Figure 2.10. Effects of GO-CoA-Tat on weight gain and food intake in matched wt vs. ghrelin knockout animals on an MCT diet.

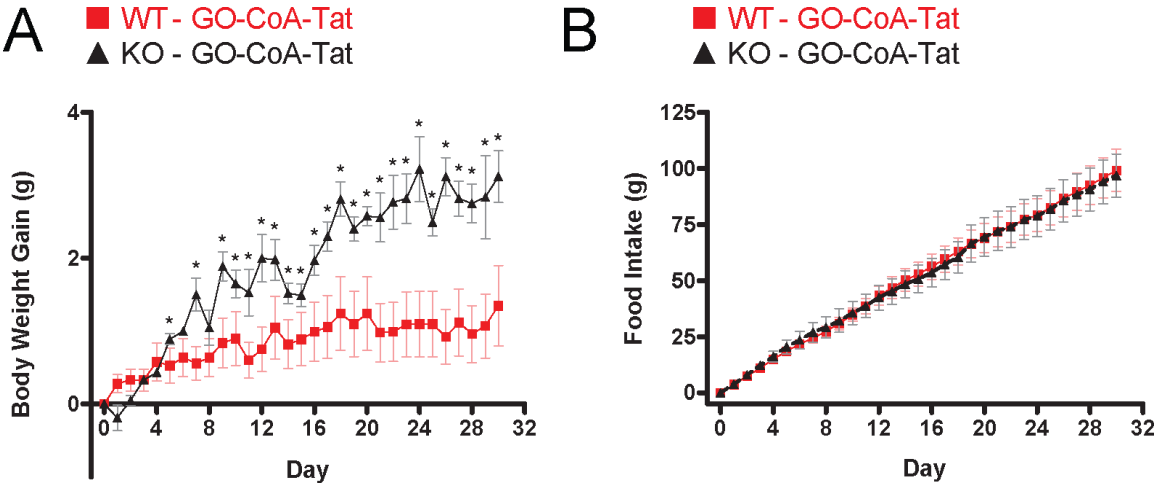

Legend, Figure 2.10. (A) Body weights of wild type mice (n=6) and ghrelin knockout mice (n=4) on an MCT diet since birth after 1 mo. of treatment with GO-CoA-Tat (11 μmol/kg). Other than ghrelin, these animals are genetically matched littermates. Standard errors are shown and * denotes $p<0.05$. The average initial weights of the wt and ghrelin knockout animals are 21.5 g and 19.7 g, respectively. (B) The corresponding food intake for the experiment in Fig. S6A, standard errors shown.

Figure 2.11. Body weight, fat mass, lean mass, and food intake of wt mice on a high fat diet after treatment with GO-CoA-Tat.

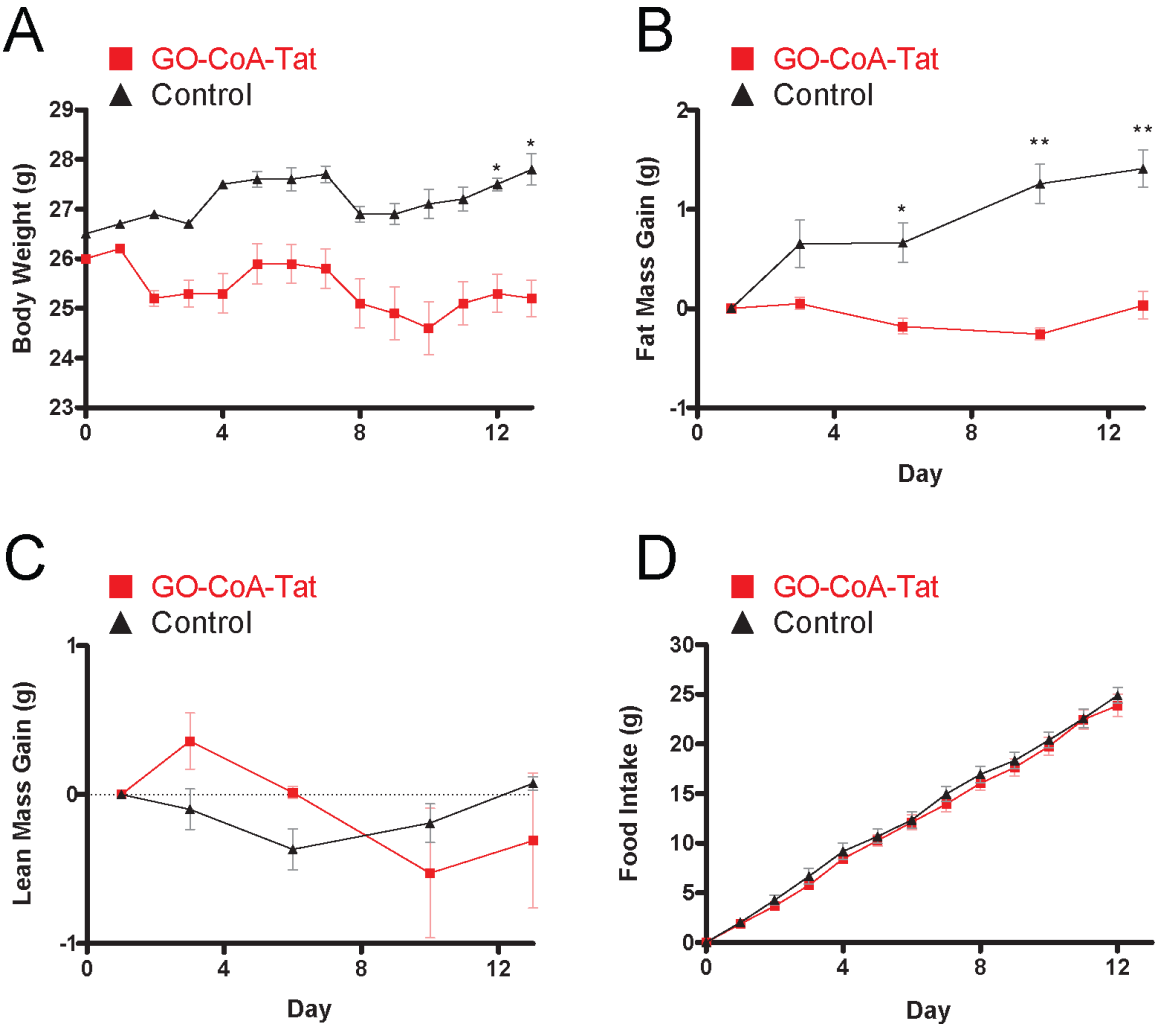

Legend, Figure 2.11. (A) Body weights of mice after treatment with GO-CoA-Tat (Red, 8 μmol/kg, n=3) or D4-Tat (Black, n=3) are shown along with standard errors. (B-D) Fat mass, lean mass, food intake are shown for the experiment in Fig. S7A. Statistically significant points ($p<0.05$) are denoted with *.

Figure 2.12. Effect of GO-CoA-Tat on insulin in human islets.

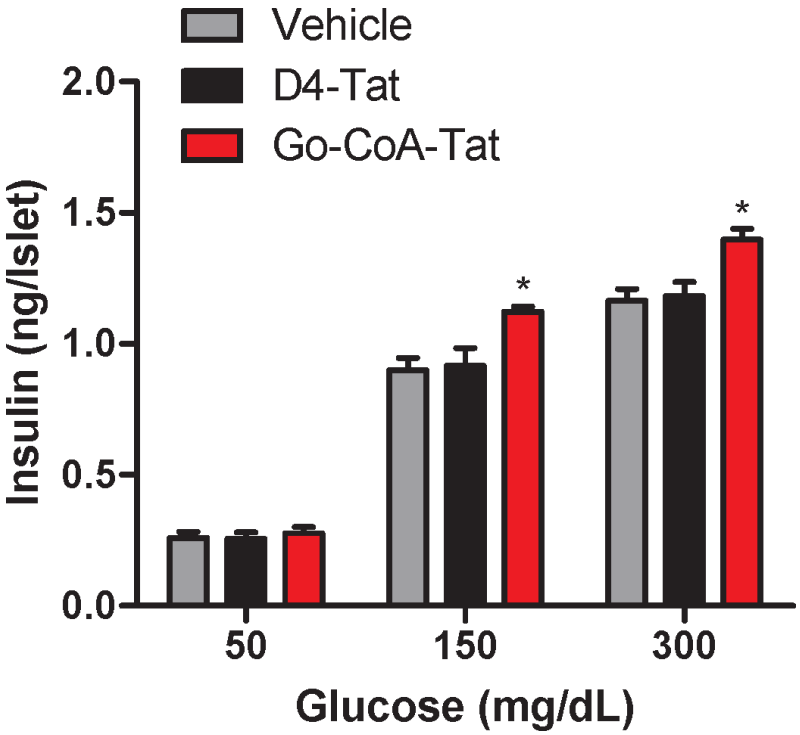

Legend, Figure 2.12. Incubation with 5 μM compound GO-CoA-Tat compared to vehicle or D4-Tat causes a statistically significant increase (*$p<0.05$) in insulin production when human islets are incubated in 150 mg/dl and 300 mg/dl glucose (n=9). Standard errors shown.

Figure 2.13. GO-CoA-Tat increases insulin, decreases glucose levels, and down-regulates islet cell UCP2 mRNA.

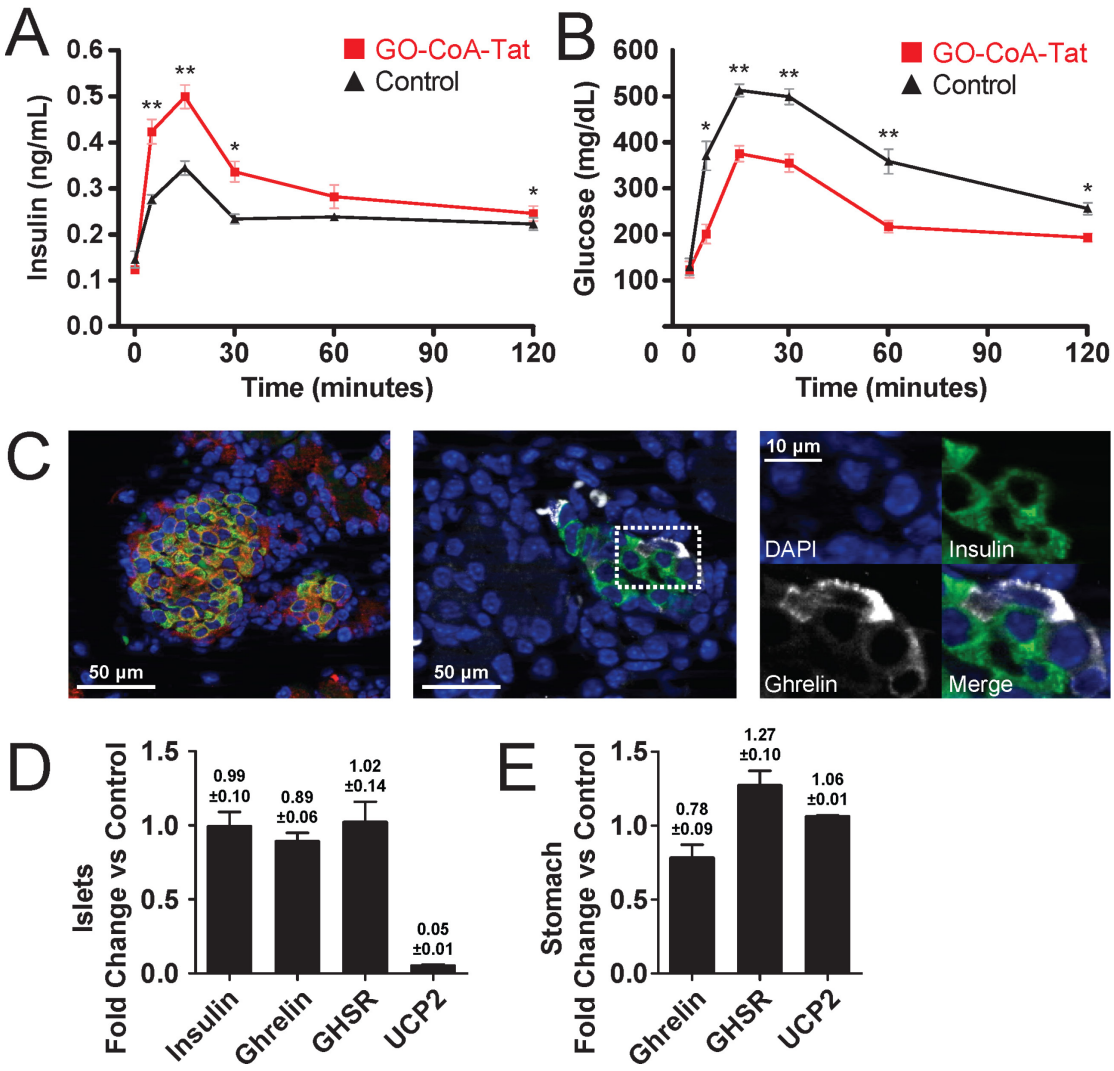

Legend, Figure 2.13. (A) C57BL6 wt mice raised on normal mouse chow and treated with 8 µmol/kg GO-CoA-Tat (n=4) experienced a statistically significant increase in insulin secretion and (B) a statistically significant decrease in blood glucose as compared to control mice (treated with D4-Tat (n=4)) when compound was administered 24 h prior to IP glucose challenge (2.5g/kg) (*p <0.05, **p<0.01, std. errors shown). (C) Immunohistochemical staining of mouse islets. Left panel – insulin (green) ghrelin receptor (GHSR) (red) and cell nuclei stained with DAPI (blue). Middle panel – staining of islet for ghrelin (white) and insulin (green) demonstrates dual staining and ghrelin positive and insulin negative cells. Right panel – close-up of unmerged images in boxed area of middle panel. (D) QRT-PCR of islets and (E) gastric fundus isolated from mice treated with inhibitor 24 h prior to isolation and mRNA expression relative to control (n=3).

Figure 2.14. Intraperitoneal glucose tolerance test in wt and KO animals on an MCT diet.

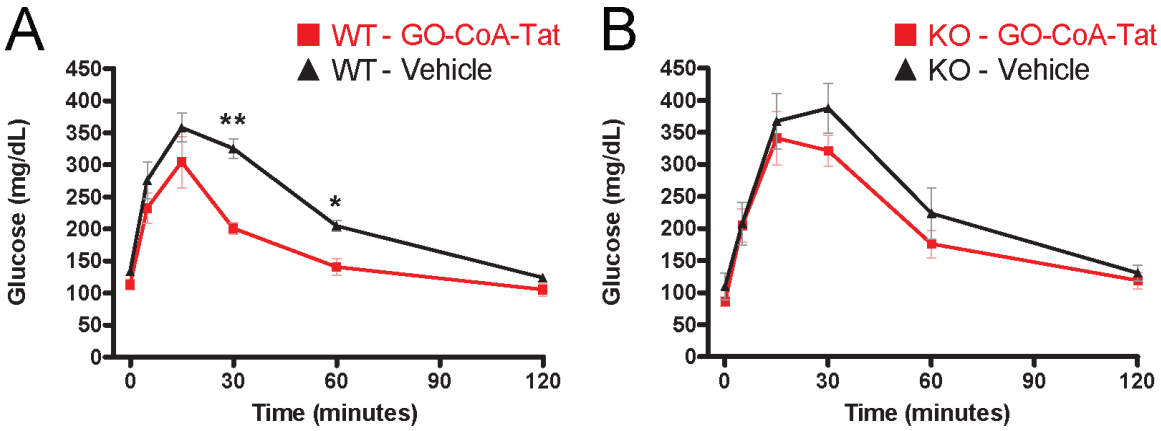

Legend, Figure 2.14. (A) After 6 h pretreatment with GO-CoA-Tat (11 μmol/kg) or vehicle, wt mice (n=5) on an MCT diet were fasted for 18 h and then an IPGTT (2.5 g/kg) performed and glucose values measured as shown. * denotes $p<0.05$. (B) Glucose response to a tolerance test as performed as in Fig. S9A except using similar age ghrelin knockout mice (n=5). Standard errors are shown.

To further understand the effects of GO-CoA-Tat, we studied its effects on body weight and adiposity in ghrelin knockout mice. In contrast to its behavior in wt mice, GO-CoA-Tat did not significantly alter weight, fat, or lean mass in ghrelin knockout mice (Figure 2.7F,G; Figure 2.8B). In a separate long term treatment study, we confirmed that during the course of one month of GO-CoA-Tat administration, ghrelin knockout mice gained more weight than otherwise genetically and age-matched matched wt mice (Figure 2.10A). Since initial body weights in ghrelin knockout mice were reduced compared to wt mice (19.7 g vs. 21.5 g), these data suggest that the GO-CoA-Tat treatment in the wt animals induces functional loss of ghrelin, bringing wt and knockout animals closer together. The food intake in these GO-CoA-Tat-treated wt and ghrelin knockout mice

was similar (Figure 2.10B) suggesting that the weight differences might be caused by differences in metabolic activity as suggested by recent GOAT knockout studies (Kirchner et al., 2009), although we have not directly tested this. Finally, in an additional wt mouse study, we showed that GO-CoA-Tat slowed weight gain in wt mice fed a high fat diet. In that study we observed a relative reduction of fat mass without a change in lean mass, but no effect on food intake (Figure 2.11). Taken together, these studies suggest that GO-CoA-Tat can specifically reduce acyl ghrelin via GOAT inhibition and thereby prevent weight gain in mice.

It has been reported that acyl ghrelin can influence glucose homeostasis and insulin secretion in pancreatic islet cells (Dezaki et al., 2007; Dezaki et al., 2008; Granata et al., 2010; Sun et al., 2006; Yada et al., 2008; Zhao et al., 2010a), although the precise impact has varied among different studies (Gauna et al., 2004; Kirchner et al., 2009; Sun et al., 2006; Tong et al., 2010; Zhao et al., 2010b). We pre-treated human islet cells with GO-CoA-Tat and showed that these cells displayed a statistically significant increase in insulin response to a glucose challenge when exposed to GO-CoA-Tat (Figure 2.12). These results suggest that acyl ghrelin plays a direct role in blunting insulin response, similar to what has recently been reported in humans (Tong et al., 2010). To investigate this in vivo, we studied wt mice that received an intraperitoneal glucose challenge of 2.5 g/kg after pre-treatment with GO-CoA-Tat. These mice show a significant increase in insulin response (Figure 2.13A) that was accompanied by a reduction in blood glucose (Figure 2.13B). We repeated this glucose challenge in ghrelin knockout animals and, under these conditions, GO-CoA-

Tat did not have a significant effect compared either to vehicle or to its impact on wt animals analyzed in parallel (Figure 2.14). These data support the hypothesis that GO-CoA-Tat's effects on glucose regulation are mediated by acyl ghrelin inhibition. It is interesting that glucose tolerance tests in GOAT knockout versus WT mice have shown mixed results (Kirchner et al., 2009; Zhao et al., 2010a) which may suggest that the acute pharmacologic action of acyl ghrelin inhibition is important for the insulin and glucose response observed here.

To further investigate the connection between GOAT inhibition and insulin regulation, we studied pancreatic islets isolated from mice treated with GO-CoA-Tat. As shown in Fig. 4, the insulin-producing ß-cells stained positive for GHSR and islets exhibited a small population of ghrelin expressing cells, which are distinct from ß-cells (Figure 2.13C). QRT-PCR of islets isolated from mice treated with GO-CoA-Tat demonstrated a 20-fold reduction in UCP2 mRNA (encoding uncoupling protein 2, a suppressor of insulin secretion) levels as compared to islets isolated from D4-tat treated mice (Figure 2.13D) but no change in levels of insulin, ghrelin, or GHSR mRNAs. Additionally, QRT-PCR showed non-statistically significant effects on UCP2 in the gastric fundus (Figure 2.13E). Taken together, these data point to a tissue-specific role for GOAT inhibition in suppressing UCP2 levels and enhancing insulin release in response to glucose. That GOAT inhibition modulates UCP2 levels so dramatically further substantiates the connection of acyl ghrelin to obesity and type 2 diabetes (Andrews et al., 2008; Joseph et al., 2002; Zhang et al., 2001).

Directly targeting the biosynthesis of the active acyl ghrelin hormone offers several potential advantages over receptor antagonists. First, these enzyme inhibitors may not need to cross the blood-brain barrier unlike acyl ghrelin receptor blockers, for which many of the key sites of action are in the brain (Broglio et al., 2004; Kojima et al., 1999). Second, receptor antagonists may drive higher acyl ghrelin formation and increase acyl /desacyl ghrelin ratios (Ariyasu et al., 2005; Broglio et al., 2004; Gauna et al., 2004; Zhang et al., 2008) that could be blunted by targeting the biosynthetic pathway. Finally, targeting an enzyme may have advantages over targeting an abundant receptor. Although GOAT inhibitor GO-CoA-Tat has some limitations as a peptide-based agent, we anticipate that future synthetic derivatization will be able to further maximize its pharmacodynamic and/or pharmacokinetic properties. In summary, this report lays the foundation for an approach to pharmacologic management of metabolic disorders through targeted GOAT blockade. We note that this strategy also has potential application to the targeting of other GOAT-related MBOAT (membrane bound O-acyl transferase) family members implicated in lipid metabolism and in important cancer-related signaling pathways such as hedgehog and Wnt (Hofmann, 2000).

Materials and Methods

Chemical Synthesis (Compounds 1-6, D4-Tat, Ghrelin-27-biotin, L5bp, F4bp)

All reagents for chemical synthesis were purchased from Aldrich or Acros Organics. All commercially available reagents were used as purchased without further purification. Preparative HPLC isolation of bisubstrate analog inhibitors, peptides, and control compounds was performed on a reverse-phase C-18 column (25 × 2.14 cm) (Microsorbtm-100, Rainin), eluted with a gradient of water (0.05% TFA) (mobile phase A) and acetonitrile (0.05% TFA) (mobile phase B). Ghrelin-27-biotin (GSSFLSPEHQRVQQRKESKKPPAKLQPK(Biotin)G) and D4-Tat were prepared using the Fmoc strategy. Synthesis of GO-CoA-Tat and related derivatives was analogous to previously described methods (Hines and Cole, 2004; Lau et al., 2000) and began with ghrelin and used the Fmoc strategy. Variable lengths of ghrelin peptide (3 to 10 C-terminal residues) were employed and Ser3 in ghrelin was replaced with Alloc (allyloxycarbonyl) protected-1,2-diaminopropionic acid. GO-CoA-Tat derivatives F4BP and L5BP were synthesized analogously by replacing Phe4 or Leu5, respectively, with benzoylphenylalanine (Bachem) and also contained an epsilon-amino linked biotin at a Lys inserted between Ahx and Tat. Orthogonal deprotection of Alloc using tetrakis (triphenylphosphine) palladium (0) to give the free amino group was carried out followed by reaction with racemic α-bromo octanoic anhydride (octanoic anhydride and bromoacetic anhydride for compounds 2 and 4, respectively). Conjugation with coenzyme A was performed by reacting the α-bromo-amide with CoASH. To a stirred solution of

bromo-amide peptide (concentration 2-10 mM in ddH_2O) was added dropwise a solution of CoASH (2.0–3.0 equivalent) in a 1.0 M aqueous buffer solution of triethylammonium bicarbonate (pH 8.0) at room temperature. After 48-72 h, the mixture was purified by anion exchange to remove excess CoASH and then lyophilized overnight, and the residue was subjected to preparative HPLC to isolate the desired products. The HPLC column was eluted with a gradient of water (0.05% TFA) (mobile phase A) and acetonitrile (0.05% TFA) (mobile phase B) (0 min, 5% B; 5–65 min, linear increase to 60% B; 10 mL/min), and was monitored at 214 nm or 260 nm. The collected fractions were concentrated under reduced pressure and lyophilized to give the final products as white solids. Their MALDI and ES-mass spectrometry data were consistent with the calculated values and the final concentrations of the compounds in aqueous solution for assay were determined by amino acid analysis.

Molecular Cloning of mGOAT cDNA

mGOAT cDNA was cloned by a two-stage nested RT-PCR scheme from mouse stomach. Total RNA was extracted from the proximal half of a mouse stomach (a gift from Kathryn O'Donnell Mendell), using a tissue homogenizer and an RNeasy® Kit (Qiagen). cDNA was prepared by reverse transcription with Invitrogen SuperScript™ II RT. 2 μL of cDNA was amplified with primers TTTACAAGGGCACCGCTTAG / CAAGGCATCTTCTGGCATTT. 1 μL of the reaction mixture was then further amplified with nested primers GCCACCATGGATTGGCTCCAGCTC /

GAGATGAAGGGCAGGGAAA]. A band at ~1.3kB was excised from the gel and ligated into pCR® 2.1-TOPO® (Invitrogen).

GOAT was amplified from this vector using primers designed for 5' blunt ligation and 3' EcoRI cleavage, then cloned into the pαH vector (a gift from Jason McLellan, derived from pHLsec (S3) using KpnI (blunted) and EcoRI. A 3xFlag® tag (Sigma) was added to the C-terminus using QuikChange® mutagenesis (Stratagene), replacing the manufacturer's protocol with the two-stage procedure developed by Wang and Malcolm (Wang and Malcolm, 1999).

Preparing Stably Transfected GOAT/Preproghrelin HeLa and HEK 293T Cells

In order to obtain a consistently high level of coherent expression of human preproghrelin (hPPG) and mouse ghrelin O-acyltransferase (mGOAT) genes, we constructed an expression cassette of hPPG cDNA in conjunction with mGOAT cDNA and an intervening encephalomyocarditis virus internal ribosome entry site (ECMV-IRES) in the pCEP4-puro vector driven by the CMV promoter. Briefly, the mGOAT coding sequence with a synonymous mutation (C165T, and the amino acid residue remains alanine) introduced using Quickchange II Site-directed Mutagenesis (Stratagene) was inserted in an intermediate plasmid (pRS416) together with ECMV-IRES by a three-piece ligation strategy. The IRES-mGOAT fusion gene was subsequently cut from the intermediate plasmid, purified and then inserted into pCEP4 with the hPPG coding sequence between the CMV promoter and the IRES-mGOAT cassette by a second three-

piece ligation. The resultant expression cassette was sequence-verified and the plasmid is referred to as phPPG-mGOAT. For HeLa transfection 3 μL of FuGENE 6 (Roche) was used per 1 μg DNA. For HEK 293T transfection 2 μL Lipofectamine 2000 (Invitrogen) was used per μg DNA. For puromycin selection and maintenance, cells were cultured with 2.5 μg/ml (HeLa) or 1 μg /ml puromycin (HEK 293T).

Cell Culture, Cell Lysate Preparation and Immunoassay Measurements of Acyl and Desacyl Ghrelin

The HeLa and HEK cell populations transfected stably with phPPG-mGOAT were grown in RPMI 1640 medium (Sigma) supplemented with 10% inactivated fetal bovine serum, puromycin (as above), 0.01% octanoic acid, and 4 mM glutamine were routinely passaged twice a week. In some experiments the cells were treated with one of seven compounds to assess inhibition of acyl ghrelin production. Cell lysate was prepared in RIPA buffer as follows. HeLa cells ($2.5x10^7$ cells estimated using an automated counter (Countess, Invitrogen) were harvested by adding trypsin (0.05%, Invitrogen) after a PBS wash. The cells were transferred to 15 mL plastic conical tubes and centrifuged at 800g in a table-top centrifuge for 5 min. The pellet was then washed with PBS and resuspended in 0.6 mL of ice-cold RIPA buffer (Sigma, catalog number R0278) containing 10% (v/v) protease inhibitor cocktail (Sigma, catalog number P8215). The mixture was then vortexed briefly for lysis and the mixture was then centrifuged at 2000g for 20 min (see **Figure 2.15** for protease inhibitor optimization; we use one-fourth of the RIPA/protease cocktail for

measuring desacyl ghrelin compared with acyl ghrelin). The supernatant was then stored at –80°C for further analysis (samples stored in this way were stable for at least several weeks). To assess levels of acyl ghrelin and desacyl ghrelin in cell lysates, samples were analyzed using a commercially available double-antibody sandwich based Enzyme Immunometric Assay (Alpco Diagnostics) using a modified protocol, in which the binding of the samples was done first on the ELISA plate coated with monoclonal antibody specific to the C-terminal part of ghrelin and after washing the plate, the acetylcholinesterase-Fab' conjugate which recognizes the N-terminal part (of acyl or desacyl ghrelin) was added to the wells to form a sandwich. Incubation was carried out for 3 h for each antibody. Standard curves generated with acyl and desacyl ghrelin standards (provided by ALPCO and concentrations confirmed by amino acid analysis) dissolved in the RIPA/protease cocktail buffer were linear in the range up to 250 pg/mL and concentrations as low as 10 pg/mL could reliably be detected. Similar acyl and desacyl ghrelin values were obtained with a Millipore kit measured in the same fashion. In general, acyl and desacyl ghrelin were in the range of 1-10 pg/10^7 cells using this approach.

Figure 2.15. Untransfected HeLa cell lysates spiked with acyl ghrelin.

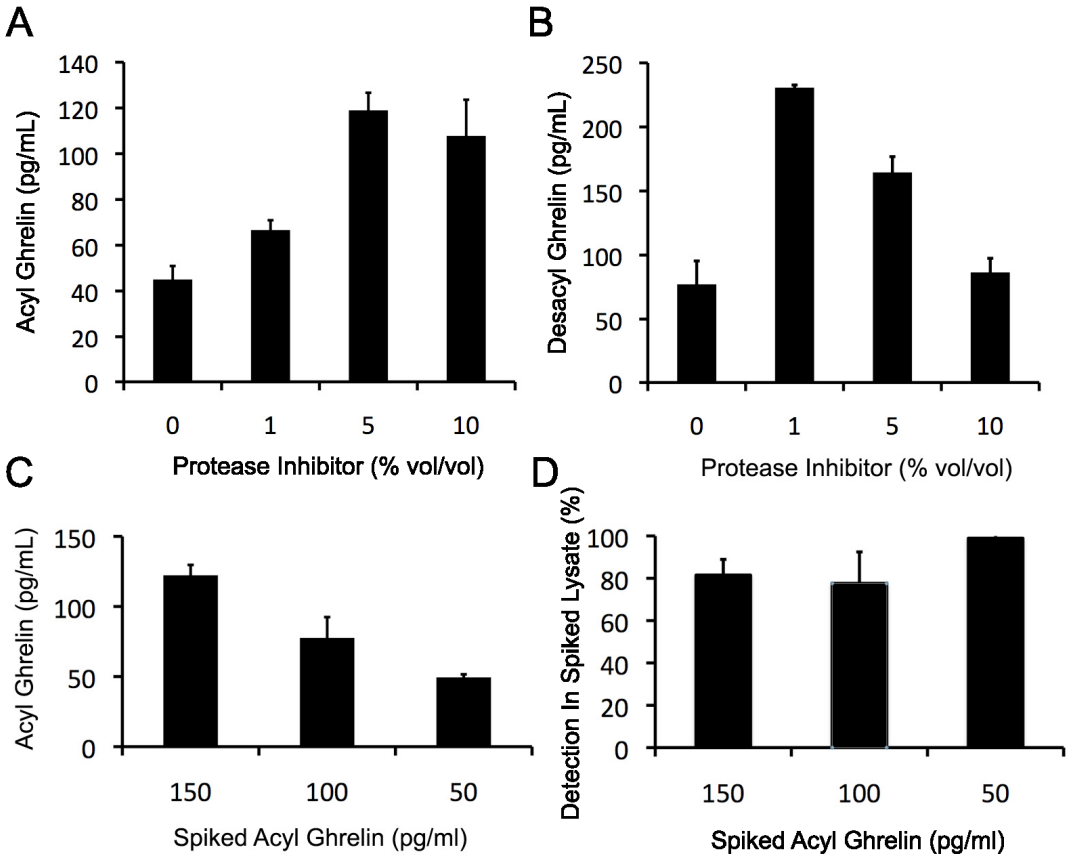

Legend, Figure 2.15. Untransfected HeLa cell lysates spiked with acyl ghrelin (to make 150 pg/mL) (A) or desacyl ghrelin (to make 250 pg/mL) (B). In a RIPA lysate, protease inhibitor concentration ranging from 1% to 10% was added. For (C) and (D) - Acyl Signal spiked into 6.5x106 untransfected HeLa cells in 0.5 mL of RIPA buffer and a 0.2 mL aliquot was added to the plate. Standard errors are shown.

GOAT Transfection and Microsomal Isolation from Mammalian Cells

GnTI-deficient HEK293T cells (S5) were grown in Freestyle 293T media (Invitrogen) supplemented with 2 mM L-glutamine and 1% FBS in an atmosphere containing 8% CO_2. On the day of transfection, 400 mL of cells were set up at a concentration of 2×10^6/mL. Cells were transfected with plasmids using Polyethylenimine

"Max" high potency linear PEI (Polysciences) as described by Aricescu et al. (*S3*). Briefly, 1 μg/ml of DNA was mixed with 3 μg/mL of transfection reagent in unsupplemented Hybridoma SFM medium (Invitrogen) equivalent to 1/20th final culture volume, incubated for 20 min at room temperature, and added to the cells. Cells were harvested for experiments after 4 d and washed once with PBS.

Each pellet of HEK293T GnTI- cells was resuspended in 20 mL Buffer D (50 mM Tris-HCl, pH 7.4, 150 mM NaCl, 1 mM sodium-EGTA, 30 μg/mL Phenyl methyl sulfonyl fluoride, 3 μg/ml Pepstatin A, and a Complete Protease Inhibitor Cocktail Tablet, EDTA-free (Roche, 1 tab/40 mL buffer)). Cells were lysed using a Dounce homogenizer (type B pestle, 30 strokes). Lysates were centrifuged at 2,000g at 4°C for 10 min, and the supernatant was transferred to a new tube and centrifuged again under the same conditions. The supernatant was then centrifuged at 100,000g at 4°C for 30 min and the supernatant discarded. The microsome pellet was resuspended in Tris-buffered saline (TBS) (50 mM Tris HCl, pH 7.4, 150 mM NaCl) and insoluble material was removed by centrifuging at 1,000 × g for 1 min. Aliquots were prepared for immunoblot analysis or flash-frozen in liquid nitrogen and stored at -80°C until the time of assay. Protein concentrations were measured using the BCA assay (Thermo) supplemented with 0.5% Triton X-100.

GOAT Acyltransferase Assay

The assay protocol was modified from Yang et al. (Yang et al., 2008c). The assay mixture contained 50 mM HEPES, pH 7.0, 1 μM octanoyl-CoA (33 dpm/fMol, American

Radiolabeled Chemicals), 10 μM Ghrelin27-Biotin, 50 μg microsome protein, and 50 μM palmitoyl CoA (Avanti Polar Lipids). Reactions were initiated by the addition of membrane protein and incubated at 37°C for 5 min. Where indicated, GO-CoA-Tat was pre-incubated for 5 min with the membrane protein. Reactions were quenched by the addition of 850 μL of quench buffer (TBS + 2% (w/v) SDS) pre-mixed with 150 μL Streptavidin Plus UltraLink Resin (Pierce) and incubated for 15 min on a rotating mixer. This mixture was transferred to a Poly-Prep® chromatography column (Bio-Rad) and washed with 30 mL wash buffer (TBS + 0.1% SDS). The mixture was transferred to a 1.5 mL microcentrifuge tube containing 1ml quench buffer, boiled at 98°C for 5 min, and subjected to scintillation counting.

Baculoviral Infection and Insect Cell Culture for Microsomal GOAT preparation

For baculoviral expression (Yang et al., 2008b), mGOAT containing a C-terminal 3xFlag tag was subcloned into pFastBac1 (Invitrogen) from pαH using EcoRI and HindIII, and high titer baculovirus was generated according to the manufacturer's instructions. 3 L of SF9 cells in a sparged culture flask were infected at a density of 2-4x10^6 cells/mL, harvested 48 h later, and washed once with PBS; GOAT recovery was found to be linear with cell density in this range. GOAT-containing microsomes were prepared as in Yang et al. (Yang et al., 2008b) with modification. Briefly, cells were resuspended in ice cold buffer D (see mammalian cell protocol), then lysed in a 40mL Dounce homogenizer using 40 strokes of the loose pestle. The lysate was centrifuged at 4,000g for 10min and then the

supernatant was transferred to a new tube and centrifuged again. This supernatant was further centrifuged at 100,000g for 30 min and the membrane fraction was resuspended in HEPES buffered saline (50mM HEPES pH 7.0, 150mM NaCl) using a Dounce homogenizer. Protein concentration was measured as described above, then microsomes were aliquoted, flash-frozen in liquid nitrogen, and stored at -80˚C until the time use.

Photo-crosslinking and FLAG affinity purification

GOAT-3xFlag Membrane aliquots from insect cells were thawed and diluted with an equal volume buffer E (HBS supplemented with 2.5 μg/ml aprotinin, 5 μg/mL pepstatin A, 5 μg/ml leupeptin, and 1 mM EGTA), then passed 10 times through a 25 gauge needle to homogenize the mixture. Each 300 μL photoassay mixture contained 4.0 mg/mL total protein and 5 μM photo-crosslinking compound with or without 100 μM GO-CoA-Tat added as a competitor. Assay mixes were pre-incubated on ice for 1h then cross-linked for 30 min in a stirred, water-cooled quartz cuvette using a UV lamp with 360 nm filter. Samples were then diluted to 1.5 mg/mL, solubilized overnight (~10 h) with buffer E supplemented with 1% Fos-Choline 16 (Anatrace), and clarified by centrifugation for 30 min at 100,000g. EZview Red ANTI-FLAG M2 Affinity Gel was pre-equilibrated according to the manufacturer's instructions and 30 μL resin was then added to each solubilized sample and allowed to bind overnight (~20 h). Flow-through was then removed by centrifugation and the resin was transferred to filter columns (Pierce) and washed 3 times with 500 μL Buffer E supplemented with 0.1% Fos-Choline 16. GOAT-3xFlag was

then eluted overnight using 60 μL Buffer E supplemented with 1mg/ml 3xFlag peptide (Sigma) and 0.1% Fos-Choline 16 and subjected to immunoblot analysis. Biotinylation was detected using streptavidin (Pierce) followed by polyclonal anti-streptavidin (Abcam) and exposed for 3 s.

Cell Viability Assay

The viability of the HepG2 cell line treated with varying concentrations of GO-CoA-Tat was determined using a LIVE/DEAD viability assay kit (Molecular Probes). Cells were incubated with two probes, 2 μM calcein-AM (green color) for 30 min and 4 μM ethidium homodimer-1 (EtdD-1, bright red color) for 10 min, for intracellular esterase activity and plasma membrane integrity, respectively. Calcein-AM was excited using the 500 nm laser line, and the emitted fluorescence was detected through a 535 nm long-pass filter. EtdD-1 was excited using the 514 nm laser line, and the emitted fluorescence was detected through a 550 nm long-pass filter. Red fluorescent (EtdD-1) cells were counted as dead, and green fluorescent (Calcein-AM) were counted as viable. In cases of dual partial red and green staining, cells were counted as dead. HeLa cell viability was determined using automated trypan blue exclusion with standard protocol on a Countess automated cell counter (Invitrogen).

Human Islet Experiments

Fresh human cadaveric islets were provided by the National Islet Cell Resource Center. Average purity and viability were 70% and 85%, respectively. For human islet experiments, islets were incubated in serum-free RPMI media with 5 μM GO-CoA-Tat for 24 h prior to a static incubation assay for 30 min in glucose free RPMI media with 50, 150 and 300 mg/dl glucose added and the insulin secreted into the medium was assessed by ELISA (Alpco Diagnostics).

Acetyltransferase Assays

The specificity of GO-CoA-Tat with the acetyltransferases p300, PCAF, and AANAT was measured using an α-ketoglutarate dehydrogenase (α–KGDH) coupled spectrophotometric assay (Szewczuk et al., 2007). Recombinant acetyltransferase domains and histone tail peptides were prepared as described previously (De Angelis et al., 1998; Thompson et al., 2004; Zheng et al., 2005). The production of CoASH by the acetyltransferase is coupled to the formation of NADH, which is monitored at 340 nm (ε_{340} = 6230 M^{-1} cm^{-1}) in a Beckman DU-640 spectrophotometer. All reactions contain 200 μM thiamine pyrophosphate, 5 mM $MgCl_2$, 1 mM DTT, 50 μg/mL BSA, 200 μM NAD, 2.4 mM α-ketoglutarate, 10 μM GO-CoA-Tat, and 50 μM acetyl-CoA. Reactions with p300 were performed in 100 mM HEPES, pH 7.9, and contained 0.1 units α–KGDH and 200 μM H4-15, a 15-mer peptide substrate based on the sequence of the histone H4 tail. p300 reactions were incubated at 30°C prior to initiation with addition of 100 nM p300 and take

place at 30°C. Reactions with PCAF were performed in 100 mM HEPES, pH 7.9, and contained 0.037 units α–KGDH and 100 μM H3-20, a 20-mer peptide substrate based on the sequence of the histone H3 tail. PCAF reactions were incubated at 30°C for 10 minutes prior to initiation with addition of 100 nM PCAF and took place at 30°C. Reactions with AANAT were performed in 100 mM NH_4OAc, pH 6.8, and contained 0.1 units α–KGDH and 200 μM tryptamine. AANAT reactions were incubated at 25°C for 10 minutes prior to initiation with addition of 10.83 nM AANAT and took place at 25°C. All reactions were followed over the linear portion of the progress curve, providing the initial velocity *via* linear regression.

Murine Experiments

All mice were treated ethically and followed protocols approved at Johns Hopkins University and the University of Cincinnati. C57BL/6J wt and ghrelin knockout male mice used in these experiments were greater than 8 weeks old and maintained on normal chow (Teklad 5.7% fat LM-485), medium chain triglyceride (MCT, 10% MCT, 40% sucrose, Teklad TD08622), or high fat diet (Bioserve 35.5% fat, 36.3% carbohydrate, F1850) as indicated at least one week prior to each experiment. In studies where food intake was monitored, animals were age-matched and maintained in individual cages. GO-CoA-Tat or control treatments (vehicle, D4-Tat) were performed no more than once daily intraperitoneally. For glucose tolerance tests, compound was administered to non-fasted, age-matched mice 6 hours prior to an 18 h fast upon which time a 2.5 g/kg intraperitoneal

glucose tolerance test (IP-GTT) was performed on conscious mice. Blood was sampled from the tail vein at 0, 15, 30, 60 and 120 min post IP-GTT. Glucose was measured with a glucometer (LifeScan OneTouch) and insulin values were assessed by ELISA (Alpco Diagnostics). Lean and fat mass was assessed with QNMR every three days (EchoMRI). For each body measurement, the average of three separate scans was obtained and body weights are shown as three day rolling averages throughout. Blood chemistries and cell counts were measured at the Johns Hopkins phenotyping core and IGF1 and growth hormone were measured by ELISA assay.

Blood Collection for Acyl and Desacyl Ghrelin Measurements

Blood samples (ca. 0.5 mL) from age-matched mice (>16 week old male mice) were obtained by transcardial puncture and were transferred immediately (within 1 min) into tubes with the same volume of buffer containing 50 mM EDTA, 4 mM p-hydroxymercuribenzoic acid (PHMB) and 1 M NaCl and kept on ice. Collections were staggered to match controls with treated samples. Within 30 min, samples were centrifuged at 3000 × g for 10 min at +4˚C and then supernatants were transferred into separate tubes and immediately treated with 100 µl of 1N HCl per mL of blood plasma and then tubes were centrifuged at 3000 × g for 5 min at +4˚C. Supernatants were transferred to cryovials and stored at -80°C. Acyl and desacyl ghrelin levels were measured using the sandwich ELISA kit from ALPCO with a 3 h incubation protocol. Similar values were obtained with a Millipore kit measured in the same fashion.

QRT-PCR

Islets were isolated as described in Song et al. (Song et al., 2008) after collagenase and DNase I digestion of the pancreas. Total RNA was extracted using Trizol. RT-PCR was performed using the one-tube RT-PCR Sybr green mix (BioRad) according to standard protocols. Fold changes in expression levels were calculated using the DDCT method. Duplicate results were analyzed using Student's t-Test.

Table 2.1. Primers used for QRT-PCR.

Insulin Fw	CGAGGCTTCTTCTACACACC	Insulin Rv	GAGGGAGCAGATGCTGGT
Glucagon Fw	CACTCACAGGGCACATTCA	Glucagon Rv	GTCCCTGGTGGCAAGATTGT
GHSR Fw	ACCTGCTCTGCAAACTCTTCCAGT	GHSR Rv	CAAACACCACCACAGCAAGCATCT
Ghrelin Fw	ACTCAGCATGCTCTGGATGGACA	Ghrelin Rv	ATGCCAACATCGAAGGGAGCATTG
UCP2-001 Fw	TGGTTGGTTTCAAGGCCACAGATG	UCP2-001 Rv	TCTCGTGCAATGGTCTTGTAGGCT
36B4 Fw	TGTTTGACAACGGCAGCATTT	36B4 Rv	CCGAGGCAACAGTTGGGTA

Immunohistochemistry

Mouse pancreas or human islets were fixed in 10% formalin or Bouin's solution, paraffin embedded and sectioned. After dewaxing, rehydration, and antigen retrieval in citrate buffer (pH 6.0), immunostaining was performed with guinea-pig anti-insulin (Linco) , rabbit anti-ghrelin (Abcam) and chicken anti-GHSR (Chemicon). Appropriate fluorescence tagged antibodies (Jackson immunoresearch) were used for antigen localization. Nuclei were counterstained using DAPI (Vector). A Zeiss Axioskop equipped with a CCD digital camera and an Apotome optical sectioning device connected to a digital image processor for pseudocoloring were used for image preparation. Images shown are 400x magnification.

CHAPTER 3 - ARCHITECTURAL ORGANIZATION OF THE METABOLIC REGULATORY ENZYME GHRELIN-O-ACYLTRANSFERASE

This chapter is reproduced from (Taylor et al., 2013), with permission.

Summary

Ghrelin O-AcylTransferase (GOAT) is a polytopic integral membrane protein required for activation of ghrelin, a secreted metabolism-regulating peptide hormone. Although GOAT is a potential therapeutic target for the treatment of obesity and diabetes and plays a key role in other physiologic processes, little is known about its structure or mechanism. GOAT is a member of the Membrane Bound O-AcylTransferase (MBOAT) family, a group of polytopic integral membrane proteins involved in lipid-biosynthetic and lipid-signaling reactions from prokaryotes to humans. Here, we use phylogeny and a variety of bioinformatic tools to predict the topology of GOAT. Using selective permeabilization indirect immunofluorescence microscopy in combination with glycosylation-shift immunoblotting, we demonstrate that GOAT contains 11 transmembrane helices and one reentrant loop. Development of the V5Glyc tag, a novel, small, and sensitive dual topology reporter, facilitated these experiments. The MBOAT family invariant residue His338 is in the ER lumen, consistent with other family members, but conserved Asn307 is cytosolic,

making it unlikely that both are involved in catalysis. Photocrosslinking of synthetic ghrelin analogs and inhibitors demonstrates binding to the C-terminal region of GOAT, consistent with a role of His338 in the active site. This knowledge of GOAT architecture is important for a deeper understanding of the mechanism of GOAT and other MBOATs and could ultimately enhance the discovery of selective inhibitors for these enzymes.

Introduction

GOAT is a polytopic integral membrane protein required for the octanoylation of ghrelin, a weight- and glucose-modulating peptide hormone produced primarily in the stomach, upper GI tract, and brains of vertebrates (Gutierrez et al., 2008; Kojima et al., 1999; Yang et al., 2008a). Octanoylation is required for activation of the ghrelin receptor, GHSR-1a, and is the only known example of protein octanoylation in higher organisms (Ozawa et al., 2009). Because dietary fats and those from local fatty acid metabolism can be directly conjugated to ghrelin (Kirchner et al., 2009; Lopez et al., 2008; Nishi et al., 2005), it can be viewed as a "fat sensor" from the brain to the body or within the brain itself, modulating energy balance. Supporting this, inhibition of GOAT in mice prevented weight gain on a high fat diet and improved glucose control (Barnett et al., 2010) and may represent an attractive target for the treatment of obesity and diabetes. Additionally, ghrelin has been implicated in a host of other physiologic processes, including gastric motility (Trudel et al., 2002), learning, memory, and reward behavior (Carlini et al., 2002; Diano et al., 2006; Egecioglu et al., 2010), cardiovascular function (Baldanzi et al., 2002; Okumura

et al., 2002; Schwenke et al., 2008), and survival in extreme starvation(Goldstein et al., 2011; Li et al., 2012; Yi et al., 2012).

GOAT is a member of the MBOAT superfamily (Membrane Bound O-AcylTransferase) (Hofmann, 2000), which is composed of many multispanning membrane proteins from prokaryotes and eukaryotes, including 11 in humans. MBOAT members have been shown to be critical for lipid biosynthesis, sterol acylation, and acyl modification of secreted proteins including ghrelin, Hedgehog (HHAT), Wnt proteins (PORC), and yeast GPI-anchored proteins (GUP1) (Bosson et al., 2006; Chen et al., 2004b; Hardy and Resh, 2012; Petrova et al., 2013; Resh, 2012; Takada et al., 2006). MBOAT proteins contain a highly conserved asparagine (N307 in GOAT) and an invariant histidine (H338 in GOAT) separated by 30-45 residues; these residues have been proposed to be catalytic. There are two additional regions of conservation in the family, at the N- and C-terminal boundaries of loop 5 on GOAT, where it adjoins surrounding hydrophobic regions. The topology of a few MBOATs has been analyzed, and the invariant histidine has been shown to be lumenal in these cases (Guo et al., 2005a; Pagac et al., 2011). Based on the modification of lumenal, secreted proteins and on lumenal location of the conserved histidine, the active site for the MBOAT family has been proposed to be conserved on the lumenal face (Pagac et al., 2011; Yang et al., 2008a).

For several MBOATs including GOAT, mutation of this conserved histidine eliminates acyl transfer activity (Bosson et al., 2006; Guo et al., 2005b; Lee et al., 2008; Lin et al., 2003; McFie et al., 2010; Yang et al., 2008a). Detailed studies of catalysis by these

purified enzymes is generally hindered by the challenge of solubilization in active conformations (Tamaki et al., 2007; Taylor et al., 2012b; Yang et al., 2008b); notable exceptions to this are ACAT1, also known as SOAT1, a robust enzyme that transfers long chain fats from Coenzyme A (CoA) to cholesterol and has been extensively characterized (reviewed in (Chang et al., 2009)), and HHAT, which N-palmitoylates hedgehog proteins (Buglino and Resh, 2008). In contrast to other MBOAT members, for HHAT, some catalytic activity was retained upon alanine mutation of the conserved histidine (Buglino and Resh, 2010). Thus, assignment of this histidine as catalytic is not yet definitive.

GOAT octanoylates serine-3 of proghrelin in the ER lumen after signal peptide cleavage. A range of fatty acids can be processed by GOAT, and the most likely acyl donors are acyl-CoAs (reviewed in (Taylor et al., 2012b)). Because fatty acyl-CoAs are known to be cytosolic, for example those produced during fatty acid β-oxidation, the ER membrane represents a barrier that these acyl-CoAs must cross. In this regard, GOAT has been postulated to be a possible acyl-CoA transporter (Yang et al., 2008a). Determination of the topology of GOAT is a critical step to defining its detailed structure and mechanisms. GOAT has been proposed to contain 8 transmembrane helices (TMs)(Yang et al., 2008a), but this has not been experimentally investigated.

In this study, we examine GOAT topology in detail, first computationally and then experimentally. Our data suggest that GOAT contains 11 TMs and segregate the invariant H338 and conserved N307 to opposite sides of the ER membrane. Photocrosslinking

binding studies map binding of acyl ghrelin analogs to the C-terminal region of GOAT and demonstrate that purified GOAT can bind ligand as a monomer.

Materials and Methods

All reagents were purchased at the highest quality available from Sigma-Aldrich or Acros Organics unless otherwise indicated. Commercially available reagents were used without further purification.

Cell Culture

HeLa cells were maintained in DMEM (Invitrogen) with 10% heat-inactivated FBS and Penicillin-Streptomycin. Transfections were done using Fugene 6 or Fugene HD (Promega) according to the manufacturer's instructions, with 2 μg GOAT DNA and 6 μl reagent per 35 mm dish or 6-well plate well. SF9 cells were maintained in ISFM media, an affordable serum-free synthetic medium, made as reported in (Inlow et al., 1989), with minor modification (in preparation).

Cloning

For human-cell expression, GOAT-3xFlag was cloned into the CAG vector as described previously (Barnett et al., 2010) with a modified multiple-cloning site. N- and C-terminal tags were placed immediately before the first or after the last residue of GOAT

without any extraneous sequence by incorporating tag sequences into oligonucleotide primers. Internally V5-tagged GOAT clones were prepared using fusion PCR (Yon and Fried, 1989). Individual point mutants were made using a modified QuikChange protocol (Stratagene). Asn-free and Lys-free GOAT were made in one round of polymerization using MISO mutagenesis, as described in Figure 2a of a previous study (Mitchell et al., 2013) as were V5Glyc clones. N-terminal deletion ΔN-H1 starts with a Met at residue 32. ΔN-H1-2, ΔN-H1-3, and ΔN-H1-3 constructs start with Met56 and ATG codons substituted at positions 81 and 109, respectively, to define the first residue of the constructs. ΔC-H10-11 and ΔC-H11 are truncated after residues 357 and 399, respectively. N-IBV-1-GOAT and N-IBV-2-GOAT are GOAT-3xFlag with an N-terminal fusion of the first 20 and 10 residues, respectively, of the M glycoprotein from infectious bronchitis virus (IBV, an avian coronavirus). Asn3 and Asn6 of this sequence are glycosylated in IBV-M, previously called the E1 protein (Swift and Machamer, 1991). All clones were fully sequence verified. Baculovirus constructs were made using the Bac2Bac system (Life Technologies, Carlsbad CA) according to the manufacturer's instructions.

Selective Permeabilization Immunofluorescence

200,000 HeLa cells were plated on glass coverslips, transfected 8-16 hours after plating, and incubated for 40 hours. For complete permeabilization, cells were fixed in 3% paraformaldehyde for 10 min, and fixative was then quenched using PBS containing 10 mM glycine and 0.2% Na-Azide (PBS/gly). Cells were incubated for 3 min in 0.5% Triton

X-100 in PBS/gly and then washed twice with PBS/gly. For selective permeabilization, dishes were placed on ice, washed with ice cold KHM (20 mM HEPES pH 7.4, 110 mM potassium acetate, 2 mM magnesium acetate), and kept on ice. The cells were permeabilized with 75 μg/ml digitonin (EMD Biosciences) in KHM for 10 min. Cells were washed twice with ice cold KHM, moved to room temperature, and fixed as above.

Staining with primary and secondary antibodies was carried out for 20 min at room temperature by inverting coverslips onto Parafilm containing 45 μl drops of PBS/gly supplemented with 1% BSA and appropriate antibodies. Antibodies used were Mouse anti-Flag M2 (1:500, Sigma), Rabbit anti-Flag (1:1000, Sigma F7425), Mouse anti-V5 (1:5000, Invitrogen), mouse anti-Myc 9E10 (1 μg/ml), rabbit anti-GFP (1:500, Molecular Probes), mouse anti-GFP (1:500, Roche 11814460001), rabbit anti-SSR1 (2 μg/ml Sigma HPA011276, recognizes residues 230-286). Coverslips were washed and incubated analogously with secondary antibodies: Alexa Fluor® 488 conjugated anti-mouse IgG (1:1000) and Alexa Fluor 568 conjugated anti-rabbit IgG (1:1000). As controls, untransfected cells were stained identically and primary antibodies were omitted. DNA was stained prior to imaging with Hoechst 33285 (0.1 μg/ml, 5 min) and coverslips were mounted using glycerol with 100 mM N-propyl gallate. Epifluorescent images were collected at room temperature using an Axioscop microscope with 63x and 40x objectives (Zeiss, Jena, Germany) equipped for epifluorescence using an ORCA-03G CCD camera (Hamamatsu, Japan) and iVision software (BioVision). For equal comparison of staining between permeabilizations, within each construct, for each antibody, an optimal exposure

time was first determined and then this fixed exposure time was used for both permeabilizations. Signal intensity was then assigned based on the optimal V5 exposure times as follows: ++++, <30 ms; +++, 30-60 ms, ++; 60-150 ms; +, 150-500 ms exposure; –, not clearly above background. Image layouts were done in Adobe Photoshop CS6 and Illustrator CS6.

For co-localization of GOAT with CFP-KDEL, coverslips were treated as above except that fixation was in methanol for 20 min at -20°C. Confocal images were acquired with a Cascade QuantEM 512SC camera (Photometrics) attached to a Zeiss AxioImager (63x objective) with a Yokogawa spinning disk confocal scanner and Slidebook software (Intelligent Imaging Innovations).

Synthesis

Peptide synthesis was performed using the Fmoc strategy. GO-CoA-Tat, GO-Tat, and GO-CoA-Tat F4BP were prepared as previously described (8). In brief, amide-linked ghrelin analogs Ser3 in ghrelin replaced with Alloc (allyloxycarbonyl) protected-1,2-diaminopropionic acid, orthogonally deprotected using palladium catalysis, and then reacted with octanoic acid in the presence of HATU (1-[Bis-(dimethylamino)methyliumyl]-1H-1,2,3-triazolo[4,5-b]pyridine-3-oxide hexafluorophosphate), reacted with octanoic anhydride, or reacted with derivatives thereof. For Ghrelin28-Oct-Diazirine, 7,7'-Diazo octanoic acid was used at this step. This was prepared by using the method described in the literature (Church and Weiss, 1970), and its structure and purity confirmed by 1H NMR. Synthesized peptides were purified using a

reversed-phase C-18 column, and their MALDI and ES mass spectrometry data were consistent with the calculated values. The final concentrations of the compounds in aqueous solution for assay were determined by amino acid analysis. Ghrelin sequences synthesized correspond to human ghrelin (GSSFLSPEHQRVQQRKESKKPPAKLQPKR).

Bioinformatics

GOAT sequences were identified using BLASTp. Annotation of chicken GOAT was corrected to include the first exon. Dog and green anole (*anolis carolinensis*) GOAT sequences were identified by megaBLAST and tBLASTx searches from their draft genomes and annotated. Sequences were aligned using MUSCLE (Edgar, 2004). Conserved domains and residues were identified using CDD (Marchler-Bauer et al., 2013), querying mouse GOAT against MBOAT pfam03062 (Hofmann, 2000). A battery of topology prediction servers were queried with GOAT sequences from various organisms, starting with mouse and human sequences. A multiple sequence alignment was submitted wherever possible. Older methods such as TMHMM 2.0 (Krogh et al., 2001), TMpred (Hofmann, 2000), SOSUI (Hirokawa et al., 1998), TopPred (Claros and von Heijne, 1994), and MEMSAT 3 (Jones, 2007) gave very different results from species-to-species, even between the highly conserved human and mouse GOATs; the range was from 4-11 TMs. The consensus prediction servers TOPCONS (Bernsel et al., 2009) and ConPred II (Arai et al., 2004) both run a number of algorithms including the above, in order to make better predictions. However, for GOAT, the results from both servers were similarly inconsistent

between species and thus hard to interpret. HMMtop (Tusnady and Simon, 2001) and PolyPhobius (Kall et al., 2007) can use a multiple sequence alignment as input. While this improved the results somewhat as compared to the aforementioned algorithms, these algorithms predict only 7 and 8 TMs, respectively. Both missed TMs predicted by MemBrain and MEMSAT-SVM that were subsequently validated experimentally. MemBrain and MEMSAT-SVM predictions were used as a basis for our study and are discussed in Results. For MemBrain, predictions for each organism were overlaid on the multiple species alignment and TM propensity plots were overlaid and aligned.

GOAT Purification

Mouse GOAT with C-terminal TEV-3xFlag tag was expressed in SF9 cells at 3-6×106/ml in 1-6 L aerated spinner flasks using 72 h baculoviral infection with MOI ~10. Cells were harvested and all subsequent steps carried out on ice or at 4˚C. Lysis was performed using a microfluidizer in 4 packed cell volumes of HBS+PI (50 mM HEPES pH 7.0, 150 mM NaCl, 2 μg/ml aprotinin, 2.5 μg/ml leupeptin, 2 μg/ml pepstatin A, and 1 mM EDTA). Lysate was cleared for 10 min at 15,000×g and then microsomes were collected at 120,000×g for 2-6 h, flash frozen on liquid nitrogen, and stored at -80˚C. Microsomes were resuspended in 10-volumes HBS+PI in a 40 ml Dounce homogenizer, solubilized for 1 hr at 4˚C with 1% Fos-Choline 16 (FC-16, Anatrace), and cleared for 30 min at 100,000×g. Supernatant was bound to pre-equilibrated flag agarose in batch for 1-3 h and then transferred to a column, washed with HBS+PI + 0.05% FC-16 and with the

same buffer containing 500 mM NaCl, then washed with HBS without protease inhibitors and cleaved overnight with His6-TEV protease in 10 mM HEPES pH 8.0, 100 mM NaCl, 0.005% FC-16, 2 mM DTT. Supernatant was collected, 20 mM imidazole added, and then His6-TEV protease removed using Ni-affinity. Sample was then further purified by ion exchange chromatography (HiTrap SP FF, GE), eluted in the same buffer containing 300 mM NaCl without imidazole, and concentrated to 2-10 mg/ml.

MALDI-TOF Mass Spectrometry

MALDI-TOF mass spectrometry of intact GOAT was performed by Tatiana Boronina in the Johns Hopkins Proteomics Core Facility using a Voyager DE STR (Applied Biosystems). 3 μg purified, tag-cleaved mouse GOAT was desalted using PLRP-S 300A/10-15 μm material (Polymer Labs / Agilent) packed in a pipet tip pre-equilibrated with 12% acetonitrile and 0.1% TFA, washed 3 times in the same buffer, and eluted with 90% acetonitrile / 0.1% TFA. 2 pMol GOAT was spotted in a sinapinic acid matrix (Laser BioLabs, France) in either 50% ethanol/0.1% TFA or 40% acetonitrile/0.1% TFA. Calibration was with AB SCIEX C3 standards (5-17 kDa) in adjacent spots under identical conditions.

Analytical Ultracentrifugation

Sedimentation velocity analytical ultracentrifugation (SV-AUC) was done on a Beckman XL-I at 10°C with an An-60Ti rotor at 40,000 RPM with total run time 12.5 h.

Purified tag-cleaved GOAT samples in a buffer containing 10 mM HEPES pH 7.0, 300 mM NaCl, and 0.0008% FC-16 were diluted to 0.8, 0.3, and 0.1 A280, corresponding to 6.8, 2.6, and 0.9 μM. Data shown (see below) are from the highest concentration; results from other cells were similar. Analysis was performed as described in Results.

Competition Photocrosslinking

Each 200 μL reaction mixture in HBS+PI+0.005% FC-16 contained 0.2-2.0 μM purified GOAT and 1 μM photocrosslinking compound with or without 200 μM competitor. Competitors were pre-incubated for 1 h and photocrosslinkers for 15 min at 4°C. Reactions were crosslinked with a UV lamp with 360 nm filter in a stirred quartz cuvette, water-cooled to 4°C using a circulating bath. GO-CoA-Tat F4BP was exposed for 10 min, Ghrelin28-Oct-F4BP for 2 min, and Ghrelin28-Oct-Diazirine for 15 min. Samples were then analyzed on SDS-PAGE, blotted for biotin (as above) and stained with colloidal Coomassie brilliant blue (CBB, Invitrogen) as a loading control.

Microsomal GOAT Octanoyltransfer Assay

SF9 microsomes containing GOAT-3xFlag and control microsomes from empty vector SF9 cells were prepared as above except that lysis was using a Dounce homogenizer. Assays were carried out as described in (Yang et al., 2008b) and (Taylor et al., 2012b), with modification. 25 μg of SF9 microsomes (BCA) in 50 μl HBS (pH 7.0), were incubated at 30°C for 5 min with 10 μM C-terminally biotin-tagged human ghrelin (Ghrelin27-Biotin),

60 μM palmitoyl CoA, and 1 μM 3H-octanoyl-CoA (high specific activity, American Radiolabeled Chemicals). Reactions were quenched and solubilized by adding 1 ml 2% SDS in TBS containing streptavidin beads, and bound for >15 min. Beads were washed with 25 ml TBS + 0.1% SDS on small columns and then scintillation counted.

Microsomal Photocrosslinking and Partial Proteolysis

Each 1200 μl crosslinking reaction contained 5 μM GO-CoA-Tat F4BP, and 5 mg total microsome protein from either GOAT-3xFlag containing microsomes or control microsomes, which were made using empty-virus infected SF9 cells. Reactions were carried out as described (Barnett et al., 2010), solubilized by diluting to 1.5 mg/ml with 1% FC-16 for 30 min at 4˚C, and then cleared for 30 min at 100,000×g. 0.4-40 μg sequencing grade modified trypsin (Promega) or buffer was added to each sample and incubated for 15 min at 37˚C. Protease was quenched with 20 μg/ml aprotinin and 20 μg/ml leupeptin and samples were bound to pre-equilibrated anti-Flag agarose (Sigma) overnight. Beads were washed 3 times with HBS+PI with 0.1% FC-16 and eluted with 1 mg/ml 3xFlag peptide (Sigma) in the same buffer then separated with SDS-PAGE. Biotin detection was using streptavidin (Pierce) followed by polyclonal anti-streptavidin (Abcam).

Results

Bioinformatic Predictions of GOAT Topology

To predict GOAT's membrane topology, we started with the assumption that topology should be conserved across species. Sixteen GOAT sequences were identified and, in the cases of dog, green anole, and chicken, annotated. A battery of web-based topology prediction servers were then tested, but most individual algorithms and consensus prediction servers gave very different results from species-to-species, even between the highly conserved human and mouse GOATs; the range was from 4-11 TMs (See *Materials and Methods*).

In contrast, two more recently developed programs, MemBrain (Shen and Chou, 2008) and MEMSAT-SVM (Nugent and Jones, 2012), stood out in their consistency of results across species. MemBrain and MEMSAT-SVM incorporate newer machine-learning algorithms, phylogeny and PSI-BLAST strategies, and current knowledge about membrane protein structure such as short and very long helices (<16 or >40 residues) and reentrant loops (also referred to as half-TMs or half-helices). Results from both programs were nearly identical, including predicted helical boundaries, except where described below. MemBrain-predicted TMs for each species are highlighted in Figure 3.1, with a total of 12 candidate TMs identified in consensus. For clarity, we numbered TMs and loops in accordance with our final model. Corresponding TM propensities for each species are overlaid in **Figure 3.2**A. Some species are predicted individually to be 11 or 13 TMs. Note that TMs 1,5, 8, and 9 were predicted to be either a TM or a reentrant loop, depending on

species. TM-7 is predicted to be one long TM by MemBrain in 13/16 species, but in dog, horse, and green anole it predicts this region as one TM and one reentrant loop.

Figure 3.1. Bioinformatic analysis of GOAT sequences identifies 12 candidate transmembrane helices (TMs).

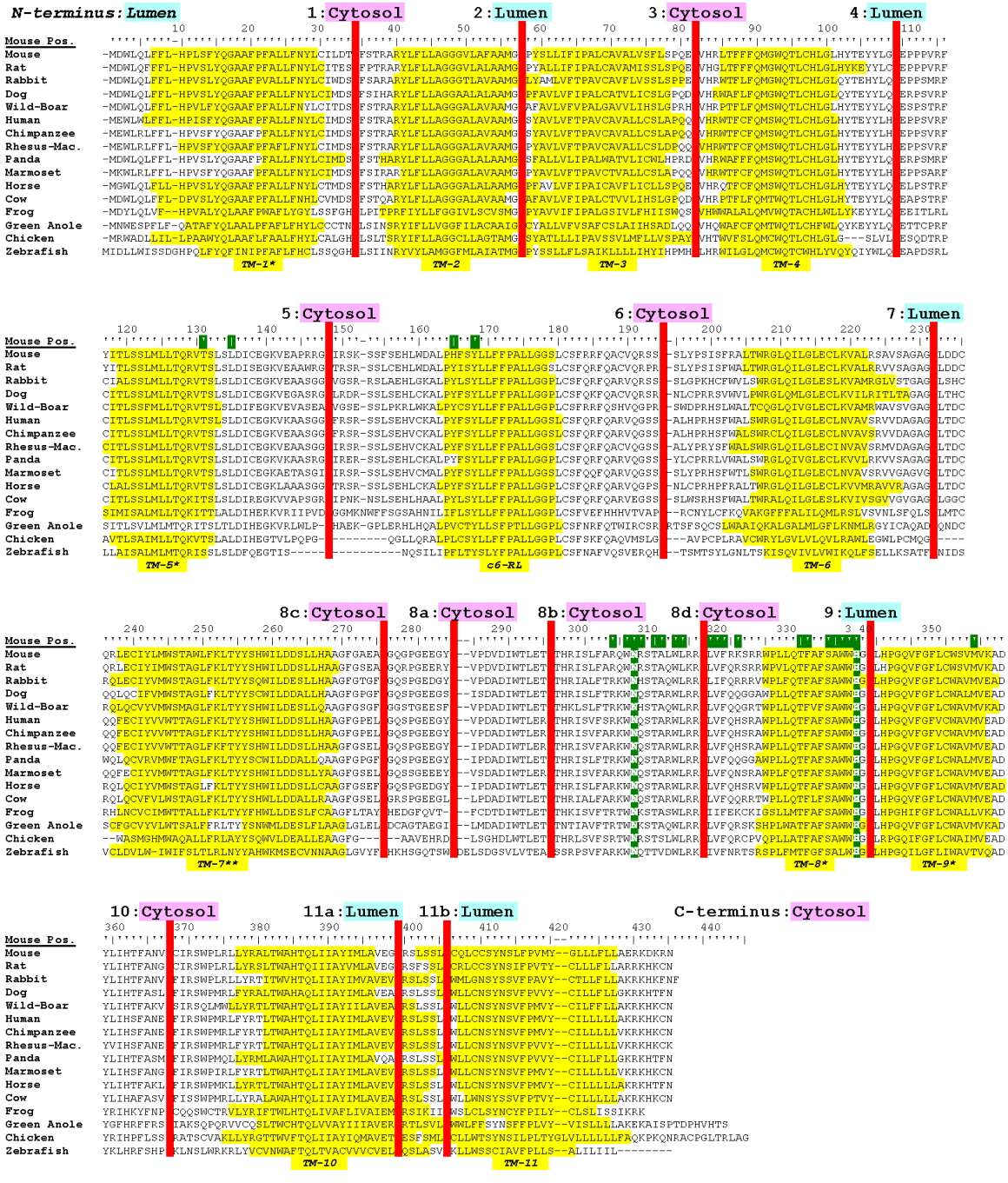

Legend, Figure 3.1. GOAT Multiple Sequence Alignment across 16 species with MemBrain-predicted candidate TMs highlighted in yellow; for clarity, TMs and loops are numbered in accordance with our final model. * Predicted to be either a full-length TM or a reentrant loop. ** TM-7 was predicted to be either one long TM or a reentrant loop plus one standard-length TM. c6-RL, candidate 6 reentrant loop, this region was found to be non-transmembrane, likely a reentrant loop. Highly conserved N307 and invariant H338 residues are highlighted in green; in every case H338 is predicted to be part of TM-9 (green + yellow highlight). Additional highly conserved MBOAT residues (NCBI Conserved Domain Database pfam03062, 1.5 bits (39)) are highlighted in green in the upper bar. Positions selected for epitope tag insertion are shown as red bars, and their localizations experimentally determined in this work are listed above. GOAT protein sequences were aligned using MUSCLE (38). Dog and Green Anole sequences were identified and annotated from their genomes; Chicken annotation was corrected to include the first exon (contains TMs 1 and 2).

Figure 3.2. Comparison of new vs. prior GOAT topology models.

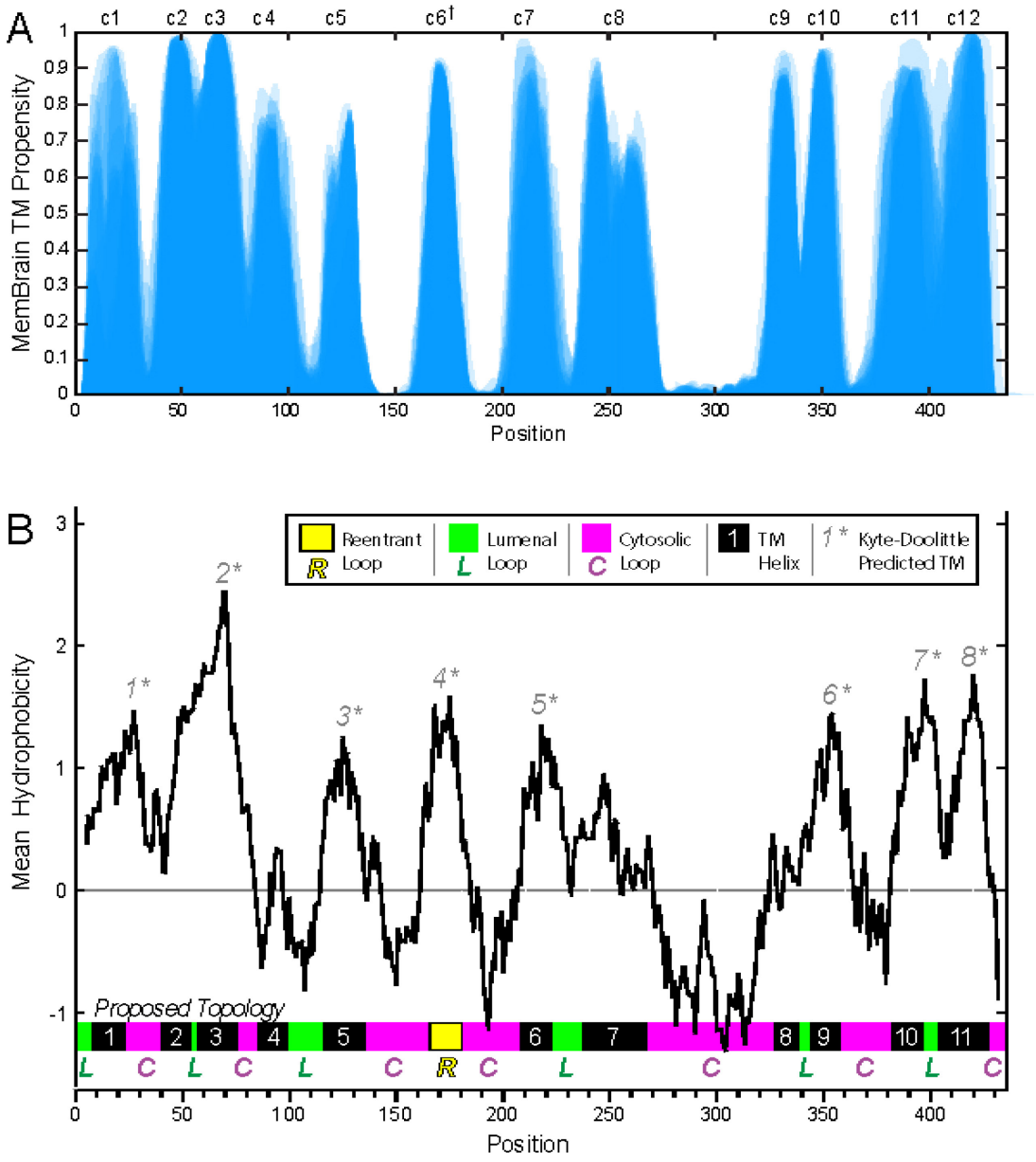

Legend, Figure 3.2. (A) Aligned overlay of MemBrain helical propensities by position for 16-species GOATs. Darker color indicates a more consistent prediction. Candidate TMs are labeled c1-c12 above the figure. † Candidate TM-6 was found to be non-TM. (B) Kyte & Doolittle mean hydrophobicity profile for mouse GOAT, with 18-residue scan window. *, TMs predicted by this method are shown above the hydrophobic peaks. Our proposed topology of GOAT is shown in the thick bar at the bottom of the graph, with TMs in black, lumenal loops in green, cytosolic loops in pink, and a possible reentrant loop in yellow.

TM-8 and TM-9 are predicted to be two separate TMs by MemBrain in 14/16 species, with the 2-3 residue turn between the TMs containing MBOAT invariant H338 at the border of TM-9. Our data (below) suggest this prediction is correct. In contrast, MemBrain predicts one long TM in this region for Rabbit and Zebrafish. MEMSAT-SVM predicts this region as one long TM in all cases. No signal peptide is predicted for GOAT by MemBrain, MEMSAT-SVM, PolyPhobius, or SignalP (Petersen et al., 2011). MemBrain does not predict orientation for helices, but MEMSAT-SVM predicts that GOAT's N-terminus is lumenal and its C-terminus is cytosolic.

We compared the new computational results to those obtained using a Kyte & Doolittle scanning hydropathy window (**Figure 3.2**B). As previously reported (Yang et al., 2008a), this method predicts 8 TMs. In comparison, the consensus MemBrain results predict 12 TMs (**Figure 3.2**A and inset bar **Figure 3.2**B).

Topology determination using selective permeabilization

To experimentally determine the topology of GOAT, we first verified its predicted localization to the ER by co-transfection with CFP-KDEL, an ER marker containing a strong, cleaved signal peptide and the KDEL retention sequence. Upon expression, GOAT-3xFlag and CFP-KDEL colocalize (Figure 3.3A).

To test the topology predictions, we designed GOAT constructs containing N-terminal and C-terminal tags. In addition GOAT constructs were generated with internal epitope tags inserted in the loops between candidate TMs, aligning to gaps where possible

(red bars, Figure 3.1). Because the boundary between TMs-10 and 11 was not clearly defined across species, we created two positions, 11a and 11b. Position 8b was added later due to masking of V5 epitopes installed at 8a (see below), and positions 8c and 8d were added with V5Glyc tags (below). We next screened Flag, 3xFlag, and V5 tags for compatibility with proper translation of GOAT's N-terminus, which contains a non-cleaved internal signal sequence (validated below). The V5 tag was selected for testing because its net charge is neutral. Staining of an N-V5 tag was indistinguishable from C-terminal 3xFlag tagged GOAT, but N-Flag and N-3xFlag tags resulted in poor expression and aggregated protein (not shown).

Mouse GOAT clones were then made with various internal and terminal epitope tags. The V5-tag was installed at the N- and C-termini and at all internal positions except 8c and 8d (red bars, Figure 3.1). To ensure that the internal tag did not perturb overall topology, "flipping" the C-terminus to the opposite side of the membrane, all clones maintain a constant C-terminal 3xFlag tag (except when C-terminally V5 or 3xMyc tagged as noted). We then investigated the topology of these clones using indirect immunofluorescence with selective permeabilization of the plasma membrane. Parallel wells were transfected with constructs of interest, and either fully permeabilized with Triton X-100 (TX) or selectively permeabilized at the plasma membrane with digitonin (Dig, Figure 3.3B). To verify the success of the permeabilization, in each experiment we employed control proteins of known localization in parallel: transfected lumenal CFP-KDEL and endogenous SSR1, an ER transmembrane protein with a cytosolic epitope. Both proteins

were detected with Triton X-100 permeabilization, but only the cytosolic SSR1 epitope was detected with digitonin permeabilization.

Figure 3.3. Mapping GOAT's topology by selective permeabilization of the plasma membrane and indirect immunofluorescence.

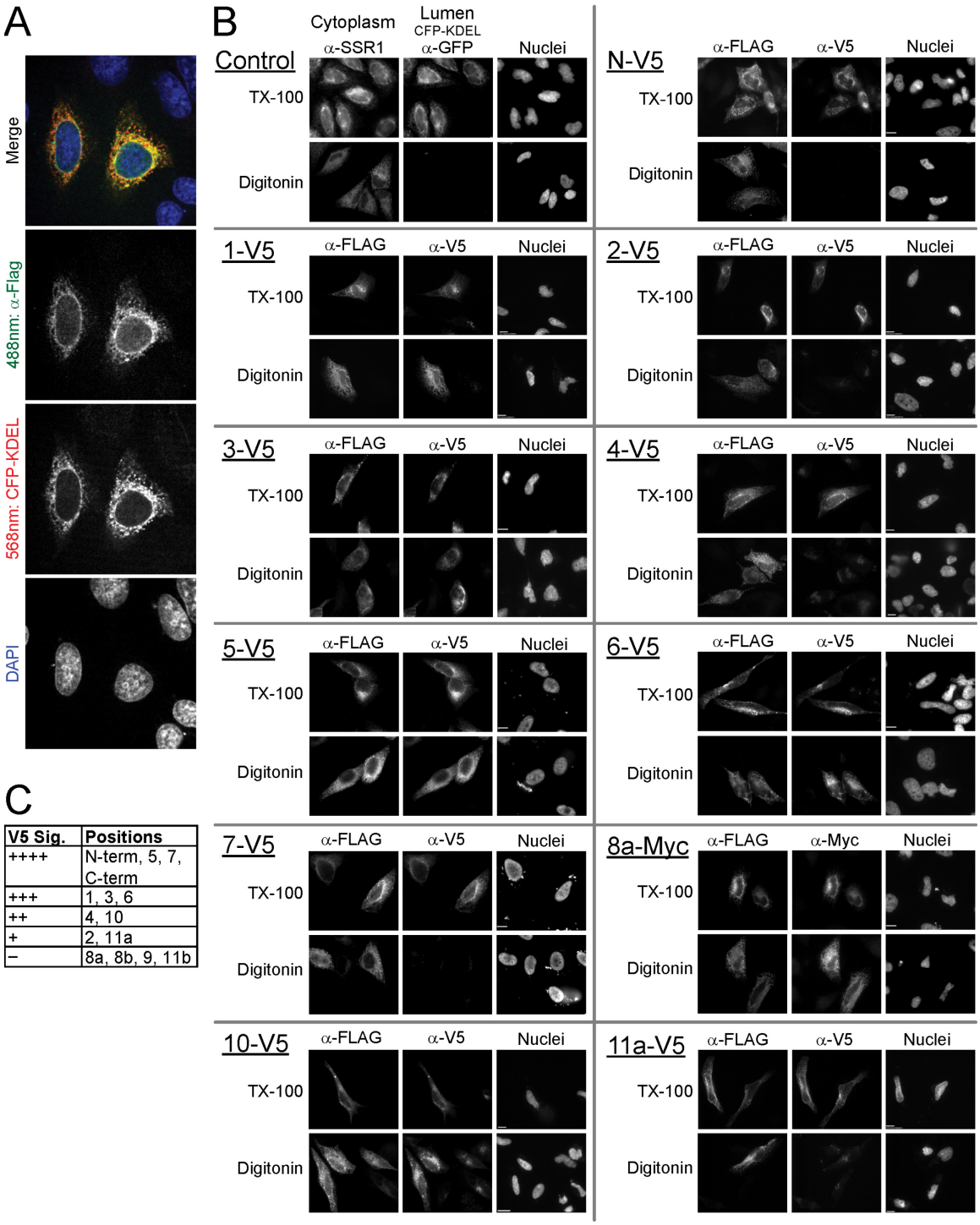

C

V5 Sig.	Positions
++++	N-term, 5, 7, C-term
+++	1, 3, 6
++	4, 10
+	2, 11a
–	8a, 8b, 9, 11b

Legend, Figure 3.3. (A) Mouse GOAT bearing a C-terminal 3xFlag tag is localized to the ER in HeLa cells, as seen by co-localization with co-transfected CFP-KDEL, an ER marker; images are a confocal projection. (B) Selective permeabilization experiments mapping the position of internal V5 epitopes. Two dishes of HeLa cells were transfected with a GOAT cDNA bearing an internal V5 or Myc epitope tag; all constructs have a C-terminal 3xFlag tag as an internal control. Selective permeabilization with digitonin revealed cytosolic but not lumenal epitopes, whereas full permeabilization with Triton X-100 (TX-100) revealed all accessible epitopes. Lumenal epitopes were thus visible with TX-100 only. As a control, two dishes were stained for proteins with known cytosolic and lumenal epitopes and permeabilized identically; in this case we used endogenous SSR1 (cytosolic) and transfected CFP-KDEL (lumenal). Identical exposures and image normalization for both permeabilizations ensure fair side-by-side comparison. (C) V5 Signal strength in indirect immunofluorescence of V5-Tagged constructs from Figure 3.3B and Figure 3.4D, see *Materials and Methods*.

Figure 3.4. Selected human GOAT constructs recapitulate mouse GOAT results and one construct retains enzymatic activity.

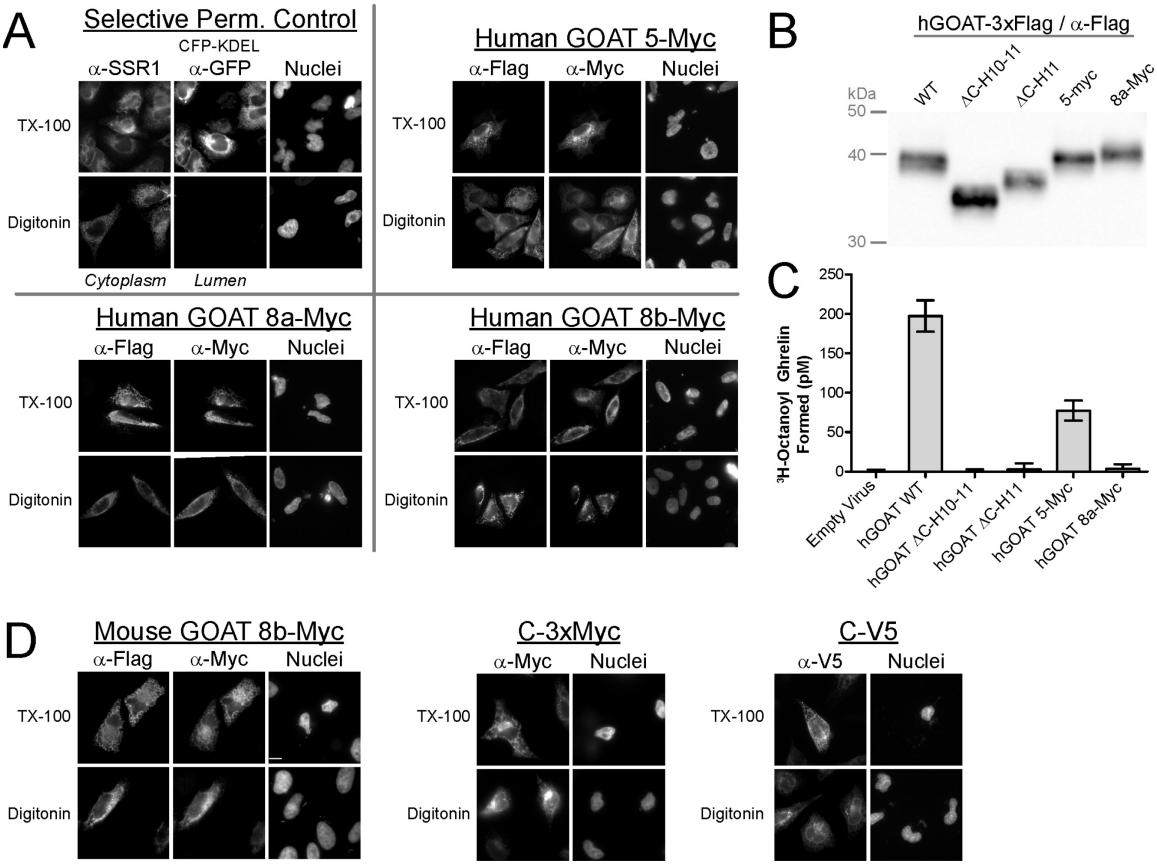

Legend, Figure 3.4. (A) Selective permeabilization of human GOAT constructs bearing the indicated internal Myc epitope tag with constant C-terminal 3xFlag tags. (B) Anti-Flag immunoblot of human GOAT constructs in SF9 cell microsomes. ΔC-H10-11 construct lacks C-terminal helices 10 and 11, ΔC-H11 lacks C-terminal helix 11. (C) Activity assay of constructs in (b). ^{3}H-octanoyl-CoA (2,2',3,3') and C-terminally biotinylated human ghrelin were added to 25 μg total microsome protein in a 50 μl reaction for 10 minutes at 30°C, and then ghrelin was immobilized on streptavidin-linked polyacrylamide beads, washed, and scintillation counted. Each bar represents an average of duplicates and standard deviations are shown. (D) Selective permeabilization of Mouse GOAT with three different C-terminal epitope tags and an additional internal Myc tag. Construct with Myc tag at position 8b also has a C-terminal 3xFlag tag.

GOAT's C-terminus was consistently localized in the cytosol in all constructs, with the 3xFlag tag readily detectable (Figure 3.3B). Ability to detect the V5 tag varied from construct to construct (relative signal strength is shown in Figure 3.3C), but overall the technique was successful and allowed determination of topology at most positions. Notably, N- and C-termini were found to be on opposite sides of the membrane, requiring an odd number of TMs. Both positions 5 and 6 were found to be cytosolic, suggesting that the strongly predicted, hydrophobic c6 does not cross the membrane. We suggest that this segment represents a reentrant loop.

The C-terminal part of the protein was more challenging, with the V5 tag undetectable at positions 8a, 8b, 9, or 11b. This was likely due to masking of the epitope rather than an expression problem, since the internally-tagged proteins were expressed well as revealed by C-terminal 3xFlag staining (not shown). We therefore installed Myc tags in these positions, as well as in positions 2, 4, 10, and 11a. The Myc tag was strongly detected at positions 8a and 8b, with clear cytosolic localization (Figure 3.3B, Figure 3.4D). Note that this localizes the conserved MBOAT fingerprint residue N307 to the cytosol. Neither V5 nor Myc tag was visible at position 9 or 11b; the proteins were expressed as seen by 3xFlag staining, but these epitopes may have been masked in the context of the short loops. Myc tags at positions 2, 4, and 11a all gave results consistent with V5 tags at these positions, but with a less robust signal to noise ratio. Myc signal from position 10 was not detectable.

To confirm the cytosolic localizations of positions 5 and 8, we made parallel constructs in human GOAT, repeated the selective permeabilizations (Figure 3.4A), and

expressed them in SF9 cells for activity assays (Figure 3.4B and C). We also made two C-terminal deletion mutants, ΔC-H11 and ΔC-H10-11, predicted to lack the final and final two TMs, respectively; all SF9 constructs have C-terminal Tev-3xFlag-His tags. The 5-Myc construct showed GOAT activity within 3-fold of the untagged version, suggesting that the 5-Myc epitope tag was tolerated. In contrast, ΔC-H10-11 and ΔC-H11 as well as the 8a-Myc insertion showed no detectable GOAT enzyme activity, suggesting that these alterations might significantly perturb active site structure.

To reduce the possibility that the 3xFlag tag caused artifactual cytosolic localization of GOAT's C-terminus, we replaced the 3xFlag tag in mouse GOAT with V5 or 3xMyc tags and repeated the selective permeabilization (Figure 3.4D). These epitopes were all found to be cytosolic.

To summarize the results thus far, selective permeabilization with insertion of single epitope tags demonstrated that GOAT has an odd number of TMs, confirmed the existence of 9 out of 12 predicted TMs, and suggested that one TM domain was a reentrant loop. However, using this method, we were unable to conclusively determine the topology around position 9 or the location of the conserved His338.

The V5Glyc tag, a novel, sensitive dual-purpose topology reporter

To investigate the topology model for GOAT using a complementary approach and to probe the architecture around His338, we developed the V5Glyc tag, a novel, small dual topology reporter (DTR) allowing sensitive readout of topology by both glycosylation gel-

shift western blotting and selective permeabilization immunofluorescence microscopy. The design principles are diagrammed in Figure 3.5. We wanted to leverage the fact that N-linked glycosylation only occurs in the ER lumen. However, glycosylation is context-sensitive, requiring both appropriate sequence context for recognition by oligosaccharyltransferase (OST) and a distance from the membrane of ~12-14 amino acids (30~40Å), corresponding to the distance of the OST active site from the membrane (Nilsson and von Heijne, 1993). This is typically achieved by fusing a complete, folded protein (or domain) to the membrane protein of interest, often with a C-terminal truncation. For example, in yeast the SUC2-HIS4C DTR, installed as a C-terminal fusion with truncation, has been used extensively to map topology of a number of proteins including other MBOATs. This DTR is reliable when used under particular conditions, and has provided much insight, but can be problematic when positioned too close to the membrane (Deshaies and Schekman, 1987; Kreft et al., 2006; Pagac et al., 2011; Sengstag, 2000). Additionally, this DTR is a very large modification of ~130 kDa, much larger than the proteins of interest here, and is inconvenient to clone in-frame without using yeast homologous recombination. Fusion of the SUC2-HIS4C to C-termini (without truncation) has been shown to cause incorrect C-terminal localization in some cases (Kim et al., 2006; Kim et al., 2003). Mapping internal sites by C-terminally truncating a membrane protein, as the tag is typically used, is likely to be of low reliability for a number of reasons. C-terminal truncations alone may result in major structural perturbations, resulting in the incorrect topology determination in the MBOATs ACAT1 and ACAT2

(Chang et al., 2009). Moreover, a very large protein insertion can further perturb the overall topology. In addition, the large size of the DTR combined with truncations of various lengths makes it challenging to verify that the fusion proteins are full-length.

We hypothesized that a much smaller, flexible hairpin-like DTR consisting of two V5 epitope tags flanking a strong consensus glycosylation site could provide a consistent context for OST, increase sensitivity for immunostaining and immunoblotting, and minimize epitope masking while minimizing protein perturbation by retaining a short sequence. It could also be readily installed in-frame in the context of a full-length protein of interest.

To create a strong consensus glycosylation site, we queried the NetNGlyc server, a neural network based N-glycosylation prediction tool (Gupta et al., 2004), with candidate synthetic V5Glyc sequences in the centers of lumenal loops 2 and 4 on GOAT. We started with NXS and NXT motifs, and found that NXS was at best weakly predicted to be glycosylated (38-53% confidence), but NXT was stronger, with NVT optimal but still only with 62% confidence (7/9 "jury" agreeing). We iteratively tested a series of additional residues on either side, resulting in the sequence GYLNVTYV as a strong prediction (83% and 85% confidence when the sequence was installed in GOAT in positions 2 and 4, respectively, with 9/9 "jury" agreeing). The resulting V5Glyc tag is 36 amino acids long and its complete sequence is GKPIPNPLLGLDST-GYLNVTYV-GKPIPNPLLGLDST.

Figure 3.5. The V5Glyc tag is a novel dual-purpose topology reporter.

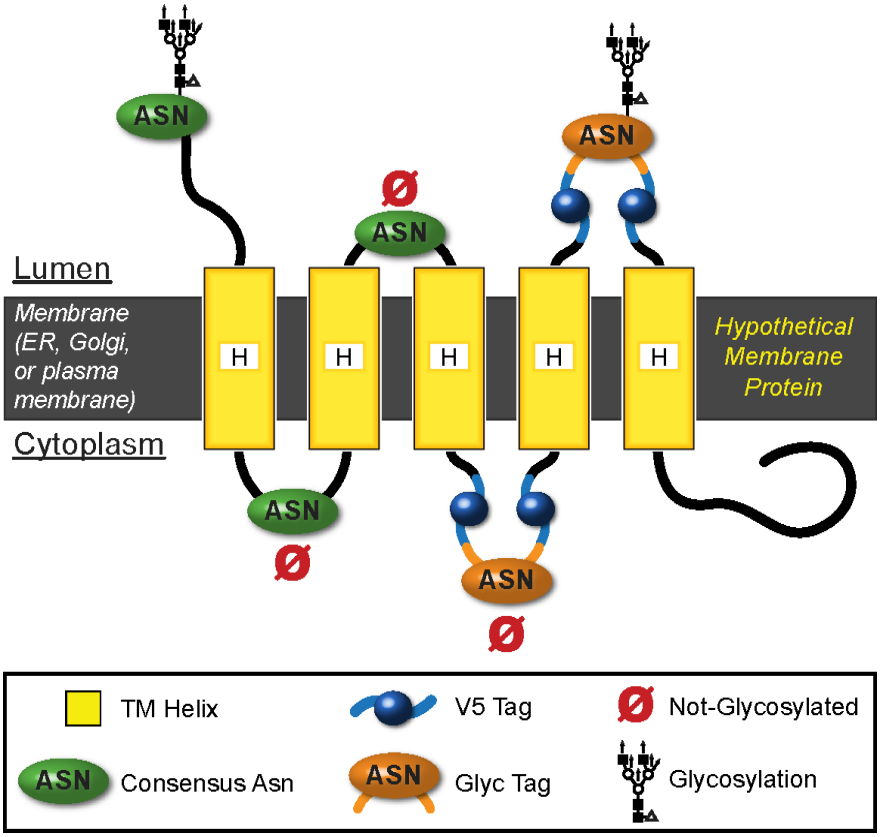

Legend, Figure 3.5. The V5Glyc tag is a neutral, hairpin-like tag containing an optimized 8-residue consensus for N-linked glycosylation, sandwiched between two V5 epitope tags. This tag was designed using the NetNGlyc server (63) to provide a consistent context that can be glycosylated if located in the ER lumen. Here, we show a hypothetical membrane protein with asparagine residues in consensus sequences (i.e. NXS or NXT motifs) on both sides of the membrane. Only lumenal asparagines in the appropriate context and spaced far enough from the membrane can be N-glycosylated.

We then installed the V5Glyc tag at all previously referenced positions in mouse GOAT and used it to probe topology by gel-shift immunoblotting (Figure 3.6A-D) and selective permeabilization immunofluorescence (selected positions shown in Figure 3.6E). GOAT's N-terminus was lumenal with complete glycosylation, removable by PNGaseF, and GOAT's C-terminus was cytosolic and thus not glycosylated (Figure 6A). The technique also confirmed localizations of all internal positions, both for those that led to

weaker-expression (Figure 3.6B) and those with strong expression (Figure 3.6D). Position 9, immediately adjacent to the H338 residue, was found to be lumenal by both PNGase sensitivity and selective permeabilization. We show key positions in Figure 6E; this approach was effective at all positions tested but two (positions 8a and 8b, where the construct did not produce full-length GOAT). Therefore, two new positions were tested in loop 8, 8c and 8d, and both were full length and found to be cytosolic (Figure 3.6C, Figure 3.6E). A summary of all topology data is presented in Table 3.1, and a full topology model taking into consideration all the data is presented in Figure 3.7.

Figure 3.6. The V5Glyc tag allows mapping of GOAT topology using two different techniques.

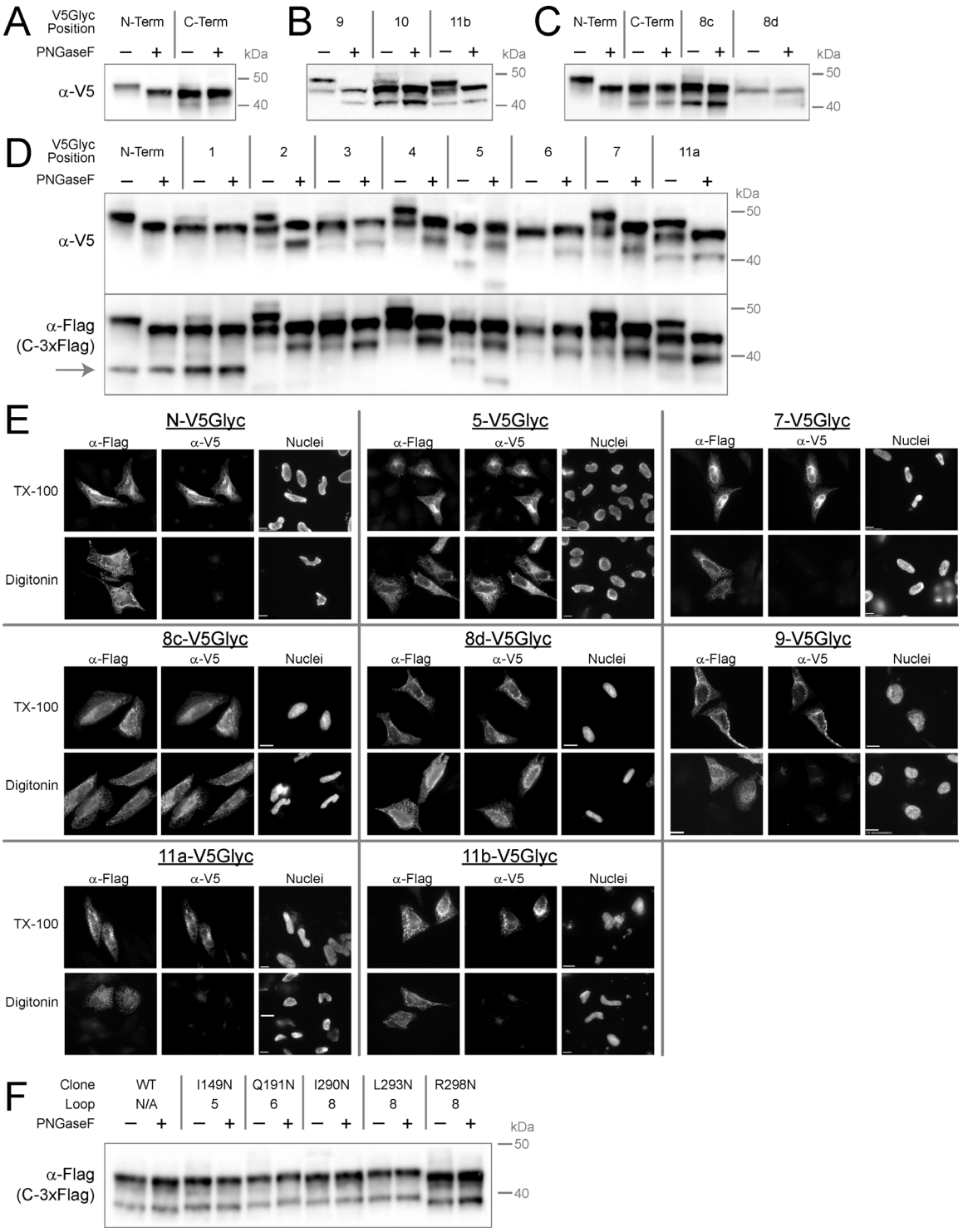

Legend, Figure 3.6. (A-D) Glycosylation gel-shift assay for localization in transfected HeLa cells. Mouse GOAT constructs with internal or terminal V5Glyc tags and a constant C-terminal 3xFlag tag were lysed 20 hours after transfection and treated with Peptide-N-Glycosidase F (PNGase F) or mock treated in identical buffer and then subjected to anti-V5 immunoblotting. Only lumenal positions can be glycosylated, and PNGase F treatment cleaves off the oligosaccharide. Constructs in (B) were less-well expressed than those in (D). Anti-Flag blot in (D) shows an additional band present (gray arrow) not seen in anti-V5 blot for N-terminal construct and position 1; this band is shown below to represent a protein starting with Met56. Note that positions 8a and 8b are not shown; no full-length GOAT could be detected from these constructs. In (C), two additional positions were tested in loop 8 (8c and 8d), and both expressed well and confirmed cytosolic location. (E) Selective permeabilization of key V5Glyc constructs reports lumenal location for challenging positions 9 and 11 and cytosolic location of loop 8; other previously suggested positions are also confirmed. As above, GOAT bearing the indicated internal V5Glyc tag was used and all constructs have a constant C-terminal 3xFlag tag. The N-terminus and positions 5 and 7 are shown because these were the most robust in our initial survey. (F) NXS or NXT codons (not V5Glyc tags) were installed in all loops longer than 24 AA, loops 5, 6, and 8. Loop 8 is longer, so three constructs were generated. None of these epitopes could be glycosylated, consistent with cytosolic locations.

Figure 3.7. GOAT Topology model as an 11-TM protein with one reentrant loop.

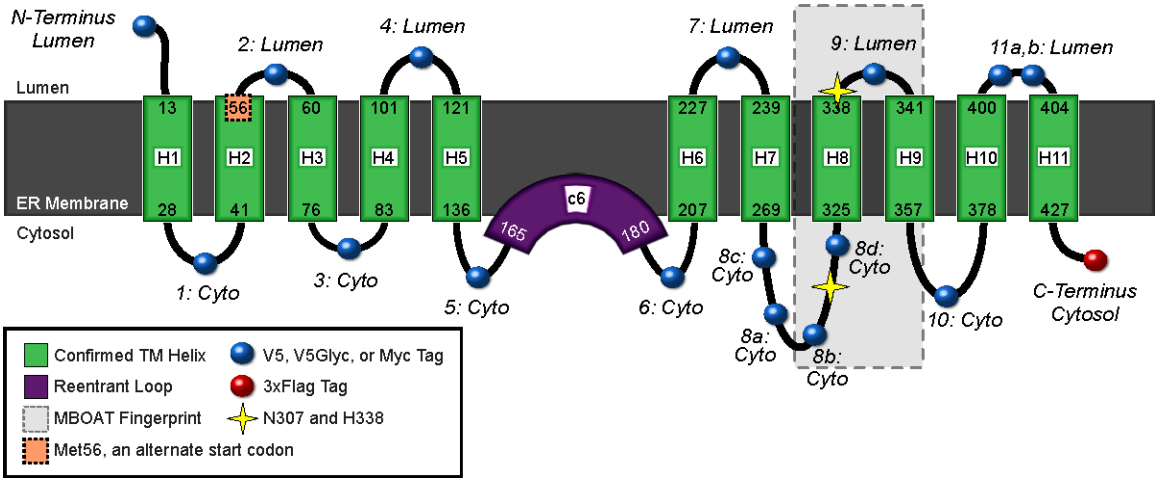

Legend, Figure 3.7. Confirmed transmembrane helices (TMs) are shown in green, spanning the ER membrane (gray). Lumen is above, cytosol below. We suggest that the hydrophobic region of GOAT "c6", predicted to be a TM domain, may be a reentrant loop, shown in purple. Relative loop length is shown by the size of the loops (black lines), but are not precisely scaled. Variable epitope tag positions used are shown as blue spheres; the constant C-terminal 3xFlag tag is a red sphere. The alternate translational start site (Met56) is highlighted in orange. Positions of the two conserved MBOAT residues (N307 and H338 in mouse and human GOAT) are shown as yellow stars, and the most-conserved region across all MBOATs is shown as a gray box (~R303-M354 in GOAT, from pfam03062 (20)). Figure design is modified from the output of MEMSAT-SVM, with permission.

Table 3.1. GOAT topology summary.

Position	V5/Myc Sel. Perm		V5Glyc			Other
			Glyc	Sel. Perm		
N-Term	L	++++	L	L	++++	Alt glyc*
1	C	+++	C	C	+++	Endogenous Asn**
2	L	+	L	L	++	
3	C	+++	C	C	+++	
4	L	++	L	L	++	
5	C	++++	C	C	++++	K141 Ubq†. Myc hGOAT; Catalytically active NXS/T Mutant***
6	C	+++	C	C	++++	NXS/T Mutant***
7	L	++++	L	L	++++	
8a	C	+++	ND	ND	ND	Myc hGOAT Three NXS/T Mutants in loop 8***
8b	C	+++	ND	ND	ND	Myc hGOAT
8c	ND	ND	C	C	++++	
8d	ND	ND	C	C	++	
9	–	–	L	L	+++	
10	C	++	C	C	++	Endogenous Asn**
11a	L	+	L	L	++	
11b	–	–	L	L	+++	
C-Term	C	++++	C	C	++++	C-3xFlag cyto in all constructs. C-3xMyc also cyto.

Legend, Table 3.1. L, lumenal; C, cytosolic; + signs indicate V5 or Myc signal level in indirect immunofluorescence. Alt Glyc*, a variety of alternate glycosylation signal sequences were installed at GOAT's N-terminus (Figure 9B) and these were all lumenal. Endogenous Asn**, an endogenous Asn in a consensus NXS/T/C site was not glycosylated. NXS/T Mutant***, a mutation creating a consensus NXS/T glycosylation site was installed in the center of this loop but could not be glycosylated (Figure 9B). Myc hGOAT, human GOAT was made with a Myc tag at this position and results agree with the mouse GOAT result. ND, not done; GOAT with V5Glyc tag installed in positions 8a and 8b did not result in full-length protein, so positions 8c and 8d were tested with this tag. †In a mass spectrometry experiment performed on full length GOAT we observed a peptide corresponding to ubiquitylation at residue K141, suggesting cytosolic localization. Relative signal strength assignment shown with variable numbers of + signs is described in *Materials and Methods.*

Met56 is an alternate start codon in Mouse GOAT, resulting in two species by SDS-PAGE

Interpretation of the gel shift blotting (Figure 3.6A-C) is somewhat complicated by the finding of at least two bands from mouse GOAT; the two predominant bands from HeLa cells have nearly identical size difference as that induced by the gel shift from N-glycosylation. We noticed that in lumenal positions, the pattern of these bands generally shift together on PNGaseF treatment (For example position 9, Figure 6B, and positions 2, 4, and 7, Figure 3.6C), suggesting that they were separate GOAT species that were both glycosylated.

We noticed that the lower band was absent from the blot for the modular V5Glyc tag but present at a smaller molecular weight in the C-terminal Flag blot when the V5Glyc tag was installed at the N-terminus and position 1 (gray arrow, Figure 3.6D). This split suggested that the two bands represent GOAT proteins with different N-termini (i.e. with two distinct translational start sites) and triggered us to map the lower band as GOAT initiating translation at Met56 (see below).

Figure 3.8. Purification of GOAT as a monomer with at least two stable bands.

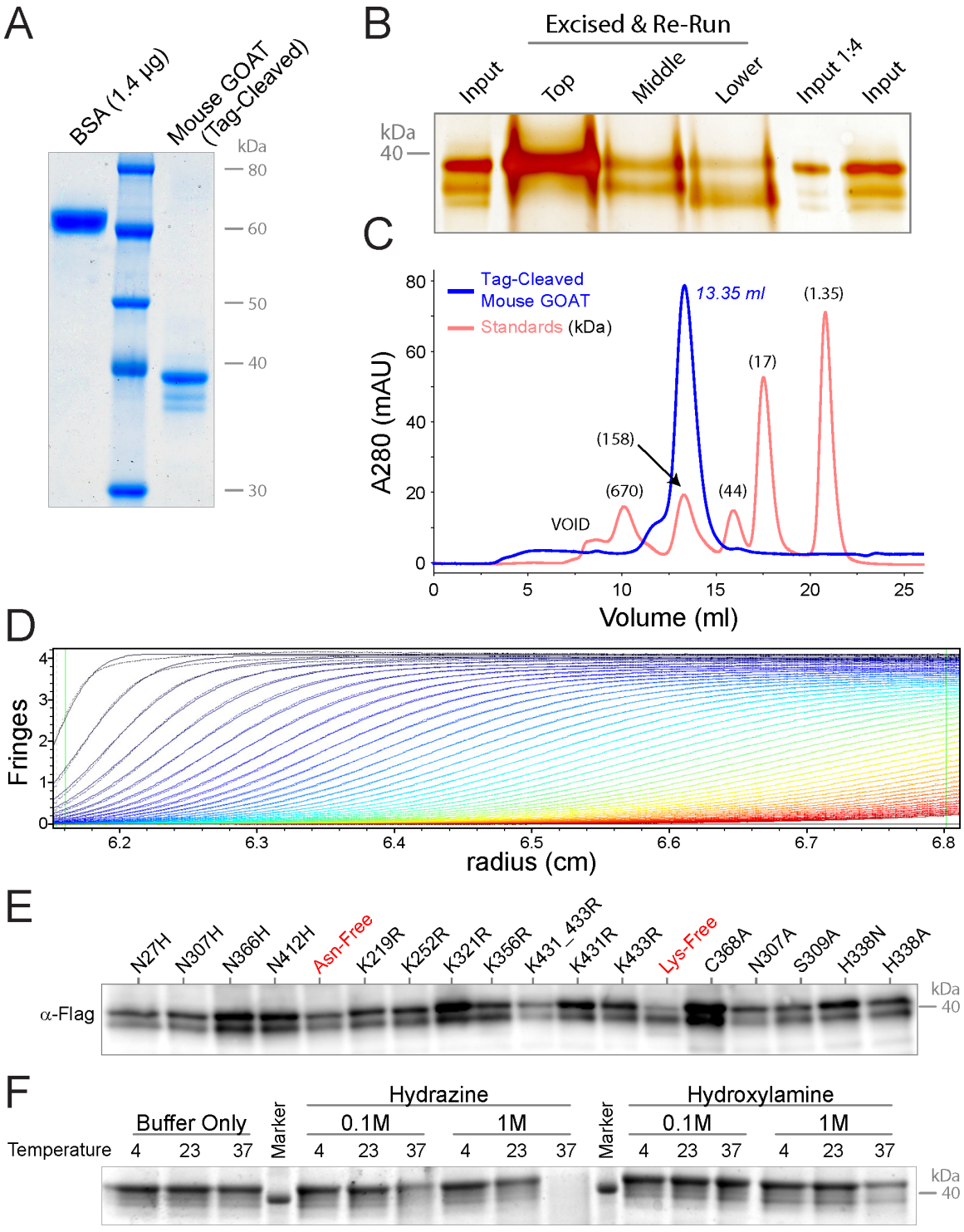

Legend, Figure 3.8. (A) Colloidal Coomassie brilliant blue (CBB) staining of purified mouse GOAT after tag cleavage and ion exchange chromatography reveals three bands. Four identical lanes of mouse GOAT were used as input for electro-elution. (B) Bands in (A) are stable species, not interconverting gel artifacts. Stained bands were excised, electro-eluted, and concentrated, and then re-run and silver stained as compared to the original purified GOAT. (C) Size exclusion chromatography of cleaved GOAT and standard proteins. Sizes of proteins in the standard are shown in parentheses. The calculated MW for monomeric GOAT in FC-16 micelles is 140.7 kDa. TEV-cleaved GOAT alone has a calculated MW of 50.6 kDa. Empty FC-16 detergent micelles alone are ~72.5 kDa and do not result in UV absorbance signal at the concentration used. (D) Interference optical monitoring data from analytical ultracentrifugation of GOAT were fit in SEDFIT to a C(s) model. Fringes over time are shown in progression from red to black; absorbance data (not shown) was similar. Approximately 90% of the signal in the sample fit to a single peak at 1.9 S, corresponding to an S(20°C, water) of 5.4 and an approximate molecular weight of 110 kDa. (E) Anti-Flag immunoblot of GOAT-3xFlag in SF9 cells with the indicated mutations shows that multiple bands seen are not due to post-translational modification on asparagine or lysine or at residues C368 or S309. Asn-free and Lys-free GOATs include all the N and K mutations listed in other constructs. (F) Treatment with hydrazine or hydroxylamine does not alter the banding pattern of purified GOAT. Mouse GOAT was incubated overnight at the indicated temperatures and concentrations with hydrazine and hydroxylamine (pH 8.0). CBB-stained gel shown; mouse GOAT used in this experiment was eluted from Flag resin using 100 mM glycine pH 3.5 and retains C-terminal the 3xFlag tag.

Mouse GOAT purified from SF9 cells (with C-terminal 3xFlag tag cleaved) produces three distinct bands on SDS-PAGE when the proteins are maximally separated and Coomassie stained (Figure 3.8A). The middle band is generally absent from immunoblots (Figure 3.8E) and may represent a co-purified protein. Mobilities of top and bottom bands when GOAT was produced in HeLa and SF9 cells were identical (not shown). We found that the two predominant bands did not change when all lysines or all asparagines were removed from GOAT by conversion to alanine residues (Figure 3.8E), suggesting they were not due to post-translational modification of these residues. C368 was mutated as part of a potential NXC motif (see below), and S309A as a potential

phosphopantetheinylation site, and these mutants too show both species. The banding pattern also did not change in response to hydroxylamine and hydrazine treatment of GOAT (Figure 3.8F), suggesting that multiple banding did not arise from fatty acid esterification.

We were concerned that the two bands might represent a gel artifact, since like many other integral membrane proteins, GOAT aggregates when heated in SDS and therefore may not be fully denatured; it also runs at a smaller-than-predicted molecular weight, again common in membrane proteins due to hydrophobicity resulting in increased SDS binding (Rath et al., 2009). We therefore excised the three bands from the gel, electro-eluted the proteins, and re-ran them in separate lanes (Figure 3.8B). The three species ran true, within the limits of our ability to separate them using this technique, suggesting that they are distinctly covalent and non-interconverting structures.

Figure 3.9. The lower GOAT band is a protein with N-terminus Met56.

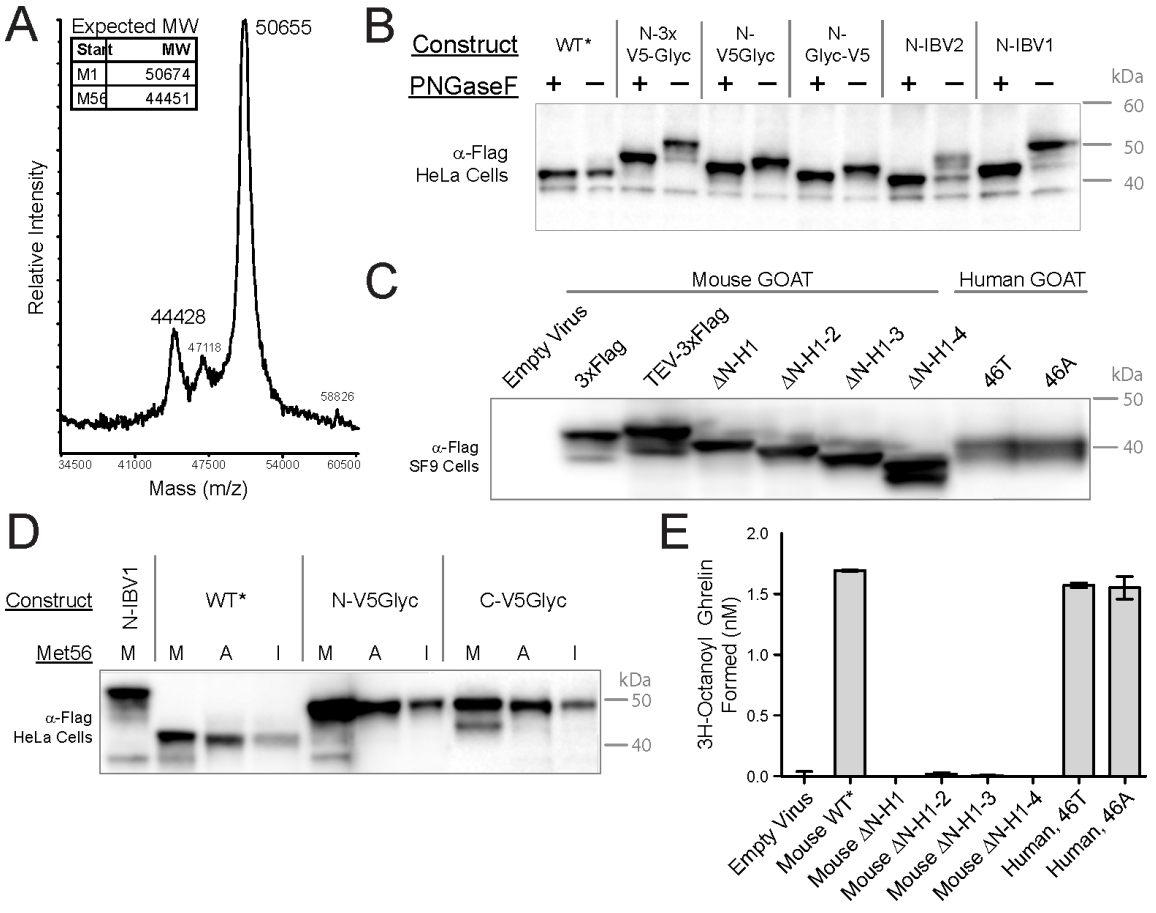

Legend, Figure 3.9. (A), MALDI-TOF of intact, purified tag-cleaved mouse GOAT. Expected molecular weights (MWs) with the indicated start codons are inset (estimated standard error on these masses is +/- 50 Da). (B) Adding N-terminal sequence shifts the upper band, but not the lower band in mouse GOAT. *, All constructs contain a C-terminal 3xFlag tag. N-IBV1 and N-IBV2 are described in *Materials and Methods*; 3xV5Glyc is V5-Glyc-V5-Glyc-V5; V5Glyc is V5-Glyc-V5; Glyc-V5 lacks the first V5 epitope of V5Glyc. (C) Anti-Flag immunoblot of SF9 microsomes of full length and helix-deleted constructs. ΔN-H1 construct lacks the first helix, ΔN-H1-2 lacks the first two helices, etc. The start codon for ΔN-H1-2 is Met56; for ΔN-H1-3 and ΔN-H1-4, a Met was installed in place of residues 81 and 109, respectively, as the first residue of the construct. All deletion mutants have a C-terminal Tev-3xFlag. Human GOAT proteins are labeled 46A and 46T because this position was expressed as either the conserved Ala or the recorded cSNP Thr. 3-fold more human GOAT-expressing microsomes were loaded than mouse GOAT-expressing microsomes, due to lower expression. **(D)** Mutation of Met56 removes the lower band from mouse GOAT. Met56 was mutated to alanine or isoleucine for the indicated constructs and all were expressed in HeLa cells. Expression levels are reduced by 5-10 fold for mutant constructs (not shown); here, 4 μg of total protein was loaded for Met constructs and 20 μg for Ala and Ile constructs. **(**E) Microsomal activity assay of TEV-3xFlag tagged GOAT constructs in (C). Each bar represents an average of duplicates and standard deviations are shown.

We analyzed purified mouse GOAT in FC-16 detergent micelles by size exclusion chromatography (SEC). Under these conditions, the solution contains a mixture of detergent micelles containing GOAT and empty detergent micelles. The empty micelles are approximately 72.4 kDa for FC-16, with aggregation number of 178 detergent molecules per micelle (Anatrace). TEV-cleaved GOAT has a MW of 50.6 kDa; as a monomer or dimer in micelles the predicted MW would be ~123 kDa or ~174 kDa, respectively. In SEC, GOAT ran as one major peak (Figure 3.8C). As compared to standard (soluble) proteins, the SEC-calculated MW for GOAT in its FC-16 micelle is 140.7 kDa. This size does not allow clear determination of whether purified GOAT is a monomer or dimer, though it is closer to a monomer position. Hydrophobic interactions between the GOAT protein and resin may result in non-ideal behavior. Note that the detergent does not result in detectable UV absorbance at these concentrations, as seen by the lack of a peak at ~70 kDa corresponding to free detergent micelles.

To further investigate the quaternary structure of GOAT, we employed sedimentation velocity analytical ultracentrifugation. As shown in Figure 3.8D, sedimentation velocity data using interference optical monitoring of GOAT were fit in SEDFIT to a C(s) model (Schuck, 2000). Approximately 90% of the signal in the sample fit to a single peak at 1.9 S, which was normalized to 5.4 S when taking into account the temperature correction factor (20°C, water). This sedimentation behavior corresponds to an approximate molecular weight of 110 kDa, consistent with monomeric GOAT in FC-16.

Although the peak was slightly asymmetric, we were unable to resolve additional, smaller species. UV absorbance data (not shown) showed similar results. Fitting the data using the program dC/dT+, which employs alternative methods of fitting data to those used by SEDFIT, calculated a similar S value and identified one major species in the experiment (Philo, 2000).

We next analyzed intact, purified GOAT by MALDI-TOF mass spectrometry (Figure 3.9A). In addition to the major GOAT peak at the expected size, a minor species with mass 44428 was found, consistent with a protein initiated at Met56. Further support that this 44428 Da peak corresponds to the lower band in SDS-PAGE can be found in its altered glycosylation pattern. Addition of various glycosylation sequences to the N-terminus of GOAT (Figure 9B and 6D), caused a size increase in the upper but not the lower band, and only the top band shifted further with glycosylation, suggesting that the faster migrating species initiates downstream of the first ATG.

Because Met56 is predicted to be the last (lumenal) residue in TM2, recovery of the lower band suggests that GOAT lacking its first two TMs might be stable. This may also be a physiologic product, and we note that Met56 is the first ATG in the second exon of GOAT. We therefore made constructs for baculoviral expression from which the first, first two, first three, and first four helices had been removed (Figure 3.9C). The size of the construct from which the first two helices have been deleted (ΔN-H1-2, start codon is Met56) co-migrated with the lower band in the full-length construct, consistent with our hypothesis. However, none of the deletion mutants were active (Figure 3.9E). We note that

although human GOAT expressed at levels lower than mouse GOAT, it had similar activity. The two different human GOAT clones have Thr or Ala at position 46; we made both after noticing that the conserved Ala residue has also been reported as Thr (Yang et al., 2008a). Indeed, a recorded human cSNP (coding single nucleotide polymorphism) specifies this polymorphism (rs7813902). Both clones performed identically in our assays.

To further confirm that Met56 can act as an alternate start codon, we mutated this residue. Met56 is conserved in all GOAT sequences evaluated except Green Anole, where it is Ile; we therefore made both M56A and M56I mutants in three different C-3xFlag-tagged GOAT constructs and expressed them in HeLa cells (Figure 3.9D). The lower band was no longer detectable in any of these mutants. We note that the mutant proteins' expression was lower than that of WT, and we loaded 5-fold more total protein in those lanes. N-IBV1 construct is shown to calibrate the lower band position.

Additional data supporting the model

Mouse GOAT is not N-glycosylated (Figure 3.8E, Figure 3.9B). However, two Asn residues are predicted to be candidates for glycosylation by the NetNGlyc server; that neither can be glycosylated is consistent with their cytosolic localizations in our model. Asn27 (79% and 9/9 Jury, +++ rating) is at the cytosolic border of TM1, and Asn366 (62% and 9/9 Jury, ++ rating) is in the middle of the cytosolic loop between TMs 9 and 10. Conserved Asn307 is in an NXS motif but is both cytosolic and not predicted to be glycosylated (48%, 7/9 "jury", - rating).

Mouse GOAT has only three loops where central installation of NXS/NXT motifs by point mutations would also allow sufficient spacing from the membrane for potential glycosylation by OST (12 residues on each side of the Asn, or 24 residues total). In loops 5 and loop 6, we installed sites on both sides of the reentrant helix (I149N and Q191N, NRS in both cases). These were predicted to be glycosylated by NetNGlyc (74% and 68%, respectively, both with 9/9 "jury" and ++ rating). Neither mutant GOAT could be glycosylated (Figure 6F). We installed three more potential sites in loop 8, with mutants I290N, L293N, and R298N making NWT, NET, and NIS sequences (prediction 51%, 58%, 67%, respectively, "Jury" 6/9, 5/9, and 8/9, respectively, + rating). These positions were not glycosylated (Figure 3.6F).

Loop 10 (20 residues) already contains Asn366, which is centrally located and in a non-standard but putative NXC motif, so we made no changes here. In summary, the lack of glycosylation in any of these sites and mutants is consistent with our model.

Additionally, Lys141 of GOAT made in SF9 cells was found to be ubiquitylated by electrospray mass spectrometry, with a trypsin site that was not cleaved and +114.04 Da shift corresponding to GG isopeptide linkage. This is consistent with cytosolic localization, since ubiquitylation can only occur on the cytosolic face of the ER membrane (Hirsch et al., 2009).

Figure 3.10. Characterization of GOAT's active site by photocrosslinking.

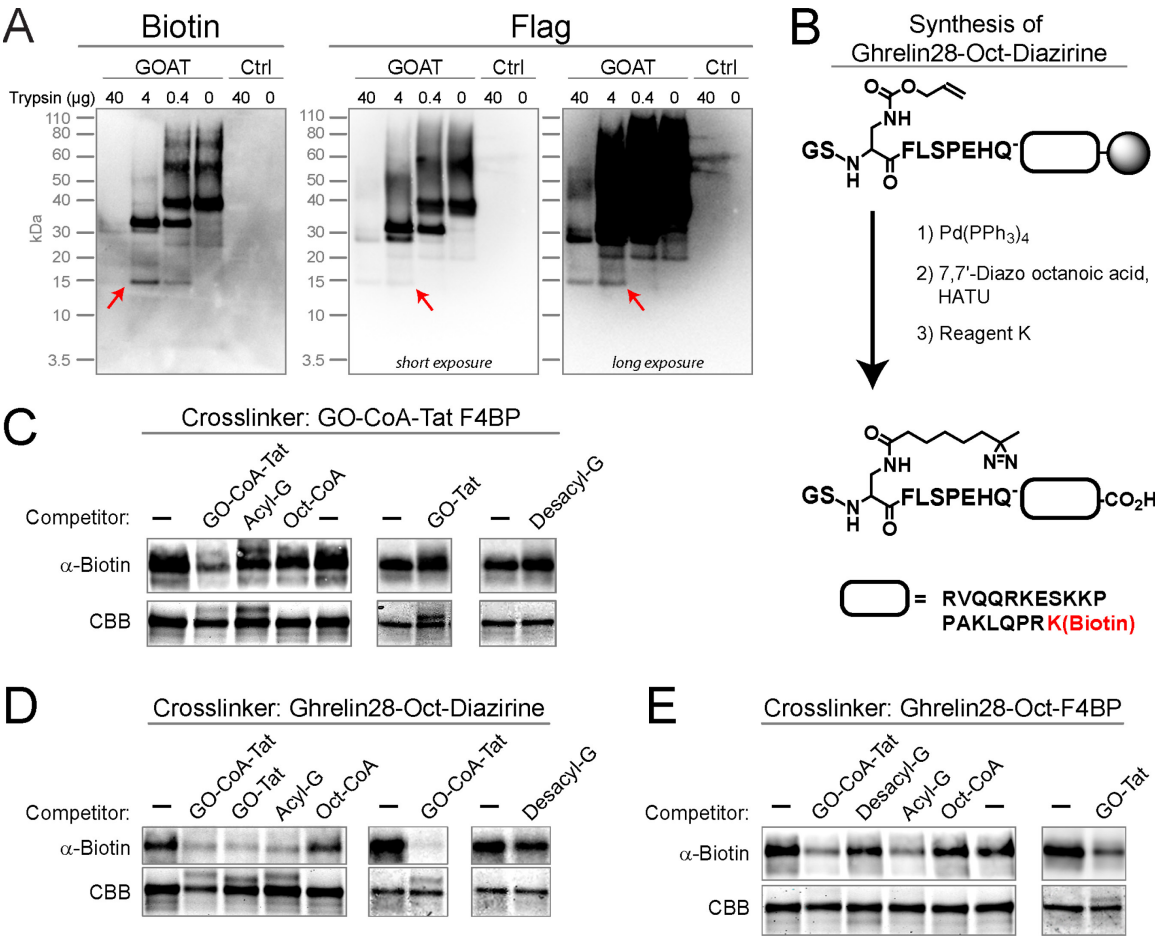

Legend, Figure 3.10. (A) Partial proteolysis of covalently photo-crosslinked mouse GOAT reveals a 15 kDa crosslinked fragment. GO-CoA-Tat F4BP (biotin-labeled) was photo-crosslinked to microsomal mouse GOAT-3xFlag or to control microsomes (Ctrl, from empty-virus infected cells). Microsomes were then solubilized, digested with trypsin, and isolated using anti-Flag beads (see *Materials and Methods*). Samples were then immunoblotted using streptavidin or anti-Flag. Note that while the biotin cannot be removed from GO-CoA-Tat F4BP during trypsin digest, the 3xFlag tag contains multiple trypsin cleavage sites, and smaller tag-cleaved species may have been lost or fallen below the limit of detection. (B) Synthetic scheme to make Ghrelin28-Oct-Diazirine, an acyl ghrelin product-analog photo-crosslinker. As a complement to GO-CoA-Tat F4BP previously reported (8), we designed another set of photoaffinity labeling agents based on the fact that the amide analogs of acyl ghrelin product have high affinity for GOAT (32). Photolabile diazirine was installed at the 7-position of the octanoic acid side chain and biotinylated lysine was installed at the C-terminus of ghrelin-28. Ghrelin28-Oct-F4BP was made similarly, using unlabeled octanoic anhydride and replacing Phe-4 with Benzoylphenylalanine. (C-E) Photocrosslinking cross-competition binding assay. Each of three biotinylated photocrosslinking compounds ((C), GO-CoA-Tat F4BP, (D),

Ghrelin28-Oct-Diazirine, (E), Ghrelin28-Oct-F4BP) was crosslinked to purified, solubilized mouse GOAT in the presence of an excess of the indicated unlabeled competitors. Separate subpanels represent separate experiments. CBB staining is used as a loading control.

Characterization of GOAT's active site by photocrosslinking

We previously reported that both microsomal and solubilized, purified GOAT can be specifically photo-crosslinked by a biotinylated analog of the bisubstrate inhibitor of GO-CoA-Tat containing UV-activatable benzoylphenylalanine in place of Phe4 (GO-CoA-Tat F4BP) (Barnett et al., 2010). Note that solubilized GOAT is not active(Taylor et al., 2012b; Yang et al., 2008b) however both with and without pre-solubilization, this crosslinking could be competed by addition of excess, unlabeled GO-CoA-Tat, suggesting specificity of the reaction to the enzyme's active site and the maintenance of a physiologically relevant fold. Therefore, to further map GOAT's active site, we performed partial proteolysis of crosslinked microsomal GOAT (Figure 3.10A). This was done by first crosslinking, then solubilizing in FC-16, digesting with different amounts of trypsin, and then purifying C-terminal fragments using anti-Flag. A 15 kDa fragment was detected in both anti-Flag and biotin blotting, suggesting that at least some of the crosslinking occurs in approximately the C-terminal 15 kDa of GOAT (see Discussion). Attempts to characterize the exact locations of photocrosslinking by mass spectrometry have so far been unsuccessful.

We next characterized the binding of various analogs and inhibitors to GOAT using photocrosslinking compounds and competitors. Based on the fact that ghrelin product analogs with amide lipid linkage have high affinity to GOAT (Yang et al., 2008a),

we synthesized two C-terminally biotinylated ghrelin product analogs with photocrosslinking moieties in the lipid (ghrelin28-Oct-Diazirine, Figure 3.10B) and on the adjacent residue in the peptide chain (ghrelin28-Oct-F4BP). Purified GOAT in FC-16 was then crosslinked with these three analogs alone or in the presence of an excess of the following unlabeled competitors: GO-CoA-Tat, acyl ghrelin (amide form), desacyl ghrelin, octanoyl-CoA, and GO-Tat (amide-linked octanoyl ghrelin product analog containing 10 residues of ghrelin followed by Ahx linker and Tat sequence). Binding of the bisubstrate crosslinker GO-CoA-Tat F4BP was only efficiently competed by GO-CoA-Tat itself (Figure 3.10C). This suggests that the bisubstrate inhibitor has a higher affinity for GOAT, perhaps by occupying a larger space in the binding site. On the other hand, the product analog photo-crosslinkers ghrelin28-Oct-Diazirine and ghrelin28-Oct-F4BP behaved similarly to each other but distinctly from the bisubstrate (Figure 3.10D, Figure 3.10E). Both product crosslinker analogs were competed by GO-CoA-Tat, suggesting that their binding to GOAT overlaps where the bisubstrate binds. Both product crosslinker analogs, which presumably attach to GOAT in distinct ways because of the location of their photoreactive groups, could also be competed by both GO-Tat and acyl ghrelin. These results suggest that the location of the photoreactive groups does not significantly affect analog binding. Octanoyl-CoA and desacyl ghrelin, which may bind more weakly to GOAT or in a non-overlapping way, did not compete or only minimally competed against both crosslinker product analog compounds.

Discussion

These studies establish the location of the 11 transmembrane spanning domains and one reentrant loop of GOAT. Using a combination of phylogeny, computational prediction, epitope mapping, and induced glycosylation, we obtained strong convergent evidence for this 11 transmembrane domain model. This new model contains three more transmembrane spanning domains than previously predicted, and also suggests that one domain predicted by the recently developed programs is instead a reentrant loop. This model also indicates that GOAT's topology is quite structurally complex. Although our evidence strongly supports this overall 11 transmembrane model, we recognize that polytopic membrane proteins are complex, and dynamic alterations of topology are formally possible. We also appreciate that the loop insertions employed, while small in size and unable to flip the C-terminus into the lumen, may perturb local structure.

Three other MBOATs have been fully mapped topologically: human ACAT1 and ACAT2 (official symbols SOAT1 and SOAT2, reviewed in (Chang et al., 2009)), and yeast Gup1p (Pagac et al., 2012). GOAT, ACAT1, and Gup1p have somewhat similar topologies, but ACAT2 is quite different than the other three. All four MBOATs have in common that the invariant histidine (His338) is lumenal or buried in the ER membrane near the lumen; this was also shown for partially-mapped yeast MBOATs Ale1p and Are1p (Pagac et al., 2012). For GOAT, ACAT1, Gup1p, and Ale1p, the histidine is at the lumenal tip of two TMs separated by only a short 2-3 residue turn. Are2p is similar, except the C-terminal

TM is likely instead a reentrant loop. The conserved asparagine (Asn307 in GOAT) was also found to be cytosolic in all six cases.

The topology models of GOAT and Gup1p are the most similar, with 12 distinct hydrophobic regions separated by relatively short hydrophilic loops, N-terminus lumenal, C-terminus cytosolic, short terminal tails, a reentrant loop near the middle of the protein, and a relatively long cytosolic loop immediately N-terminal to the hydrophobic region containing the invariant His. However, for Gup1p the N-terminal two regions were found to be reentrant loops, resulting in a model with 9 TMs.

ACAT1 topology has been studied rigorously using a variety of methods. Overall, its topology is relatively similar to GOAT, with 9 TMs, but ACAT1 has longer loops, two fewer helices, and opposite orientation of the N- and C-termini. In contrast, ACAT2 was shown to have only two transmembrane domains using selective permeabilization with two distinct epitope tags (Lin et al., 2003). These results are surprising considering ACAT2 has 10 regions predicted to be transmembrane or reentrant by MemBrain (data not shown), similar to the other MBOATs; some of the non-TM hydrophobic regions were modeled as reentrant loops. And, with the exception of some subtle differences in predicted loop regions around the invariant histidine, the positions chosen should have efficiently interrogated these locations. It is possible, therefore, that ACAT2 has a distinct topology compared to the other MBOATs.

These studies have revealed that GOAT's C-terminus can physically contact peptide and octanoyl-CoA substrates and that the bisubstrate analog encompasses both

enzyme interaction surfaces. The lumenal location of His338 suggests it could well be in the active site of the GOAT enzyme, consistent with the hypothesis of a conserved lumenal active site for the MBOAT family. In contrast, the conserved extra-lumenal position of the conserved MBOAT residue Asn307 indicates that it is unlikely to be directly involved in catalysis. However, its importance might be in substrate interactions, transport of substrates, or protein structural stability.

The finding of a FLAG-tagged ~15 kDa fragment with GO-CoA-Tat F4BP crosslinking maps the ghrelin binding site to the C-terminal region of GOAT. This could be consistent with crosslinking to the regions around TM-8 and TM-9, depending whether the crosslinked compound causes a gel shift of this smaller GOAT fragment. In any event, these results suggest that the GOAT C-terminal region is directly involved in substrate binding and/or catalysis. Additionally, this region contains three lysophospholipid acyltransferase motifs essential for activity in this subset of MBOATs (Shindou et al., 2009).

The quaternary structure of GOAT has not been investigated previously; the only MBOAT for which the quaternary structure is known is ACAT1, which is a homotetramer both in cell culture and in vitro (Yu et al., 1999). We show by analytical ultracentrifugation that purified GOAT in detergent micelles is a monomer (Figure 3.8D). Taken together with the specific binding of ghrelin photocrosslinking analogs to GOAT under nearly identical conditions (Figure 3.10C-E), this suggests that GOAT can bind ghrelin and analogs as a monomer.

Additionally, the V5Glyc glycosylation strategy developed here may be of more general utility for the analysis of membrane proteins. In particular, the flanked sequence seems to be generally well-tolerated for loop insertion and efficiently processed by oligosaccharyltransferase. It gives robust signal on both immunofluorescence and immunoblotting, and this dual topology reporter is far smaller than others previously employed, suggesting it is likely to be better tolerated for membrane protein applications.

CHAPTER 4 – MECHANISTIC ANALYSIS OF GHRELIN-O-ACYLTRANSFERASE USING SUBSTRATE

Summary

In this chapter, we explore an *in vitro* microsomal ghrelin octanoylation assay to analyze its enzymologic features. Measurement of K_m for 10-mer, 27-mer, and synthetic Tat-peptide-containing ghrelin substrates provide evidence for a role of charge interactions in substrate binding. Ghrelin substrates with amino-alanine in place of Ser3 demonstrate that GOAT can catalyze the formation of an octanoyl-amide bond at a similar rate compared with the natural reaction. A pH-rate comparison of these substrates reveals minimal differences in acyltransferase activity across pH 6.0-9.0. These data support a GOAT catalytic mechanism which is insensitive to substrate nucleophilicity.

Introduction

Ghrelin is a 28 amino-acid secreted peptide hormone that provides a neuroendocrine link between the gut and the brain, modulating metabolism in response to nutrient availability(Kirchner et al., 2009; Kojima et al., 1999; Lopez et al., 2008; Nishi et al., 2005). Ghrelin signaling requires octanoylation of Ser3, a unique modification required

for activation of the ghrelin receptor, GHSR-1a(Kojima et al., 1999; Ozawa et al., 2009) and catalyzed by the 11-transmembrane integral membrane protein Ghrelin-O-Acyltransferase (GOAT)(Gutierrez et al., 2008; Li et al., 2012; Taylor et al., 2013; Yang et al., 2008a). Ghrelin may play roles in both energy balance and hunger, depending on the circumstances (Barnett et al., 2010; Teubner et al., 2013). The metabolic consequences of GOAT activity have also been observed in the context of surviving starvation, supporting fat storage and glucagon signaling and antagonizing insulin. Accordingly, GOAT-deficient mice generated in two different ways fail to maintain blood glucose in conditions of calorie restriction(Li et al., 2012; Zhang et al., 2015; Zhao et al., 2010a), although the precise details of the experimental systems may influence this result(Yi et al., 2012).

GOAT is a member of the MBOAT family of acyltransferases, a group of polytopic integral membrane proteins that acylate lipids, sterols, and GPI-anchored proteins (Hofmann, 2000). Little is known about their enzyme mechanisms. They contain an invariant lumenal histidine and a highly conserved asparagine (Guo et al., 2005b; Matevossian and Resh, 2015; Pagac et al., 2011; Taylor et al., 2013), which are presumed to be involved in catalysis. However, in the case of HHAT, which N-palmitoylates hedgehog proteins, some activity was preserved upon mutation of the histidine to alanine (Buglino and Resh, 2010), and for GOAT, it has been demonstrated that the conserved His and Asn are on opposite sides of the ER membrane (Taylor et al., 2013). These observations in HHAT and GOAT leave open the role of specific MBOAT residues in catalysis.

A number of *in vitro* assays have been published for GOAT using microsomes prepared from insect cells (Darling et al., 2013; Darling et al., 2015; Garner and Janda, 2010, 2011; Taylor et al., 2012b; Taylor et al., 2013; Yang et al., 2008a) or human cells(Barnett et al., 2010). These assays have established N-terminal sequence requirements for recognition of ghrelin by GOAT and identified a number of peptide-based inhibitors as well as initial small-molecule scaffolds. However, mechanistic details regarding the mechanism of catalysis and contributions to binding beyond the first few ghrelin residues are lacking.

In this study, we establish and optimize an improved *in vitro* microsomal GOAT octanoylation assay using biotin-tagged ghrelin. We also describe a novel ghrelin substrate in which the natural Ser is replaced with 2,3-diaminoproprionic acid (dap, amino Ala) at position 3 and its processing by GOAT.

Materials and Methods

All reagents were purchased at the highest quality available from Sigma-Aldrich or Acros Organics unless otherwise indicated. Commercially available reagents were used without further purification.

Cloning

Mouse GOAT with and without a C-terminal 3xFlag tag was cloned into pFastBac1 (Life Technologies, Grand Island, NY) using EcoRI and HindIII and into pFastBac HT modified to contain an N-terminal His_{10} tag. All clones were fully sequence verified and then recombined into baculovirus by transformation of DH10Bac cells (Life Technologies) and plated on appropriate antibiotic plates with a blue-white screen per the manufacturer's instructions. Recombinant white clones were verified by two colony PCR reactions: Reaction 1 with M13F (-40) and M13Rev primers demonstrated the presence of a full-length insert and the absence of empty virus, and Reaction 2 with M13F (-40) and GOAT-Internal-Rev (5'-GGAGAGCAGGGAAAAAGAGCAAGT-3') demonstrated the presence of mouse GOAT. Final clones were further confirmed by DNA sequencing of the complete open reading frames. Baculovirus DNA was prepared for transfection by alkaline lysis with isopropanol precipitation and ethanol wash.

Cell Culture and Virus Preparation

Cell culture medium and insect cells were from Life Technologies unless otherwise noted. SF9 (*Spodoptera frugiperda*) and High Five (*Trichoplusia ni*) insect cells were maintained in suspension in 25 mL - 3 L spinner flasks (Bellco Glass, Vineland NJ) in SF-900 III and Express Five serum free media, respectively, at 27°C at a density of 0.2-6 × 10^6 per mL, with aeration at sizes 1L and larger. High Five cells were counted after trituration 30 times through a 200 µl pipet tip. P1 virus was prepared by transfecting 800,000 SF9

cells per well with 5 μg DNA on 6-well plates using Cellfectin II reagent according to the manufacturer's instructions and harvested after 3 days. P2 and P3 viruses were prepared using sequential passages with multiplicity of infection (MOI)=0.1, with GOAT expression confirmed by immunoblotting at the P2 stage. For Immunoblotting, cell pellets from 1 mL suspension culture were lysed in 250 μl 1x LDS (lithium dodecyl sulfate) loading dye (Life Technologies) containing 150 mM 2-mercaptoethanol, 2 μg/ml aprotinin, 2.5 μg/ml leupeptin, 2 μg/ml pepstatin A, 1 mM EDTA, and 1 μL benzonase nuclease (Sigma, St. Louis, MO), incubated at 37˚C for 10 min, and cleared by centrifugation for 5 min in at 21,000 × g; 4 μl was loaded per lane.

Microsome Preparation

1-3 L cultures at 2.5 × 10^6 cells/mL were infected with P3 virus at MOI ~1 for 48 hours and collected by centrifugation. Pellets from 1 L culture (~10 mL) were resuspended in 40 mL HBS (50 mM HEPES pH 7.0, 150 mM NaCl) containing 2 μg/ml aprotinin, 2.5 μg/ml leupeptin, 2 μg/ml pepstatin A, and 1 mM EDTA and lysed using 40 strokes in a 40 mL Dounce homogenizer (loose pestle). Cell debris was pelleted for 10 min at 4,000 × g and then microsomes were collected at 100,000 × g for 1 h, resuspended in 6 mL HBS with a Dounce homogenizer and then passed 10 times through a 22 gauge needle and twice through a 25 gauge needle. Aliquots were flash-frozen in liquid nitrogen and stored at -80˚C. Microsomal protein concentration was measured against a BSA standard using the

BCA assay (Thermo Fisher Scientific, Waltham, MA), supplementing the working reagent with 0.5% Triton X-100.

Chemical Synthesis

Peptide synthesis was performed using automated solid phase peptide synthesis and the Fmoc strategy. Biotin-tagged Ghrelin27 (hereafter Ghrelin27) was reported previously (Barnett et al., 2010), and was prepared analogously with a S3A mutation. To prepare Dap3-Ghrelin27, Ser3 was replaced with Alloc(allyloxycarbonyl) protected-1,2-diaminopropionic acid (dap, amino-alanine) and deprotected with $Pd(PPh_3)_4$. Biotin-tagged Ghrelin10 and its S3A and Dap3 analogs were prepared analogously, with an aminohexanoic acid linker (Ahx) between the ghrelin sequence and biotinylated lysine (GSSFLSPEHQ(Ahx)K(Biotin)G). Biotin-tagged Ghrelin10-Tat and S3A analog contained the same sequence as Ghrelin10 through K(Biotin), with Tat sequence C-terminal to K(Biotin). Ghrelin sequences synthesized correspond to human ghrelin, and sequences for all ghrelin substrates are shown in Table 1. Synthesized peptides were purified using a reversed-phase C-18 column with a gradient of acetonitrile and water (0.05% trifluoroacetic acid), and structures and purities confirmed with matrix assisted laser desorption mass spectrometry. The final concentrations of the compounds in aqueous solution for assay were based on amino acid analyses (performed at the Harvard or Yale facilities).

Microsomal Ghrelin Octanoyltransferase Assay

The assay was performed similarly to previously described methods (Taylor et al., 2012a; Taylor et al., 2013; Yang et al., 2008c), with modification. Microsomes were thawed on ice, diluted in cold HBS, passed 10 times through a 25 gauge needle, and aliquoted into pre-chilled tubes. Unless otherwise indicated, each 50 µl reaction in HBS (50 mM HEPES pH 7.0, 150 mM NaCl) contained 25 µg microsome protein, was pre-incubated at 30˚C for 5 min, and then incubated 1 min at 30˚C with 10 µM Ghrelin27, 50 µM palmitoyl-CoA (Avanti Polar Lipids, Alabaster, AL), and 1 µM ^{3}H-octanoyl-CoA (60-90 Ci/mmol (American Radiolabeled Chemicals, St. Louis, MO), diluted 1:20 with nonradioactive octanoyl-CoA (Avanti)). All components of the assay were pre-incubated at 30˚C for at least 5 min. Reactions were quenched and solubilized by adding 1 ml 2% SDS in TBS (50mM Tris pH 7.4, 150mM NaCl) containing 10 µl Pierce Streptavidin Plus UltraLink resin (Thermo) and mixed for at least 15 min. For assays containing ghrelin10-Biotin, 37.5 µl resin was used. Beads were washed with 25 ml TBS + 0.1% SDS on small columns (Bio-Rad, Hercules, CA) using a vacuum manifold and then analyzed by scintillation counting. For detergent compatibility assays, detergents were added to microsomes for the 5 min preincubation step.

Ghrelin Octanoyltransferase Assays at Varying pH

The microsomal ghrelin octanoyltransferase assay above was modified as follows: each microsomal aliquot was diluted and homogenized in 150 mM NaCl, 250 mM bis-

Tris propane to achieve the pH of interest (6-9). Each reaction contained 50 μg microsome protein, 10 μM C-terminally biotin-tagged human ghrelin-10 (ghrelin10-Biotin), 50 μM palmitoyl-CoA (Avanti), and 1 μM ^{3}H-octanoyl-CoA (radioactive diluted 1:20 with nonradioactive)). The final amount of 50 mM HEPES pH 7.0 from the frozen microsomal aliquot was 2 μl. Reactions were quenched and solubilized by adding 1 ml 2% SDS in 100 mM Tris pH 7.0, 150 mM NaCl containing 37.5 μl Pierce Streptavidin Plus UltraLink Resin (Thermo) and bound for >15 min. Error in the ratio of rates was calculated using the formula $V(xy)=X^2V(y)+Y^2V(x)+V(x)V(y)$(Bizzozero, 1995).

Chemical Reactivity of Acyl Ghrelin Analogs with Hydroxylamine or Hydrazine

Washed ghrelin assay columns were capped and incubated overnight (~12 h) with 1 mL freshly-prepared 1 M hydroxylamine pH 8.0, 1 M hydrazine pH 8.0, or 1 M MES (2-(N-morpholino)ethanesulfonic acid) pH 6.0 as a control at room temperature. The column mixtures were eluted and washed with an additional 1 mL of the same buffer, and the eluents were combined and analyzed by scintillation counting as were the washed beads as described above.

Detergent Solubilization of GOAT

To test for detergents compatible with GOAT octanoylation, we screened initially at 1.5 × critical micelle concentration and at 1 mM for the following detergents: Anzergent 3-14, APO 10, Big Chap, Brij35, C13E8, CHAPS, CHAPSO, Cholate, CycloFos 6, CycloFos

7, Cymal 6, Cymal 7, Cy-TripGlu (Chae et al., 2008), Deoxy Big Chap, Deoxycholate, Digitonin, Dodecyl Maltoside, Fos-Choline-12, Fos-Choline-13, Fos-Choline-16, GCT-3(Bae et al., Submitted), GNG-3 (Glucose Neopentyl Glycol)(Chae et al., 2013), Hexadecyl Maltoside, LysoFos-Choline 14, LysoFos-Choline 18, MNG-3 (Maltose Neopentyl Glycol)(Chae et al., 2010b), Octyl Glucoside, Ph-TripGlu (Chae et al., 2008), Sucrose Monododecanoate, Taurocholate, TDAO (Tetradecyl Dimethylamine Oxide), Tetradecyl Dimethyl Glycine, Tetradecyl Maltoside, TRIPAO (Chae et al., 2010a), and Triton X-100. Mixed micelles of cholesteryl hemisuccinate (CHS) plus CHAPS, MNG-3 (Lauryl Maltose Neopentyl Glycol), or Fos-Choline-16 were made by mixing detergent:CHS at ratios of 5:1, 10:1, and 20:1 (w/w), respectively, and added analogously at varying concentrations. Detergents found to be compatible with octanoyltransfer above the CMC were next tested by solubilization of microsomes prior to assay; solubilization was accomplished for 1 h with end-over-end mixing at 4°C and clearing by centrifugation for 30 min at 100,000 × g. No conditions were found in which solubilized mixtures retained detectable activity. GOAT-TEV-3xFlag was purified from SF9 microsomes in Fos-Choline-16 (FC-16), as described (Taylor et al., 2013), with final elution in 0.0008% FC-16 (1.5 × critical micelle concentration (CMC)), or purified analogously using 1% *n*-dodecyl-β-D-maltoside (DDM). Purified GOAT was inactive, with or without addition of control microsomes. Purified GOAT solubilized in FC-16 was exchanged during Flag affinity into a number of the above detergents at 1.5 × CMC and was inactive in all cases. All available detergents were purchased from Anatrace (Maumee, OH); digitonin was from

Calbiochem (now EMD Millipore, Billerica MA). GCT-3 was a generous gift from Pil-Seok Chae.

Results

Establishing an Improved in Vitro Ghrelin Octanoyltransfer Assay

A previously published ghrelin octanoylation assay (Barnett et al., 2010) from members of our group used a microsomal preparation from human embryonic kidney cells expressing mouse GOAT. This preparation was suboptimal for detailed enzymologic characterization due to low signal to noise ratio and low conversion of ^{3}H-octanoyl-CoA to ^{3}H-octanoyl ghrelin. In comparison, using an analogous preparation made from insect cells infected with baculovirus expressing mouse GOAT, Yang et al. (Yang et al., 2008c) achieved approximately 100-fold more signal with no apparent increase in background. Therefore, we prepared recombinant baculovirus expressing mouse GOAT in three varieties: untagged, C-terminal 3xFlag tag, and C-terminal 3xFlag tag with N-terminal His_{10} tag, infected SF9 cells, and prepared microsomes 48 hours later (Figure 1A). Control microsomes were prepared from cells infected with virus produced from empty-vector alone.

Figure 4.1. GOAT octanoylation assay establishment.

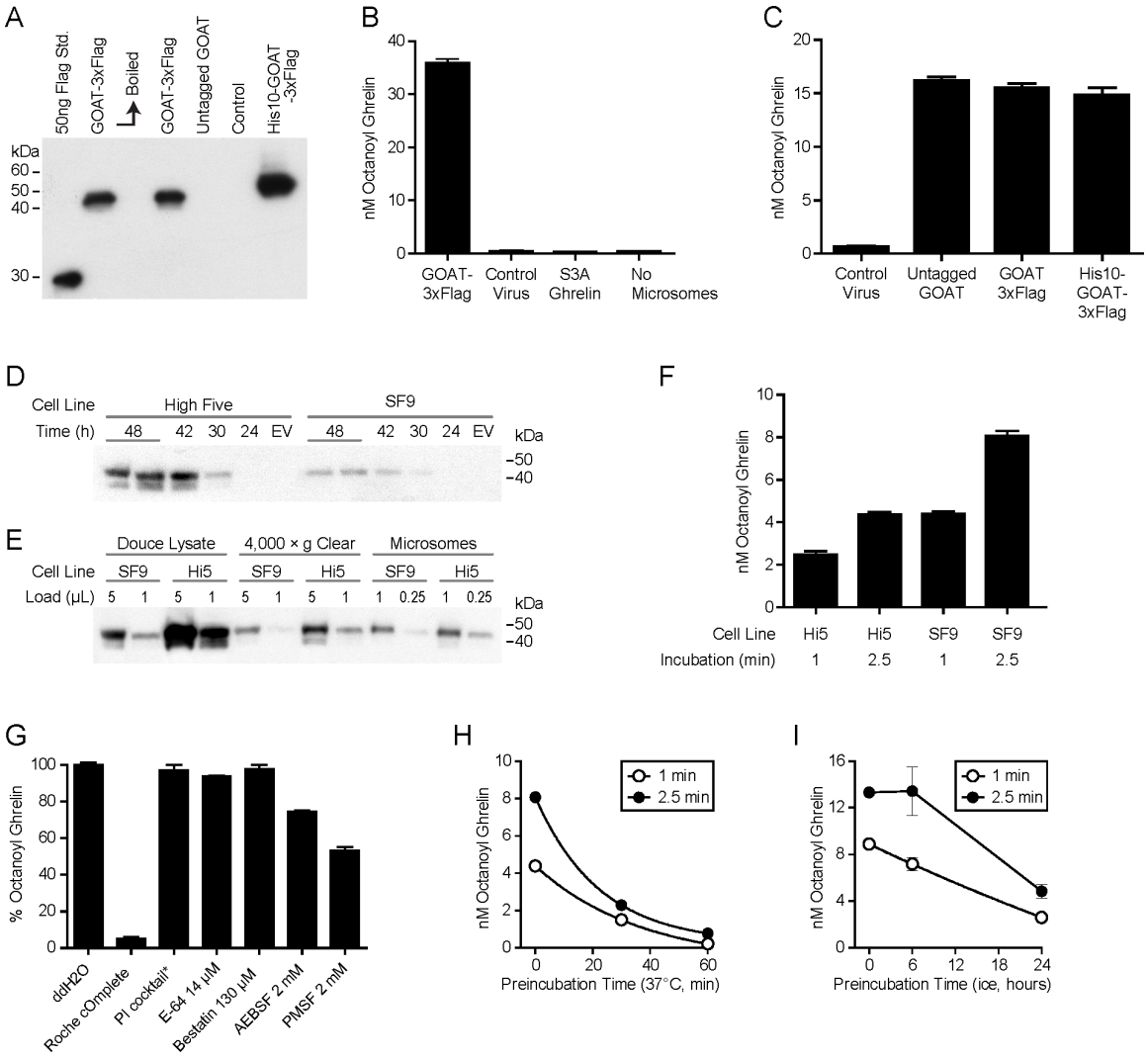

Legend, Figure 4.1. (A) Anti-Flag immunoblot of SF9 cells expressing various tagged GOAT constructs. As previously reported with GOAT expressed in human cells, boiling (10 min at 100˚C) caused aggregation of GOAT and loss of signal. Control cells are infected with virus made from empty vector. (B) GOAT octanoylation assay. Each 50 µl reaction was incubated for 5 min at 37˚C with 50 µg microsome protein, 1 µM octanoyl-CoA, 50 µM palmitoyl-CoA, 10 µM Ghrelin27. Microsomes made with control virus made from empty vector and Ghrelin27-S3A are shown as controls. (C) Activity of microsomes containing untagged GOAT, N-GOAT-3xFlag-C, and N-His_{10}-GOAT-3xFlag-C under the same conditions as (B). (D) Anti-Flag immunoblot of High Five and SF9 cells infected with GOAT-3xFlag virus for the indicated times. EV=virus made with empty vector, 48 hours. Each lane contains the equivalent of 20 µl suspension culture. (E) Microsome preparation from 1 L cultures of SF9 and High Five (Hi5) cells. Loading shows two different amounts at each step and an equivalent fraction of the total is shown at each step. (F) 25 µg microsome protein from High Five or SF9 cells were incubated for the indicated time at 37˚C with 1 µM

octanoyl-CoA, 50 μM palmitoyl-CoA, 10 μM Ghrelin27. (G) The indicated protease inhibitors were pre-incubated with GOAT microsomes for 5 min before 1 min assay. PI cocktail: 2 μg/mL Leupeptin, Aprotinin, Pepstatin A, 2mM EGTA. (H, I) GOAT microsomes stability. Microsomes were pre-incubated at the 37°C or on ice, respectively, at 95% of final assay concentration for the indicated times and then assayed for 1 or 2.5 min.

Acyltransferase assays with this SF9 microsomal GOAT preparation (Figure 1B) (Barnett et al., 2010; Taylor et al., 2012b) showed robust conversion to product, approximately 500-fold greater than that with the HEK-293 microsomal preparation and ~100-fold signal over background. This assay uses biotinylated human ghrelin (Ghrelin27-biotin) and ^{3}H-octanoyl-CoA and is comparable to that reported for proghrelin-His_8 (Yang et al., 2008b) . Ghrelin containing a Ser3Ala mutation showed undetectable (background) levels acyl transfer, despite the presence of serines at positions 2 and 6, recapitulating the known specificity of GOAT (Yang et al., 2008a; Yang et al., 2008b). Untagged and two different tagged GOAT preparations showed similar acyltransferase activity (Figure 1C).

High Five cells are an alternate lepidopteran cell line used with baculoviral expression systems that can sometimes express more recombinant protein than SF9 cells (Honegger et al., 1981). We therefore expressed GOAT-3xFlag in both High Five and SF9 cells. Optimal protein expression 48 hours after infection, and higher in High Five than SF9 (Figure 1D). Microsomes made from both cell lines (Figure 1E) were assayed for 1 min and 2.5 min (Figure 1F), and although SF9 microsomes contained less GOAT, they were more active. Therefore, SF9 cells were selected for further use.

We also systematically screened protease inhibitor conditions to determine how they impacted GOAT activity (Figure 1G). The commercial protease inhibitor tablet (Roche) compared with our standard cocktail (leupeptin, aprotinin, peptstatin A, EGTA) greatly inhibited GOAT activity.There was modest inhibition from the serine protease inhibitors AEBSF and PMSF. We next assayed the stability of microsomal GOAT activity on standing. With preincubation at 37˚C, there was an apparent exponential decay in signal with $t_{1/2}$ of approximately 20 min (Figure 1H). On ice, there was little change in signal after 6 hours, and approximately 30% of activity remained after 24 hours (Figure 1I). Efforts to obtain detergent solubilized GOAT activity were unsuccessful (see *Materials and Methods*).

Prior studies revealed that GOAT activity rapidly diminishes over time (Yang et al., 2008b). This was somewhat ameliorated with the addition of 50 μM palmitoyl-CoA to limit microsomal octanoyl-CoA hydrolysis. Our standard assay, which includes 50 μM palmitoyl-CoA shows a reduction in activity as a function of time in less than 2 minutes (Figure 2). This non-linearity persisted despite attempts to stabilize the enzyme by reducing the temperature or adjusting palmitoyl-CoA concentration. We employed the shortest practical time-pont 1 min, to approximate initial conditions for further studies. Under these conditions, there is a linear relationship between octanoyltransferase activity and the amount of microsomes added up to 25 μg (0.5ug/μL) as shown in Figure 2G. We therefore used these conditions to approximate steady-state kinetic parameters as discussed below.

Figure 4.2. GOAT octanoylation assay optimization.

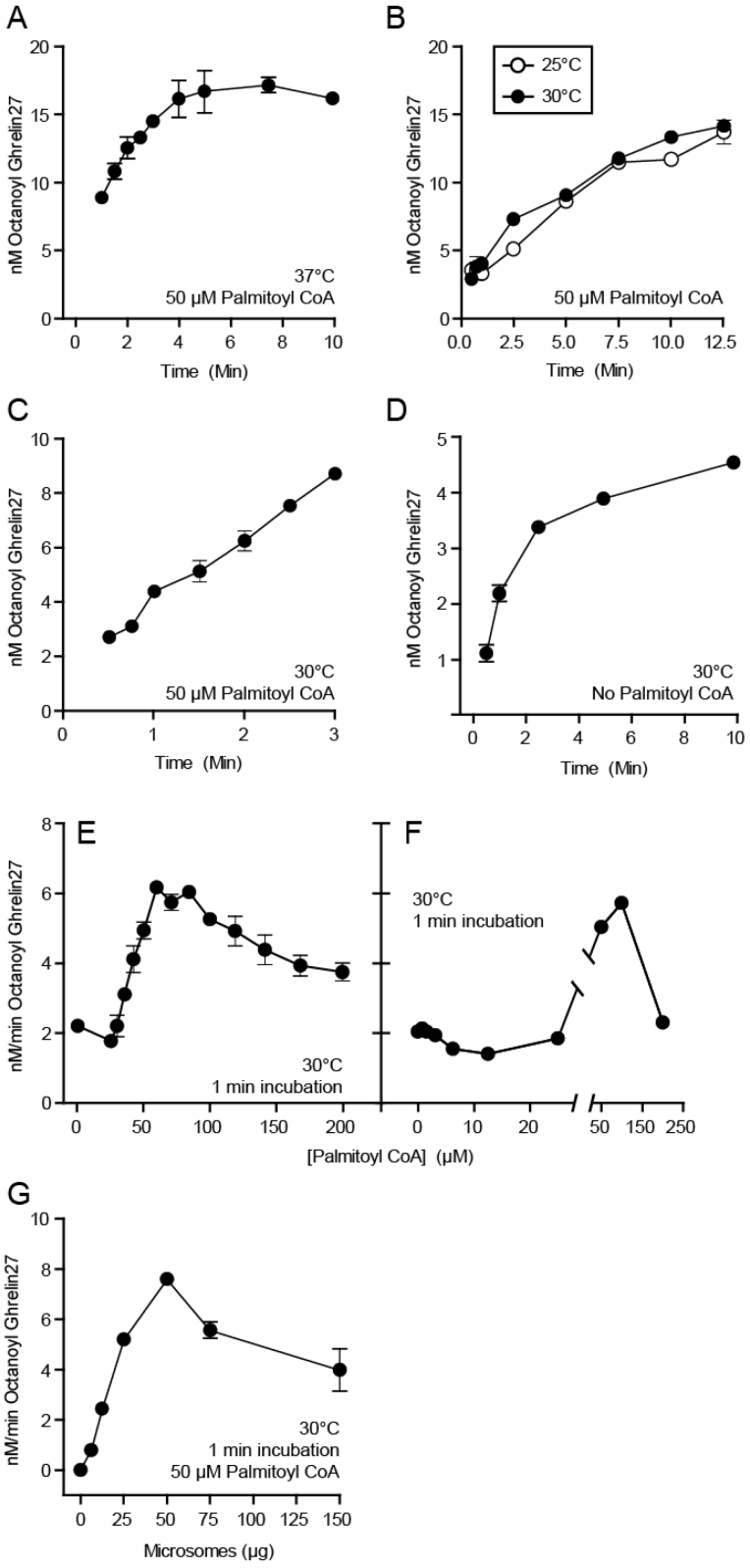

Legend, Figure 4.2. (A) Reaction mixtures containing 10 μM Ghrelin27, 1 μM octanoyl-CoA, 50 μM palmitoyl-CoA, and 25 μg microsome protein were incubated at 37°C for the indicated time and then quenched in 2% SDS. (B) Activity over time for 10 μM Ghrelin27 at 25°C and 30°C. (C) Activity over time for 10 μM Ghrelin27 at 30°C, with 50 μM palmitoyl-CoA in the reaction mixture. (D) Activity over time for 10 μM Ghrelin27 at 30°C, without 50 μM palmitoyl-CoA in the reaction mixture. (E,F) Activity in 1 min assay at 30°C with indicated concentration of palmitoyl-CoA. Error bars in F (range of duplicates) are smaller than the data points. (G) Activity in 1 min at 30°C assay containing 50 μM palmitoyl-CoA with the indicated amount of microsome protein added to the reaction mixture.

Figure 4.3. Kinetic Measurements for ghrelin substrates.

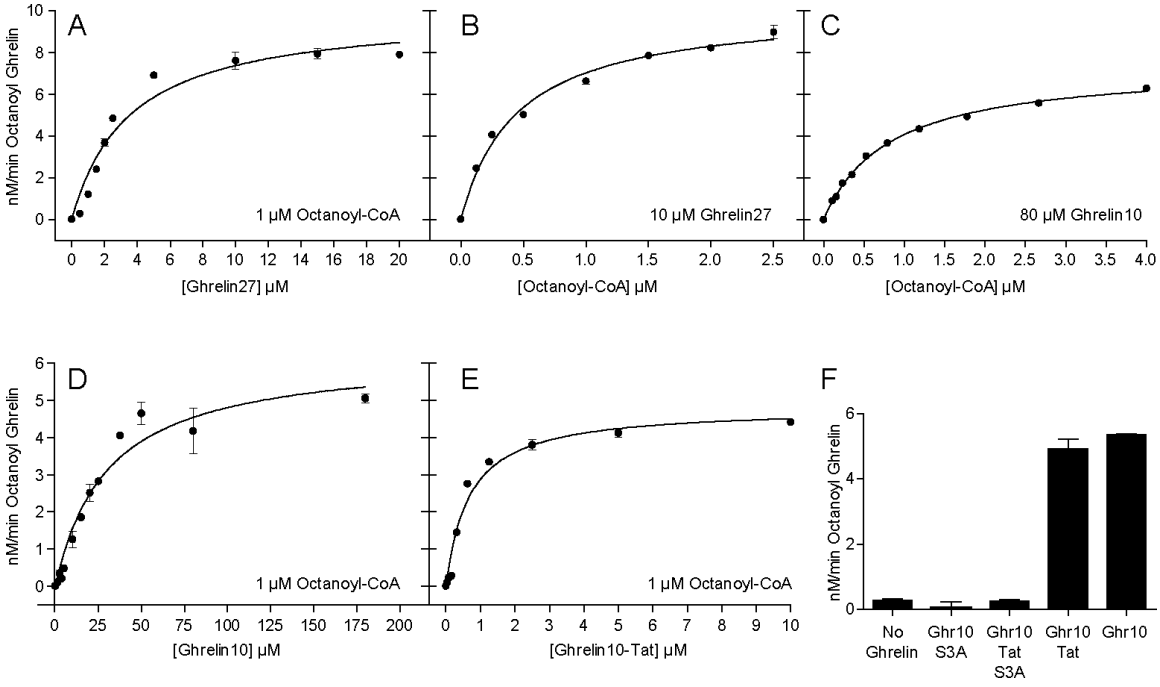

Legend, Figure 4.3. Each assay mixture was incubated at 30°C for 1 min in the presence of 50 μM palmitoyl-CoA with 25 μg microsome protein. Solid lines are best-fit to the Michaelis-Menten equation, and K_m values are shown in Table 1. (A) Ghrelin27 with 1 μM octanoyl-CoA. (B) Octanoyl-CoA with 10 μM Ghrelin27. (C) Octanoyl-CoA with 80 μM Ghrelin10. (D) Ghrelin10 with 1 μM octanoyl-CoA. (E) Ghrelin10-Tat with 1 μM octanoyl-CoA. (F) Each reaction contained 50 μM of the indicated substrate; Ghr10, Ghrelin10.

Kinetic measurements and substrate structure:activity

The GOAT reaction demonstrated apparent Michaelis-Menten kinetics with respect to the substrates ghrelin and octanoyl-CoA (Figure 3A, 3B). The apparent K_m values for octanoyl-CoA and Ghrelin27 were 0.44 and 3.5 μM, respectively, comparable to published values 0.6 and 6 μM (Yang et al., 2008b) (the latter is for proghrelin-His_8; proghrelin is likely the natural substrate for GOAT (Taylor et al., 2012b)). The apparent K_m for octanoyl-CoA was in the range of 0.4-0.8 μM depending on the ghrelin substrate.

The shorter substrate Ghrelin10 was efficiently octanoylated, but displayed ~ 10-fold higher apparent K_m than Ghrelin27 (Figure 3D and Table 1). Ghrelin10-Tat showed ~ 5-fold lower apparent K_m than Ghrelin27 (Figure 3E and Table 1). As expected, S3A ghrelin substrate mutants were not processed (Figure 3F).

Table 4.1. Ghrelin substrate sequences and apparent kinetic measurements

Substrate	Sequence	K_m (apparent), μM	V_{max} (apparent) (nmol/min/mg)
Ghrelin27	GSSFLSPEHQRVQQRKESKKPPAKLQ PK(Biotin)G	3.5 ± 0.60	230 ± 10
Dap3-Ghrelin27	GS(Dap)FLSPEHQRVQQRKESKKPP AKLQPK(Biotin)G	3.4 ± 0.61	85 ± 5
Ghrelin10	GSSFLSPEHQ(Ahx)K(Biotin)G	30.4 ± 5.1	160 ± 10
Dap3-Ghrelin10	GS(Dap)FLSPEHQ(Ahx)K(Biotin)G	33.9 ± 9.6	74 ± 8
Ghrelin10-Tat	GSSFLSPEHQ(Ahx) K(Biotin)YGRKKRRQRRR	0.68 ± 0.09	120 ± 50
Octanoyl-CoA	*(vs 10 μM Ghrelin27)*	0.44 ± 0.04	250 ± 8
Octanoyl-CoA	*(vs 80 μM Ghrelin10)*	0.81 ± 0.04	190 ± 4

Legend, Table 4.1. All reactions were carried out for 1 min at 30°C with 25 μg microsome protein and 50 μM palmitoyl-CoA. 1 μM octanoyl-CoA was used in the ghrelin measurements.

Figure 4.4. GOAT octanoylates Dap3 substrates.

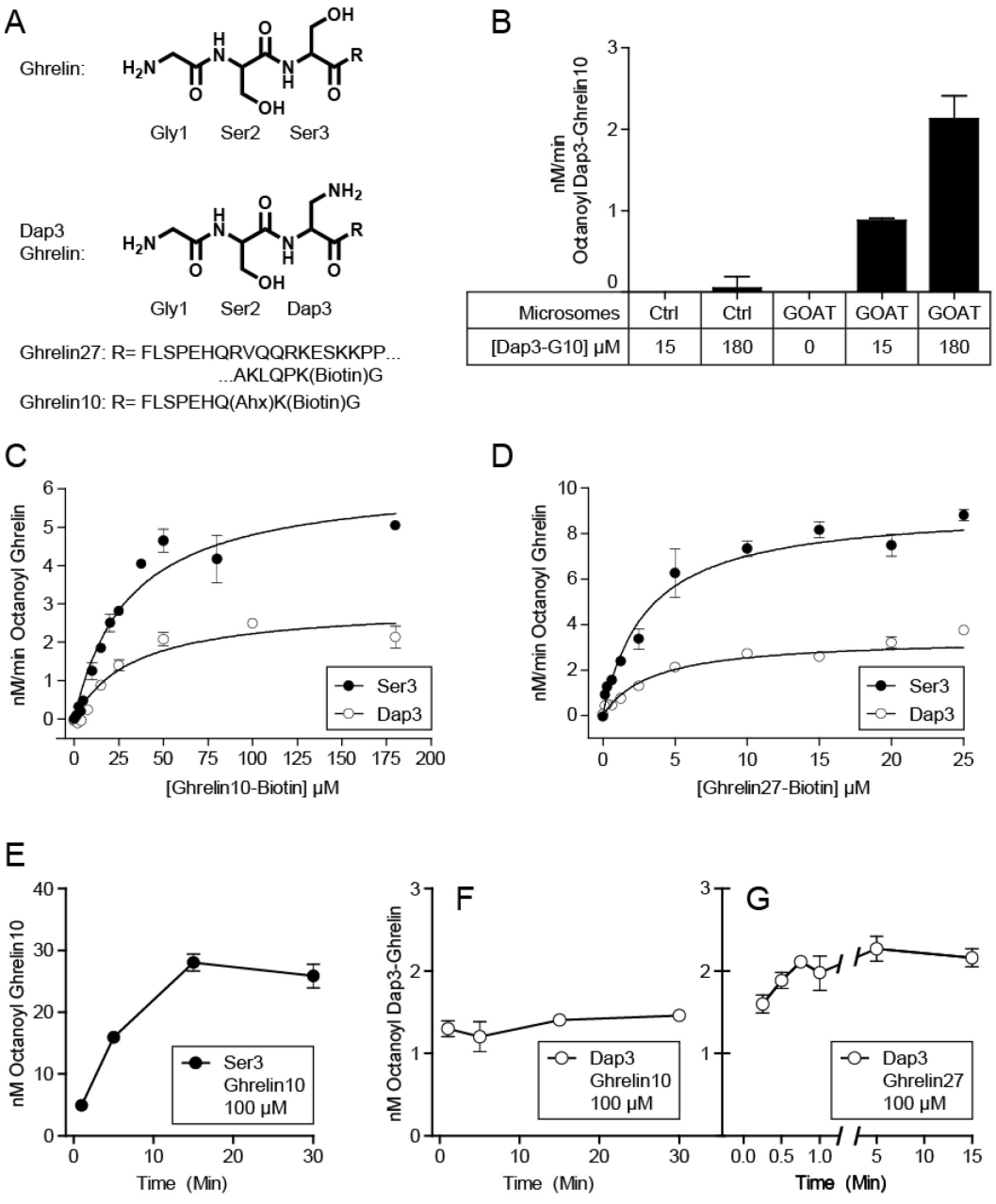

Legend, Figure 4.4. (A) Structure of Ghrelin and Dap3 (amino-alanine) analog. (B) Octanoylation of Dap3-Ghrelin10 (Dap3-G10) requires GOAT. 25 μg GOAT or empty-vector virus control microsomes were incubated for 1 min at 30°C with 1 μM octanoyl-CoA, 50 μM palmitoyl-CoA, and the indicated concentration of Dap3-Ghrelin10. (C) Kinetic measurements for Ghrelin10 and Dap3-Ghrelin10 and D, kinetic measurements for Ghrelin27 and Dap3-Ghrelin27 with 1 μM octanoyl-CoA. Solid lines are best-fit to the Michaelis-Menten equation, and K_m values are shown in Table 1. (E) Octanoylation of 100 μM Ser3 Ghrelin10 over time. Each mixture contained 25 μg membrane protein, 1 μM octanoyl-CoA, and 50 μM palmitoyl-CoA. (F,G) Octanoylation of Dap3-Ghrelin10 (100 μM) and Dap3-Ghrelin27 (10 μM) over time, respectively.

Octanoylation of Dap3 Ghreln Analogs

To explore the chemical flexibility of GOAT, We replaced Ser3 in Ghrelin27 and Ghrelin10 with amino-alanine (Dap), which substitutes the serine sidechain –OH with –NH_2. The structure of the first 3 residues of ghrelin and the Dap3 analogs are shown in Figure 4A. Dap3-Ghrelin10 can be octanoylated in the octanoyltransferase assay in a GOAT-dependent fashion (Figure 4B). Reactions for Dap3-Ghrelin10 (Figure 4C) and Dap3-Ghrelin27 (Figure 4D) display saturation kinetics, with K_m for both substrates indistinguishable from their natural Ser3 analogs (Table 1). Maximum reaction rates for both substrates was approximately 2-fold lower than for the natural Ser analogs.

Acyl ghrelin analog inhibition has previously been reported for GOAT, with more potent inhibition by amide-linked octanoyl ghrelin pentapeptides than for ester-linked peptides (Yang et al., 2008b). Therefore, we compared the formation of product over time for Ghrelin10 (Figure 4E), Dap3-Ghrelin10 (Figure 4F), and Dap3-Ghrelin27 (Figure 4G) under the standard assay conditions (30°C, 25 μg microsome protein, 1 μM octanoyl-

CoA, 50 μM palmitoyl-CoA). The Ghrelin10 (Ser3) reaction continues to increase in signal for 15 min, with linearity for at least the first 5 min; similar results were seen with Ghrelin27 (Figure 2B, C). In contrast, no additional signal is seen for Dap3-Ghrelin10 and Dap3-Ghrelin27 after 1 min (Figure 4 F,G), and therefore it appears that there is severe product inhibition for amine but less so for hydroxyl substrates.

Chemical reactivity of Dap3-Ghrelin octanoylation product

While the radioactive incorporation assay was consistent with GOAT-catalyzed amide bond formation of the Dap3-ghrelin substrates, it was formally possible that the presence of the amino group at the 3-position leads to site-switching to afford Ser ester products. To assess this possibility, we employed the nucleophilic amines hydroxylamine and hydrazine that can readily cleave ester but not amide functionalities. (Bizzozero, 1995) (Yang et al., 2008a). As a positive control, strepavidin-immobilized biotin-tagged ^{3}H-octanoylated Ghrelin10 and Ghrelin27 when treated immobilized with 1M hydroxylamine or 1M hydrazine (Nigst et al., 2012) induced substantial loss of the radioactivity into the supernatant, expected because of aminolysis of the ester linkages. In comparison,no detectable cleavage occured in the 1M MES-treated control reaction (Figure 5A). Because we had incomplete cleavage with hydroxylamine for octanoylated Ghrelin27, we selected hydrazine for the experiment with Ghrelin10 (Ser3) and Dap3-Ghrelin10 (Figure 5B). Nearly all the [^{3}H]-octanoate was released into the supernatant for octanoylated-Ghrelin10, whereas octanoylated-Dap3-Ghrelin resisted hydrazine treatemnt. These results confirm

that the octanoylated Dap3-adducts are indeed amide rather than ester modified (Honegger et al., 1981).

Figure 4.5 GOAT forms an octanoyl-amide on Dap3-Ghrelin substrates.

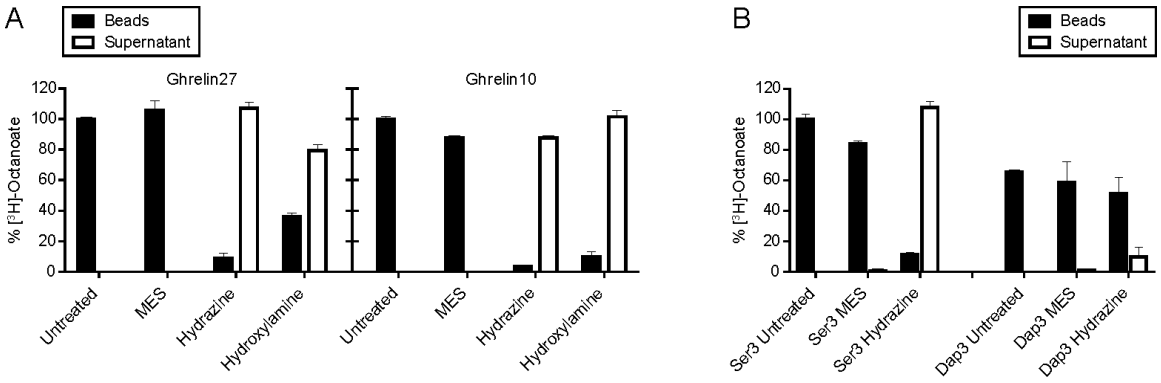

Legend, Figure 4.5. (A) Hydrazine and hydroxylamine cleavage of octanoylated ghrelin. Reaction mixtures were incubated 1 min at 30°C with 10 μM Ghrelin27 or 100 μM Ghrelin10, quenched in 2% SDS, bound to streptavidin resin, and washed. Capped columns were then incubated overnight with 1 mL of 1M hydrazine or hydroxylamine; 1 M MES buffer was used as a control. Beads and supernatants were then scintillation counted. (B) Ghrelin10 (Ser3) and Dap3-Ghrelin10 were treated with hydrazine or MES as in (A).

pH Sensitivity of Ser3 and Dap3 Ghrelin Octanoylation

Because the pK_a of the sidechain of amino-Ala (RNH_3+ to RNH_2 pKa is ~8 (Lan et al., 2010)) is dramatically different from that of the sidechain of Ser (ROH to RO- is ~13 (Bruice et al., 1962)), we hypothesized that the GOAT-catalyzed acyl transfer reactions with the two substrates might show sharply different pH sensitivities if proton transfer of the nucleophile were rate-determining. We measured the rate of ghrelin octanoylation for Ser3-containing Ghrelin10 and Dap3-Ghrelin10 at 7.5 μM (sub-saturating), and 100 μM (saturating) as shown in Figure 6. As shown, the rates for both substrates are relatively

insensitive to pH throughought the range 6-9, with no more than a 2-fold variation for each substrate. These results suggest that deprotonation of the nucleophile does not appear to be rate-limiting for the overall GOAT reaction.

Figure 4.6. Rate of Ser3 and Dap3-Ghrelin10 Substrates at pH 6-9.

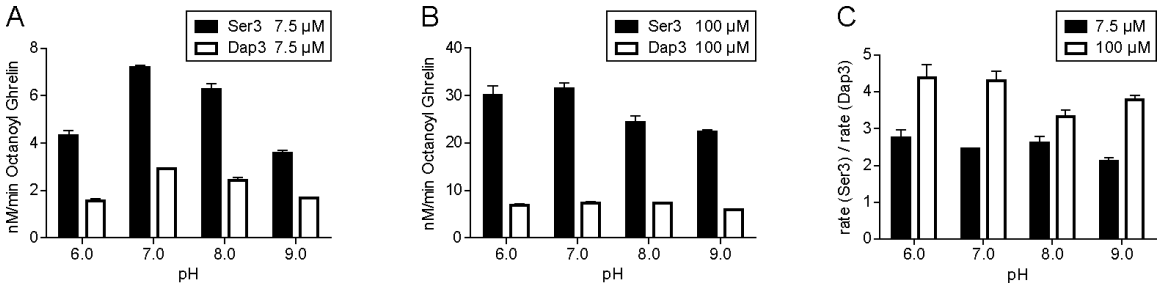

Legend, Figure 4.6. Reactions were carried out for 1 min in 100 mM Bis-Tris Propane at the indicated pH using Ghrelin10 (Ser3) and Dap3-Ghrelin10. Rates for Ser3 and Dap3 at 7.5 µM are shown in (A) and 100 µM in (B). 100 µM is saturating conditions (see Figure 4C). The ratio of the rate of the two substrates across pH 6-9 is shown in (C).

Failure to Purify Active GOAT

Because of the limitations of the microsomal assay, and given our ability to produce and purify milligram quantities of GOAT from SF9 membranes in FosCholine-16 micelles that retain the ability to bind ghrelin analogs (Taylor et al., 2013), we worked to find conditions in which GOAT could be solubilized in detergent without loss of activity. Previous attempts to solubilize active GOAT had been unsuccessful (Taylor et al., 2012b; Yang et al., 2008b). We purified and tag-cleaved GOAT as previously reported (Taylor et al., 2013) in the detergent FC-16 (final 0.0008%, 1.5 × CMC). The protein was monodisperse as previously reported but was inactive in our assay, with concentrations

tested ranging from the amount present in a standard microsomal assay (~ 10 ng) to 25 μg per 50 μL reaction. In case some required factor present in microsomes had been removed in our purification, in 50 μL reactions we mixed 50 μg control microsomes (lacking GOAT) with varying amounts of purified GOAT; there was still no activity. We exchanged GOAT from FosCholine-16 into 1.2 × CMC *n*-octyl-β-D-glucopyranoside (OG), *n*-dodecyl-β-D-maltoside (DDM), and lauryldimethylamine-*N*-oxide (LDAO) by size exclusion; GOAT aggregated in OG but a significant fraction was monodisperse in both DDM and LDAO (not shown). However, both monodisperse fractions were similarly inactive, without or with control microsomes.

We next screened 35 detergents for compatibility with the GOAT octanoyltransfer. We hypothesized that because GOAT transfers an octanoyl group, *n*-alkyl detergents might be inhibitory, especially those with chains of around 8-carbons. Therefore, we selected longer-chain detergents and a number of detergents with alternate hydrophobic moieties, including bile-salt-based detergents, a tripod amine oxide and two tripod glycosides (Chae et al., 2010a; Chae et al., 2008), maltose neopentyl glycol (MNG-3) (Chae et al., 2010b), glucose neoptentyl glycol (GNG-3)(Chae et al., 2013), and the doxycholate-based glycoside GCT-3 (Bae et al., Submitted). We also included mixed micelles of cholesteryl hemisuccinate plus CHAPS, MNG-3 (Lauryl Maltose Neopentyl Glycol), or FC-16.

Because detergents must be above the CMC to maintain soluble integral membrane protein, we screened most detergents at both ~1.5 × CMC and 1mM (~0.02-0.1% w/v),

adding detergent to the assay during preincubation; promising detergents were tested at additional concentrations. The results are shown in Supplementary Table 1. Most detergents abolished GOAT activity at concentrations above their CMC. However, a number of low-CMC detergents were compatible with octanoyltransfer at concentrations at least 5-10 fold higher than their CMC, including FC-16, GCT-3, MNG-3, and *n*-tetradecyl-N,N-dimethylglycine, and *n*-tetradecyl-β-D-maltoside.

Table 4.2. Detergent compatibility with GOAT octanoyltransferase assay.

Page 1 of 3

Detergent	CMC (mM)	mM	w/v (%)	CMCs	Activity (% Ctrl) 0.5 µg/µl	Activity (% Ctrl) 1 µg/µl
Anzergent 3-14	0.16	1.000	0.036%	6.3	**0%**	**-2%**
APO 10	4.66	1.000	0.022%	0.2	**52%**	**111%**
		10.000	0.218%	2.1	**2%**	
Big Chap	2.9	1.000	0.088%	0.3	**14%**	
		1.000	0.088%	0.3	**11%**	**86%**
		4.350	0.382%	1.5	**1%**	
		10.000	0.878%	3.4	**6%**	
Brij35	0.09	1.000	0.120%	11.1	**2%**	**-1%**
C13E8	0.1	1.000	0.055%	10.0	**-1%**	**-2%**
CHAPS	8	1.000	0.061%	0.1	**109%**	
		1.000	0.061%	0.1	**72%**	**90%**
		10.000	0.614%	1.3	**79%**	
		12.000	0.737%	1.5	**0%**	
		25.000	1.535%	3.1	**1%**	
		50.000	3.070%	6.3	**0%**	
CHAPS+Cholesteryl Hemisuccinate	8	12.000	0.737%	1.5	**2%**	
		25.000	1.535%	3.1	**-1%**	
		50.000	3.070%	6.3	**-4%**	
CHAPSO	8	1.000	0.063%	0.1	**101%**	
		12.000	0.757%	1.5	**0%**	
Cholate	9.5	1.000	0.043%	0.1	**101%**	
		14.250	0.614%	1.5	**-1%**	
CycloFos 6	2.68	1.000	0.035%	0.4	**104%**	**311%**
		3.000	0.105%	1.1		**0%**
		10.000	0.349%	3.7		**0%**
CycloFos 7	0.62	0.100	0.004%	0.2	**101%**	
		0.300	0.011%	0.5	**117%**	
		1.000	0.036%	1.6	**1%**	**0%**
Cymal 6	0.56	1.000	0.051%	1.8	**-1%**	**-1%**
Cymal 7	0.19	1.000	0.052%	5.3	**-2%**	**-1%**
Cy-TripGlu	1.8	1.000	0.067%	0.6	**4%**	
		2.700	0.180%	1.5	**1%**	
Digitonin	0.5	0.100	0.012%	0.2		**103%**
		1.000	0.123%	2.0		**2%**
Dodecyl Maltoside	0.17	1.000	0.051%	5.9	**-1%**	**-2%**
Deoxy Big Chap	1.4	1.000	0.086%	0.7	**15%**	
		2.100	0.181%	1.5	**2%**	
Deoxycholate	6	1.000	0.041%	0.2	**-2%**	
		9.000	0.373%	1.5	**0%**	

Table 4.2. Detergent compatibility with GOAT octanoyltransferase assay.

Page 2 of 3

Detergent	CMC (mM)	mM	w/v (%)	CMCs	Activity (% Ctrl) 0.5 µg/µl	Activity (% Ctrl) 1 µg/µl
Fos-Choline-12	1.5	1.000	0.035%	0.7	**2%**	
		3.000	0.105%	2.0	**-1%**	
Fos-Choline-13	0.75	1.000	0.037%	1.3	**2%**	**-2%**
Fos-Choline-16	0.013	0.001	0.000%	0.1	**93%**	
		0.010	0.000%	0.8	**87%**	
		0.020	0.001%	1.5	**100%**	
		0.100	0.004%	7.7	**93%**	
		0.140	0.006%	10.7	**93%**	
		0.245	0.010%	18.9	**91%**	
		1.000	0.041%	76.9	**-2%**	**-1%**
		1.000	0.041%	76.9	**1%**	**-1%**
		2.454	0.100%	188.8	**-3%**	
		24.540	1.000%	1887.7	**0%**	
FosCholine-16+Cholesteryl Hemisuccinate		0.140	0.006%	10.7	**44%**	
		1.000	0.041%	76.9	**-3%**	
GCT-3	0.018	0.027	0.003%	1.5	**81%**	
		0.083	0.010%	4.6	**117%**	
		0.261	0.032%	14.5	**59%**	
		0.826	0.100%	45.9	**1%**	
		0.826	0.100%	45.9	**0%**	
		2.613	0.316%	145.2	**1%**	
		8.264	1.000%	459.1	**2%**	
		8.264	1.000%	459.1	**-3%**	
		26.135	3.162%	1451.9	**0%**	
GNG-3 (Glucose Neopentyl Glycol)	1.02	1.000	0.057%	1.0	**1%**	
		3.000	0.171%	2.9	**0%**	
		9.000	0.512%	8.8	**-2%**	
Hexadecyl Maltoside	0.0006	1.000	0.057%	1666.7	**2%**	**76%**
		3.000	0.170%	5000.0	**-1%**	
		10.000	0.567%	16666.7	**1%**	
LysoFos-Choline 14	0.036	1.000	0.047%	27.8	**0%**	**-1%**
LysoFos-Choline 18	0.0003	1.000	0.052%	3333.3	**0%**	**-1%**

Table 4.2. Detergent compatibility with GOAT octanoyltransferase assay.

Page 3 of 3

Detergent	CMC (mM)	mM	w/v (%)	CMCs	Activity (% Ctrl) 0.5 µg/µl	Activity (% Ctrl) 1 µg/µl
MNG-3 (Maltose Neopentyl Glycol)	0.01	0.015	0.002%	1.5	**129%**	
		0.015	0.002%	1.5	**105%**	
		0.047	0.005%	4.7	**98%**	
		0.100	0.010%	10.0	**88%**	
		0.122	0.012%	12.2	**23%**	
		0.387	0.039%	38.7	**6%**	
		1.225	0.123%	122.5	**6%**	
		0.995	0.100%	99.5	**1%**	
		1.000	0.101%	100.0	**6%**	
		3.162	0.318%	316.2	**2%**	
		5.000	0.503%	500.0	**3%**	
		9.950	1.000%	995.0	**8%**	
		10.000	1.005%	1000.0	**-3%**	
		10.000	1.005%	1000.0	**1%**	
MNG-3+Chonlesteryl Hemisuccinate	0.01	1.000	0.101%	100.0	**4%**	
		5.000	0.503%	500.0	**1%**	
Octyl Glucoside	19.5	1.000	0.029%	0.1		**-1%**
		1.000	0.029%	0.1		**35%**
		10.000	0.292%	0.5	**-3%**	
		30.000	0.876%	1.5	**-7%**	
Ph-TripGlu	3.6	1.000	0.066%	0.3	**62%**	
		5.400	0.356%	1.5	**0%**	
Sucrose Monododecanoate	0.3	1.000	0.053%	3.3	**-1%**	**-2%**
Taurocholate	3	1.000	0.054%	0.3	**92%**	**82%**
		4.500	0.242%	1.5	**7%**	
TDAO (Tetradecyl Dimethylamine Oxide)	0.29	1.000	0.026%	3.4	**1%**	**23%**
		10.000	0.257%	34.5	**3%**	
Tetradecyl Maltoside	0.01	0.100	0.005%	10.0	**94%**	
		1.000	0.054%	100.0	**0%**	**44%**
		3.000	0.162%	300.0	**0%**	
		10.000	0.539%	1000.0	**1%**	
Tetradecyl Dimethyl Glycine	0.034	1.000	0.030%	29.4	**-1%**	**-2%**
Triton X-100	0.23	0.100	0.006%	0.4	**87%**	**133%**
		1.000	0.065%	4.3		**-1%**
TRIPAO	4.5	1.000	0.036%	0.2	**13%**	
		6.750	0.245%	1.5	**1%**	

Figure 4.7. Attempts to solubilize active GOAT.

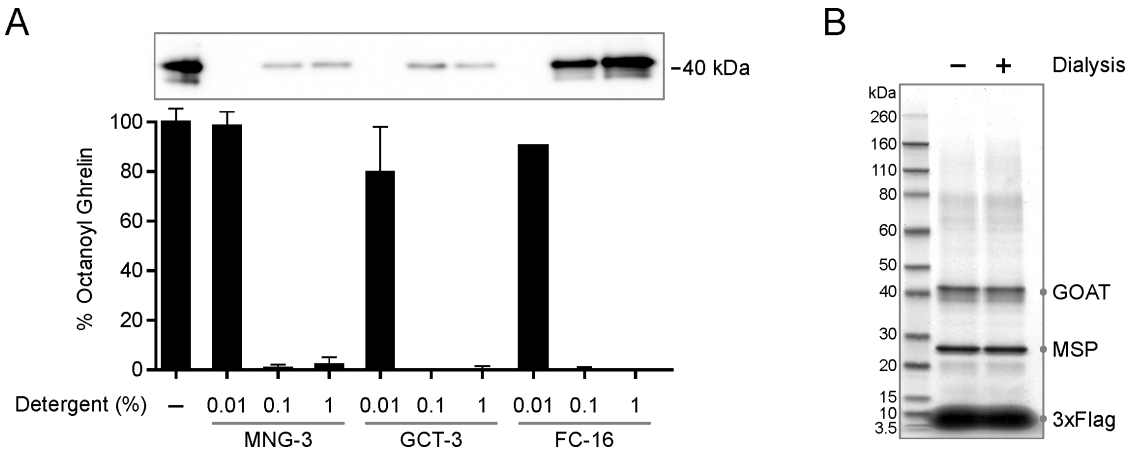

Legend, Figure 4.7. (A) GOAT-3xFlag micelles retain activity only at detergent concentrations too low to solubilize GOAT. Microsomes were incubated for 1 hour with the indicated detergents and then a fraction of each mixture was assayed for activity (lower panel). The remaining mixture was cleared by ultracentrifugation and in all cases had no activity. Top panel: α-Flag immunoblot demonstrates the amount of GOAT solubilized in each supernatant. Gel lanes correspond to the amount of protein solubilized in the assay points below. The positive control in lane 1 was not ultracentrifuged prior to gel loading. (B) Coomassie-stained SDS-PAGE of GOAT-3xFlag-MSP-POPC nanodiscs after packaging, size exclusion chromatography, and re-purification by Flag affinity. Samples are shown before and after 20-hour dialysis against HBS.

To examine whether solubilization had occurred in any of these conditions where activity seemed to remain, GOAT microsomes were solubilized for one hour with MNG-3, GCT-3, and FC-16 at 0.01%, 0.1%, and 1% (w/v) each and assayed for activity before and after ultracentrifugation (Figure 7A). Note that 0.01% is 5-20 × CMC for each detergent. No activity remained after ultracentrifugation, and activity was retained before solubilization at only 0.01% for each detergent, a condition in which no detectable GOAT was solubilzied (Figure 4.7A).

We next removed detergent by reconstitution of purified GOAT into a phosphatidylcholine bilayer, packaging 3xFlag-tagged GOAT into nanodiscs (Ritchie et al., 2009). The Membrane Scaffold Proritein (MSP)-GOAT-lipid complex was monodisperse on size exclusion in the absence of detergent, with calculated MW ~ 280 kDa (not shown), consistent with successful packaging. When this complex was immobilized by α-Flag affinity and eluted with 3xFlag peptide, the expected 2:1 ratio of MSP:GOAT was achieved and the complex was stable through multiple rounds of dialysis against buffer lacking detergent (Figure 4.7B). However, the preparation was inactive, with or without the addition of control microsomes.

Discussion

In this study we provide new insights into GOAT's catalytic mechanism, building on a number of contemporary studies (Barnett et al., 2010; Darling et al., 2013; Darling et al., 2015; Yang et al., 2008b). Using recombinant baculovirus expressing mouse GOAT in insect cells and synthetic biotin-tagged ghrelin analogs ranging from 10-27 residues in length, we identified conditions which have allowed us to approximate initial steady-state conditions. However, the inability to have a solubilized, purified catalytically active system and likely the complexity of the GOAT-catalyzed process itself still hamper a more precise enzymologic analysis.

That Ghrelin27 shows a 10-fold lower apparent K_m relative to that of Ghrelin10, suggests that the C-terminal peptide sequence contributes to binding with GOAT, the lipid bilayer, or both. These 17 additional residues include 3 Lys, 2 Arg, and 1 Glu for a net +4 positive charge, which may contribute to enhanced apparent affinity through electrostatic interactions. Supporting this hypothesis, when these 17 residues were replaced with the Tat sequence (which has a net positive charge of +8), the apparent K_m is lowered an additional 5-fold. This was also fortuitous for the design of our inhibitor GO-CoA-Tat(Barnett et al., 2010).

The ability to produce ghrlein substrates using solid phase peptide synthesis allowed us to explore the chemistry of acylation by comparing peptides bearing the natural Ser and artificial amino-alanine (Dap) at position 3, substituting the serine hydroxyl for an amine. We demonstrate that GOAT has the ability to octanoylate either hydroxyl or amine acceptor, forming an ester or amide bond (see below). The K_m for Ser3 and Dap3 versions of both ghrelin substrates were indistinguishable, but the Dap3 reaction was nonlinear within the first 30 seconds, resulting in a lower apparent rate due to severe apparent product inhibiton.

We compared the rates of Ser3 and Dap3 substrates from pH 6.0-9.0. The serine hydroxyl has a pKa of approximately 13 and will not change protonation over this range. In contrast, the pK_a of the β-NH_2 group in Dap is approximately 8 {Bruice, 1962 #704;Lan, 2010 #125}. We note that sidechain pKa may be shifted by a number of pH units in the microenvironment of an enzyme active site (Harris and Turner, 2002) and may also be

reduced in the hydrophobic context of microsomes. Thus, the combination of the rate similarity for amine and hydroxy nucleophilic substrates and the insensitivity to pH suggests that the chemical step is unlikely to be rate-limiting in the catalytic mechanism. As discussed previously, transporting and positioning octanoyl-CoA through the lipid bilayer may be the slow step for the overall GOAT reaction. Perhaps future studies that explore GOAT's role in substrate transferring may be illuminating on this point.

The ability of GOAT to funcation as both an *O*- and *N*-acyltransferase is a property shared with a number of other *O*-acyltransferases, but uncommon among *N*-acyltransferases. The *O*-acyltransferases carnitine acetyltransferase, carnitine palmitoyltransferase I, and carntine octanoyltransferase can all process amino-substrates, albeit at reduced rate; carntine palmitoyltransferase II (CPTII) showed no reactivity. As seen with GOAT, amide-linked product analogs are potent inhibitors of these enzymes (Jenkins and Griffith, 1985; Murthy et al., 1990; Yang et al., 2008b). LpxA from gram negative bacteria in which Lipid A contains only *O*-linked fatty acids can acylate either UDP-GlcNac or its amine analog UDP-GlcNac3N. In contrast, LpxA from bacteria containing only N-linked fatty acids cannot accept the hydroxyl substrate UDP-GlcNac (Sweet et al., 2004). Aminoglycoside *N*-acetyltransferase from *mycobacterium tuberculosis* AAC(2')-Ic acylates aminoglycoside antibiotics with 2' amino or 2' hydroxyl groups, with higher efficiency for 2'-amino substrates. In spite of the name, the natural substrate of this enzyme is unknown, and therefore could be either hydroxyl or amine*(Hegde et al., 2001)*.

The structure of AAC(2')-Ic supports a reaction mechanism where the 2' amino or hydroxyl is positioned for direct nucleophilic attack on acetyl-CoA (Vetting et al., 2002).

In contrast with the versatility in reaction chemistry of the majority of *O*-acyltransferases, neither Serotonin *N*-acetyltransferase nor Tetrahydrodipicolinate *N*-succinyltransferase can acylate the hydroxyl analog of their natural substrate. It was hypothesized previously that these differences in reactivity might be due to mechanistic requirements for increased nucleophilicity of the amine substrate (De Angelis et al., 1998). A corollary to this is that *O*-selectivity may be more difficult to achieve than *N*-selectivity, and therefore a deeper understanding of the mechanistic differences of these enzymes will have implications for engineering selective reactivity. This selectivity appears to be present in CPTII and was also demonstrated for the polyketide associated acyltransferase PapA5, which acylates the hydroxyl substrate octanol but not octylamine (Onwueme et al., 2004).

REFERENCES

Ali, S., Chen, J.A., and Garcia, J.M. (2013). Clinical development of ghrelin axis-derived molecules for cancer cachexia treatment. Current opinion in supportive and palliative care *7*, 368-375.

Andrews, Z.B., Liu, Z.W., Walllingford, N., Erion, D.M., Borok, E., Friedman, J.M., Tschöp, M.H., Shanabrough, M., Cline, G., Shulman, G.I., *et al.* (2008). UCP2 mediates ghrelin's action on NPY/AgRP neurons by lowering free radicals. Nature *454*, 846-851.

Arai, M., Mitsuke, H., Ikeda, M., Xia, J.X., Kikuchi, T., Satake, M., and Shimizu, T. (2004). ConPred II: a consensus prediction method for obtaining transmembrane topology models with high reliability. Nucleic acids research *32*, W390-393.

Ariyasu, H., Takaya, K., Iwakura, H., Hosoda, H., Akamizu, T., Arai, Y., Kangawa, K., and Nakao, K. (2005). Transgenic mice overexpressing des-acyl ghrelin show small phenotype. Endocrinology *146*, 355-364.

Bae, H.E., Gotfryd, K., Pacyna, J., Hussain, H., Ehsan, M., Loland, C.J., Byrne, B., and Chae, P.S. (Submitted). Doxycholate-based Glycosides (DCGs) for Membrane Protein Stabilisation.

Baldanzi, G., Filigheddu, N., Cutrupi, S., Catapano, F., Bonissoni, S., Fubini, A., Malan, D., Baj, G., Granata, R., Broglio, F., *et al.* (2002). Ghrelin and des-acyl ghrelin inhibit cell death in cardiomyocytes and endothelial cells through ERK1/2 and PI 3-kinase/AKT. J Cell Biol *159*, 1029-1037.

Barkan, A.L., Dimaraki, E.V., Jessup, S.K., Symons, K.V., Ermolenko, M., and Jaffe, C.A. (2003). Ghrelin secretion in humans is sexually dimorphic, suppressed by somatostatin, and not affected by the ambient growth hormone levels. J Clin Endocr Metab *88*, 2180-2184.

Barnett, B.P., Hwang, Y., Taylor, M.S., Kirchner, H., Pfluger, P.T., Bernard, V., Lin, Y.Y., Bowers, E.M., Mukherjee, C., Song, W.J., *et al.* (2010). Glucose and weight control in mice with a designed ghrelin O-acyltransferase inhibitor. Science *330*, 1689-1692.

Bednarek, M.A., Feighner, S.D., Pong, S.S., McKee, K.K., Hreniuk, D.L., Silva, M.V., Warren, V.A., Howard, A.D., Van Der Ploeg, L.H., and Heck, J.V. (2000). Structure-function studies on the new growth hormone-releasing peptide, ghrelin: minimal sequence of ghrelin necessary for activation of growth hormone secretagogue receptor 1a. Journal of medicinal chemistry *43*, 4370-4376.

Bernsel, A., Viklund, H., Hennerdal, A., and Elofsson, A. (2009). TOPCONS: consensus prediction of membrane protein topology. Nucleic acids research *37*, W465-468.

Bizzozero, O.A. (1995). Chemical analysis of acylation sites and species. Methods in enzymology *250*, 361-379.

Bosson, R., Jaquenoud, M., and Conzelmann, A. (2006). GUP1 of Saccharomyces cerevisiae encodes an O-acyltransferase involved in remodeling of the GPI anchor. Mol Biol Cell *17*, 2636-2645.

Broglio, F., Gottero, C., Prodam, F., Gauna, C., Muccioli, G., Papotti, M., Abribat, T., Van Der Lely, A.J., and Ghigo, E. (2004). Non-acylated ghrelin counteracts the metabolic but not the neuroendocrine response to acylated ghrelin in humans. The Journal of clinical endocrinology and metabolism *89*, 3062-3065.

Bruice, T.C., Fife, T.H., Bruno, J.J., and Brandon, N.E. (1962). Hydroxyl group catalysis. II. The reactivity of the hydroxyl group of serine. The nucleophilicity of alcohols and the ease of hydrolysis of their acetyl esters as related to their pKa. Biochemistry *1*, 7-12.

Buglino, J.A., and Resh, M.D. (2008). Hhat is a palmitoylacyltransferase with specificity for N-palmitoylation of Sonic Hedgehog. J Biol Chem *283*, 22076-22088.

Buglino, J.A., and Resh, M.D. (2010). Identification of conserved regions and residues within Hedgehog acyltransferase critical for palmitoylation of Sonic Hedgehog. PLoS One *5*, e11195.

Cao, Y., Tang, J., Yang, T., Ma, H., Yi, D., Gu, C., and Yu, S. (2013). Cardioprotective effect of ghrelin in cardiopulmonary bypass involves a reduction in inflammatory response. PLoS One *8*, e55021.

Carlini, V.P., Monzon, M.E., Varas, M.M., Cragnolini, A.B., Schioth, H.B., Scimonelli, T.N., and de Barioglio, S.R. (2002). Ghrelin increases anxiety-like behavior and memory retention in rats. Biochemical and biophysical research communications *299*, 739-743.

Chae, P.S., Guzei, I.A., and Gellman, S.H. (2010a). Crystallographic characterization of N-oxide tripod amphiphiles. Journal of the American Chemical Society *132*, 1953-1959.

Chae, P.S., Rana, R.R., Gotfryd, K., Rasmussen, S.G., Kruse, A.C., Cho, K.H., Capaldi, S., Carlsson, E., Kobilka, B., Loland, C.J., *et al.* (2013). Glucose-neopentyl glycol (GNG) amphiphiles for membrane protein study. Chem Commun (Camb) *49*, 2287-2289.

Chae, P.S., Rasmussen, S.G., Rana, R.R., Gotfryd, K., Chandra, R., Goren, M.A., Kruse, A.C., Nurva, S., Loland, C.J., Pierre, Y., *et al.* (2010b). Maltose-neopentyl glycol (MNG) amphiphiles for solubilization, stabilization and crystallization of membrane proteins. Nature methods *7*, 1003-1008.

Chae, P.S., Wander, M.J., Bowling, A.P., Laible, P.D., and Gellman, S.H. (2008). Glycotripod amphiphiles for solubilization and stabilization of a membrane-protein superassembly: importance of branching in the hydrophilic portion. Chembiochem : a European journal of chemical biology *9*, 1706-1709.

Chamoun, Z., Mann, R.K., Nellen, D., von Kessler, D.P., Bellotto, M., Beachy, P.A., and Basler, K. (2001). Skinny hedgehog, an acyltransferase required for palmitoylation and activity of the hedgehog signal. Science *293*, 2080-2084.

Chang, T.Y., Li, B.L., Chang, C.C., and Urano, Y. (2009). Acyl-coenzyme A:cholesterol acyltransferases. American journal of physiology Endocrinology and metabolism *297*, E1-9.

Chen, H.Y., Trumbauer, M.E., Chen, A.S., Weingarth, D.T., Adams, J.R., Frazier, E.G., Shen, Z., Marsh, D.J., Feighner, S.D., Guan, X.M., *et al.* (2004a). Orexigenic action of peripheral ghrelin is mediated by neuropeptide Y and agouti-related protein. Endocrinology *145*, 2607-2612.

Chen, M.H., Li, Y.J., Kawakami, T., Xu, S.M., and Chuang, P.T. (2004b). Palmitoylation is required for the production of a soluble multimeric Hedgehog protein complex and long-range signaling in vertebrates. Genes & development *18*, 641-659.

Church, R.F.R., and Weiss, M.J. (1970). Diazirines. II. Synthesis and properties of small functionalized diazirine molecules. Observations on the reaction of a diaziridine with the iodine-iodide ion system. J Org Chem *35*, 2465-2471.

Claros, M.G., and von Heijne, G. (1994). TopPred II: an improved software for membrane protein structure predictions. Computer applications in the biosciences : CABIOS *10*, 685-686.

Clevers, H. (2006). Wnt/beta-catenin signaling in development and disease. Cell *127*, 469-480.

Cowley, M.A., Smith, R.G., Diano, S., Tschöp, M., Pronchuk, N., Grove, K.L., Strasburger, C.J., Bidlingmaier, M., Esterman, M., Heiman, M.L., *et al.* (2003). The distribution and mechanism of action of ghrelin in the CNS demonstrates a novel hypothalamic circuit regulating energy homeostasis. Neuron *37*, 649-661.

Cruz, C.R., and Smith, R.G. (2008). The growth hormone secretagogue receptor. Vitamins and hormones *77*, 47-88.

Cummings, D.E., Purnell, J.Q., Frayo, R.S., Schmidova, K., Wisse, B.E., and Weigle, D.S. (2001). A preprandial rise in plasma ghrelin levels suggests a role in meal initiation in humans. Diabetes *50*, 1714-1719.

Darling, J.E., Prybolsky, E.P., Sieburg, M., and Hougland, J.L. (2013). A fluorescent peptide substrate facilitates investigation of ghrelin recognition and acylation by ghrelin O-acyltransferase. Anal Biochem *437*, 68-76.

Darling, J.E., Zhao, F., Loftus, R.J., Patton, L.M., Gibbs, R.A., and Hougland, J.L. (2015). Structure-activity analysis of human ghrelin O-acyltransferase reveals chemical determinants of ghrelin selectivity and acyl group recognition. Biochemistry *54*, 1100-1110.

Date, Y., Kojima, M., Hosoda, H., Sawaguchi, A., Mondal, M.S., Suganuma, T., Matsukura, S., Kangawa, K., and Nakazato, M. (2000). Ghrelin, a novel growth hormone-releasing acylated peptide, is synthesized in a distinct endocrine cell type in the gastrointestinal tracts of rats and humans. Endocrinology *141*, 4255-4261.

De Angelis, J., Gastel, J., Klein, D.C., and Cole, P.A. (1998). Kinetic analysis of the catalytic mechanism of serotonin N-acetyltransferase (EC 2.3.1.87). J Biol Chem *273*, 3045-3050.

De Vriese, C., Gregoire, F., De Neef, P., Robberecht, P., and Delporte, C. (2005). Ghrelin is produced by the human erythroleukemic HEL cell line and involved in an autocrine pathway leading to cell proliferation. Endocrinology *146*, 1514-1522.

Deshaies, R.J., and Schekman, R. (1987). A yeast mutant defective at an early stage in import of secretory protein precursors into the endoplasmic reticulum. J Cell Biol *105*, 633-645.

Dezaki, K., Kakei, M., and Yada, T. (2007). Ghrelin uses Galphai2 and activates voltage-dependent K+ channels to attenuate glucose-induced Ca2+ signaling and insulin release in islet beta-cells: novel signal transduction of ghrelin. Diabetes *56*, 2319-2327.

Dezaki, K., Sone, H., and Yada, T. (2008). Ghrelin is a physiological regulator of insulin release in pancreatic islets and glucose homeostasis. Pharmacology & therapeutics *118*, 239-249.

Diano, S., Farr, S.A., Benoit, S.C., McNay, E.C., da Silva, I., Horvath, B., Gaskin, F.S., Nonaka, N., Jaeger, L.B., Banks, W.A., *et al.* (2006). Ghrelin controls hippocampal spine synapse density and memory performance. Nature neuroscience *9*, 381-388.

Dornonville de la Cour, C., Lindstrom, E., Norlen, P., and Hakanson, R. (2004). Ghrelin stimulates gastric emptying but is without effect on acid secretion and gastric endocrine cells. Regul Pept *120*, 23-32.

Edgar, R.C. (2004). MUSCLE: multiple sequence alignment with high accuracy and high throughput. Nucleic acids research *32*, 1792-1797.

Egecioglu, E., Jerlhag, E., Salome, N., Skibicka, K.P., Haage, D., Bohlooly, Y.M., Andersson, D., Bjursell, M., Perrissoud, D., Engel, J.A., *et al.* (2010). Ghrelin increases intake of rewarding food in rodents. Addiction biology *15*, 304-311.

Garner, A.L., and Janda, K.D. (2010). cat-ELCCA: a robust method to monitor the fatty acid acyltransferase activity of ghrelin O-acyltransferase (GOAT). Angewandte Chemie *49*, 9630-9634.

Garner, A.L., and Janda, K.D. (2011). A small molecule antagonist of ghrelin O-acyltransferase (GOAT). Chem Commun (Camb) *47*, 7512-7514.

Gauna, C., Meyler, F.M., Janssen, J.A., Delhanty, P.J., Abribat, T., van Koetsveld, P., Hofland, L.J., Broglio, F., Ghigo, E., and van der Lely, A.J. (2004). Administration of acylated ghrelin reduces insulin sensitivity, whereas the combination of acylated plus unacylated ghrelin strongly improves insulin sensitivity. The Journal of clinical endocrinology and metabolism *89*, 5035-5042.

Goldstein, J.L., Zhao, T.J., Li, R.L., Sherbet, D.P., Liang, G., and Brown, M.S. (2011). Surviving Starvation: Essential Role of the Ghrelin-Growth Hormone Axis. Cold Spring Harb Symp Quant Biol.

Granata, R., Baragli, A., Settanni, F., Scarlatti, F., and Ghigo, E. (2010). Unraveling the role of the ghrelin gene peptides in the endocrine pancreas. Journal of molecular endocrinology *45*, 107-118.

Groschl, M., Uhr, M., and Kraus, T. (2004). Evaluation of the comparability of commercial ghrelin assays. Clinical chemistry *50*, 457-458.

Gualillo, O., Lago, F., and Dieguez, C. (2008). Introducing GOAT: a target for obesity and anti-diabetic drugs? Trends in pharmacological sciences *29*, 398-401.

Guan, X.M., Yu, H., Palyha, O.C., McKee, K.K., Feighner, S.D., Sirinathsinghji, D.J., Smith, R.G., Van der Ploeg, L.H., and Howard, A.D. (1997). Distribution of mRNA encoding the growth hormone secretagogue receptor in brain and peripheral tissues. Brain research Molecular brain research *48*, 23-29.

Guo, Z.Y., Chang, C.C., Lu, X., Chen, J., Li, B.L., and Chang, T.Y. (2005a). The disulfide linkage and the free sulfhydryl accessibility of acyl-coenzyme A:cholesterol acyltransferase 1 as studied by using mPEG5000-maleimide. Biochemistry *44*, 6537-6546.

Guo, Z.Y., Lin, S., Heinen, J.A., Chang, C.C., and Chang, T.Y. (2005b). The active site His-460 of human acyl-coenzyme A:cholesterol acyltransferase 1 resides in a hitherto undisclosed transmembrane domain. J Biol Chem *280*, 37814-37826.

Gupta, R., Jung, E., and Brunak, S. (2004). Prediction of N-glycosylation sites in human proteins (In Preparation).

Gutierrez, J.A., Solenberg, P.J., Perkins, D.R., Willency, J.A., Knierman, M.D., Jin, Z., Witcher, D.R., Luo, S., Onyia, J.E., and Hale, J.E. (2008). Ghrelin octanoylation mediated by an orphan lipid transferase. Proc Natl Acad Sci U S A *105*, 6320-6325.

Hardy, R.Y., and Resh, M.D. (2012). Identification of N-terminal residues of Sonic Hedgehog important for palmitoylation by Hedgehog acyltransferase. J Biol Chem *287*, 42881-42889.

Harris, T.K., and Turner, G.J. (2002). Structural basis of perturbed pKa values of catalytic groups in enzyme active sites. IUBMB life *53*, 85-98.

Hegde, S.S., Javid-Majd, F., and Blanchard, J.S. (2001). Overexpression and mechanistic analysis of chromosomally encoded aminoglycoside 2'-N-acetyltransferase (AAC(2')-Ic) from Mycobacterium tuberculosis. J Biol Chem *276*, 45876-45881.

Heller, R.S., Jenny, M., Collombat, P., Mansouri, A., Tomasetto, C., Madsen, O.D., Mellitzer, G., Gradwohl, G., and Serup, P. (2005). Genetic determinants of pancreatic epsilon-cell development. Dev Biol *286*, 217-224.

Hines, A.C., and Cole, P.A. (2004). Design, synthesis, and characterization of an ATP-peptide conjugate inhibitor of protein kinase A. Bioorganic & medicinal chemistry letters *14*, 2951-2954.

Hirokawa, T., Boon-Chieng, S., and Mitaku, S. (1998). SOSUI: classification and secondary structure prediction system for membrane proteins. Bioinformatics *14*, 378-379.

Hirsch, C., Gauss, R., Horn, S.C., Neuber, O., and Sommer, T. (2009). The ubiquitylation machinery of the endoplasmic reticulum. Nature *458*, 453-460.

Hofmann, K. (2000). A superfamily of membrane-bound O-acyltransferases with implications for wnt signaling. Trends in biochemical sciences *25*, 111-112.

Honegger, A., Hughes, G.J., and Wilson, K.J. (1981). Chemical modification of peptides by hydrazine. The Biochemical journal *199*, 53-59.

Howard, A.D., Feighner, S.D., Cully, D.F., Arena, J.P., Liberator, P.A., Rosenblum, C.I., Hamelin, M., Hreniuk, D.L., Palyha, O.C., Anderson, J., *et al.* (1996). A receptor in pituitary and hypothalamus that functions in growth hormone release. Science *273*, 974-977.

Inlow, D., Shauger, A., and Maiorella, B. (1989). Insect Cell Culture and Baculovirus Propagation in Protein-Free Medium. J Tissue Culture Methods *12*.

Iwakura, H., Li, Y., Ariyasu, H., Hosoda, H., Kanamoto, N., Bando, M., Yamada, G., Hosoda, K., Nakao, K., Kangawa, K., *et al.* (2010). Establishment of a novel ghrelin-producing cell line. Endocrinology *151*, 2940-2945.

Jenkins, D.L., and Griffith, O.W. (1985). DL-aminocarnitine and acetyl-DL-aminocarnitine. Potent inhibitors of carnitine acyltransferases and hepatic triglyceride catabolism. J Biol Chem *260*, 14748-14755.

Jones, D.T. (2007). Improving the accuracy of transmembrane protein topology prediction using evolutionary information. Bioinformatics *23*, 538-544.

Joseph, J.W., Koshkin, V., Zhang, C.Y., Wang, J., Lowell, B.B., Chan, C.B., and Wheeler, M.B. (2002). Uncoupling protein 2 knockout mice have enhanced insulin secretory capacity after a high-fat diet. Diabetes *51*, 3211-3219.

Kadowaki, T., Wilder, E., Klingensmith, J., Zachary, K., and Perrimon, N. (1996). The segment polarity gene porcupine encodes a putative multitransmembrane protein involved in Wingless processing. Genes & development *10*, 3116-3128.

Kaiya, H., Kojima, M., Hosoda, H., Koda, A., Yamamoto, K., Kitajima, Y., Matsumoto, M., Minamitake, Y., Kikuyama, S., and Kangawa, K. (2001). Bullfrog ghrelin is modified by n-octanoic acid at its third threonine residue. J Biol Chem *276*, 40441-40448.

Kall, L., Krogh, A., and Sonnhammer, E.L. (2007). Advantages of combined transmembrane topology and signal peptide prediction--the Phobius web server. Nucleic acids research *35*, W429-432.

Kamegai, J., Tamura, H., Shimizu, T., Ishii, S., Sugihara, H., and Wakabayashi, I. (2001). Chronic central infusion of ghrelin increases hypothalamic neuropeptide Y and Agouti-related protein mRNA levels and body weight in rats. Diabetes *50*, 2438-2443.

Kanamoto, N., Akamizu, T., Hosoda, H., Hataya, Y., Ariyasu, H., Takaya, K., Hosoda, K., Saijo, M., Moriyama, K., Shimatsu, A., *et al.* (2001). Substantial production of ghrelin by a human medullary thyroid carcinoma cell line. The Journal of clinical endocrinology and metabolism *86*, 4984-4990.

Kim, H., Melen, K., Osterberg, M., and von Heijne, G. (2006). A global topology map of the Saccharomyces cerevisiae membrane proteome. Proc Natl Acad Sci U S A *103*, 11142-11147.

Kim, H., Melen, K., and von Heijne, G. (2003). Topology models for 37 Saccharomyces cerevisiae membrane proteins based on C-terminal reporter fusions and predictions. J Biol Chem *278*, 10208-10213.

Kirchner, H., Gutierrez, J.A., Solenberg, P.J., Pfluger, P.T., Czyzyk, T.A., Willency, J.A., Schurmann, A., Joost, H.G., Jandacek, R.J., Hale, J.E., *et al.* (2009). GOAT links dietary lipids with the endocrine control of energy balance. Nature medicine *15*, 741-745.

Kojima, M., Hosoda, H., Date, Y., Nakazato, M., Matsuo, H., and Kangawa, K. (1999). Ghrelin is a growth-hormone-releasing acylated peptide from stomach. Nature *402*, 656-660.

Kojima, M., and Kangawa, K. (2005). Ghrelin: structure and function. Physiological reviews *85*, 495-522.

Korbonits, M., Ciccarelli, E., Ghigo, E., and Grossman, A.B. (1999). The growth hormone secretagogue receptor. Growth hormone & IGF research : official journal of the Growth Hormone Research Society and the International IGF Research Society *9 Suppl A*, 93-99.

Kreft, S.G., Wang, L., and Hochstrasser, M. (2006). Membrane topology of the yeast endoplasmic reticulum-localized ubiquitin ligase Doa10 and comparison with its human ortholog TEB4 (MARCH-VI). J Biol Chem *281*, 4646-4653.

Krogh, A., Larsson, B., von Heijne, G., and Sonnhammer, E.L. (2001). Predicting transmembrane protein topology with a hidden Markov model: application to complete genomes. Journal of molecular biology *305*, 567-580.

Ku, J.M., Andrews, Z.B., Barsby, T., Reichenbach, A., Lemus, M.B., Drummond, G.R., Sleeman, M.W., Spencer, S.J., Sobey, C.G., and Miller, A.A. (2015). Ghrelin-related peptides exert protective effects in the cerebral circulation of male mice through a nonclassical ghrelin receptor(s). Endocrinology *156*, 280-290.

Lan, Y., Langlet-Bertin, B., Abbate, V., Vermeer, L.S., Kong, X., Sullivan, K.E., Leborgne, C., Scherman, D., Hider, R.C., Drake, A.F., *et al.* (2010). Incorporation of 2,3-diaminopropionic acid into linear cationic amphipathic peptides produces pH-sensitive vectors. Chembiochem : a European journal of chemical biology *11*, 1266-1272.

Lau, O.D., Kundu, T.K., Soccio, R.E., Ait-Si-Ali, S., Khalil, E.M., Vassilev, A., Wolffe, A.P., Nakatani, Y., Roeder, R.G., and Cole, P.A. (2000). HATs off: selective synthetic inhibitors of the histone acetyltransferases p300 and PCAF. Mol Cell *5*, 589-595.

Lee, H.C., Inoue, T., Imae, R., Kono, N., Shirae, S., Matsuda, S., Gengyo-Ando, K., Mitani, S., and Arai, H. (2008). Caenorhabditis elegans mboa-7, a member of the MBOAT family, is required for selective incorporation of polyunsaturated fatty acids into phosphatidylinositol. Mol Biol Cell *19*, 1174-1184.

Li, B., Zeng, M., He, W., Huang, X., Luo, L., Zhang, H., and Deng, D.Y. (2015). Ghrelin protects alveolar macrophages against lipopolysaccharide-induced apoptosis through growth hormone secretagogue receptor 1a-dependent c-Jun N-terminal kinase and Wnt/beta-catenin signaling and suppresses lung inflammation. Endocrinology *156*, 203-217.

Li, R.L., Sherbet, D.P., Elsbernd, B.L., Goldstein, J.L., Brown, M.S., and Zhao, T.J. (2012). Profound hypoglycemia in starved, ghrelin-deficient mice is caused by decreased gluconeogenesis and reversed by lactate or fatty acids. J Biol Chem.

Lin, S., Lu, X., Chang, C.C., and Chang, T.Y. (2003). Human acyl-coenzyme A:cholesterol acyltransferase expressed in chinese hamster ovary cells: membrane topology and active site location. Mol Biol Cell *14*, 2447-2460.

Liu, J., Prudom, C.E., Nass, R., Pezzoli, S.S., Oliveri, M.C., Johnson, M.L., Veldhuis, P., Gordon, D.A., Howard, A.D., Witcher, D.R., *et al.* (2008). Novel ghrelin assays provide evidence for independent regulation of ghrelin acylation and secretion in healthy young men. The Journal of clinical endocrinology and metabolism *93*, 1980-1987.

Lopez, M., Lage, R., Saha, A.K., Perez-Tilve, D., Vazquez, M.J., Varela, L., Sangiao-Alvarellos, S., Tovar, S., Raghay, K., Rodriguez-Cuenca, S., *et al.* (2008). Hypothalamic fatty acid metabolism mediates the orexigenic action of ghrelin. Cell metabolism *7*, 389-399.

Lu, S.C., Xu, J., Chinookoswong, N., Liu, S., Steavenson, S., Gegg, C., Brankow, D., Lindberg, R., Veniant, M., and Gu, W. (2009). An acyl-ghrelin-specific neutralizing antibody inhibits the acute ghrelin-mediated orexigenic effects in mice. Molecular pharmacology *75*, 901-907.

Marchler-Bauer, A., Zheng, C., Chitsaz, F., Derbyshire, M.K., Geer, L.Y., Geer, R.C., Gonzales, N.R., Gwadz, M., Hurwitz, D.I., Lanczycki, C.J., *et al.* (2013). CDD: conserved domains and protein three-dimensional structure. Nucleic acids research *41*, D348-352.

Matevossian, A., and Resh, M.D. (2015). Membrane topology of hedgehog acyltransferase. J Biol Chem *290*, 2235-2243.

McFarlane, M.R., Brown, M.S., Goldstein, J.L., and Zhao, T.J. (2014). Induced ablation of ghrelin cells in adult mice does not decrease food intake, body weight, or response to high-fat diet. Cell metabolism *20*, 54-60.

McFie, P.J., Stone, S.L., Banman, S.L., and Stone, S.J. (2010). Topological orientation of acyl-CoA:diacylglycerol acyltransferase-1 (DGAT1) and identification of a putative active site histidine and the role of the n terminus in dimer/tetramer formation. J Biol Chem *285*, 37377-37387.

Mitchell, L.A., Cai, Y., Taylor, M., Noronha, A.M., Chuang, J., Dai, L., and Boeke, J.D. (2013). Multichange Isothermal Mutagenesis: a new strategy for multiple site-directed mutations in plasmid DNA. ACS Synth Biol.

Morton, G.J., and Schwartz, M.W. (2001). The NPY/AgRP neuron and energy homeostasis. International journal of obesity and related metabolic disorders : journal of the International Association for the Study of Obesity *25 Suppl 5*, S56-62.

Murray, S., Tulloch, A., Gold, M.S., and Avena, N.M. (2014). Hormonal and neural mechanisms of food reward, eating behaviour and obesity. Nature reviews Endocrinology *10*, 540-552.

Murthy, M.S., Ramsay, R.R., and Pande, S.V. (1990). Acyl-CoA chain length affects the specificity of various carnitine palmitoyltransferases with respect to carnitine analogues. Possible application in the discrimination of different carnitine palmitoyltransferase activities. The Biochemical journal *267*, 273-276.

Nigst, T.A., Antipova, A., and Mayr, H. (2012). Nucleophilic reactivities of hydrazines and amines: the futile search for the alpha-effect in hydrazine reactivities. The Journal of organic chemistry *77*, 8142-8155.

Nilsson, I.M., and von Heijne, G. (1993). Determination of the distance between the oligosaccharyltransferase active site and the endoplasmic reticulum membrane. J Biol Chem *268*, 5798-5801.

Nishi, Y., Hiejima, H., Hosoda, H., Kaiya, H., Mori, K., Fukue, Y., Yanase, T., Nawata, H., Kangawa, K., and Kojima, M. (2005). Ingested medium-chain fatty acids are directly utilized for the acyl modification of ghrelin. Endocrinology *146*, 2255-2264.

Nugent, T., and Jones, D.T. (2012). Detecting pore-lining regions in transmembrane protein sequences. BMC bioinformatics *13*, 169.

Nussbaum, S.R., Zahradnik, R.J., Lavigne, J.R., Brennan, G.L., Nozawa-Ung, K., Kim, L.Y., Keutmann, H.T., Wang, C.A., Potts, J.T., Jr., and Segre, G.V. (1987). Highly sensitive two-site immunoradiometric assay of parathyrin, and its clinical utility in evaluating patients with hypercalcemia. Clinical chemistry *33*, 1364-1367.

Okumura, H., Nagaya, N., Enomoto, M., Nakagawa, E., Oya, H., and Kangawa, K. (2002). Vasodilatory effect of ghrelin, an endogenous peptide from the stomach. Journal of cardiovascular pharmacology *39*, 779-783.

Onwueme, K.C., Ferreras, J.A., Buglino, J., Lima, C.D., and Quadri, L.E. (2004). Mycobacterial polyketide-associated proteins are acyltransferases: proof of principle with Mycobacterium tuberculosis PapA5. Proc Natl Acad Sci U S A *101*, 4608-4613.

Ozawa, A., Speaker, R.B., 3rd, and Lindberg, I. (2009). Enzymatic characterization of a human acyltransferase activity. PLoS One *4*, e5426.

Pagac, M., de la Mora, H.V., Duperrex, C., Roubaty, C., Vionnet, C., and Conzelmann, A. (2011). Topology of 1-acyl-sn-glycerol-3-phosphate acyltransferases SLC1 and ALE1 and related membrane-bound O-acyltransferases (MBOATs) of Saccharomyces cerevisiae. J Biol Chem *286*, 36438-36447.

Pagac, M., Vazquez, H.M., Bochud, A., Roubaty, C., Knopfli, C., Vionnet, C., and Conzelmann, A. (2012). Topology of the microsomal glycerol-3-phosphate acyltransferase Gpt2p/Gat1p of Saccharomyces cerevisiae. Molecular microbiology *86*, 1156-1166.

Parang, K., Till, J.H., Ablooglu, A.J., Kohanski, R.A., Hubbard, S.R., and Cole, P.A. (2001). Mechanism-based design of a protein kinase inhibitor. Nature structural biology *8*, 37-41.

Pasca di Magliano, M., and Hebrok, M. (2003). Hedgehog signalling in cancer formation and maintenance. Nature reviews Cancer *3*, 903-911.

Petersen, T.N., Brunak, S., von Heijne, G., and Nielsen, H. (2011). SignalP 4.0: discriminating signal peptides from transmembrane regions. Nature methods *8*, 785-786.

Petrova, E., Rios-Esteves, J., Ouerfelli, O., Glickman, J.F., and Resh, M.D. (2013). Inhibitors of Hedgehog acyltransferase block Sonic Hedgehog signaling. Nat Chem Biol *9*, 247-249.

Philo, J.S. (2000). A method for directly fitting the time derivative of sedimentation velocity data and an alternative algorithm for calculating sedimentation coefficient distribution functions. Anal Biochem *279*, 151-163.

Porporato, P.E., Filigheddu, N., Reano, S., Ferrara, M., Angelino, E., Gnocchi, V.F., Prodam, F., Ronchi, G., Fagoonee, S., Fornaro, M., *et al.* (2013). Acylated and unacylated ghrelin impair skeletal muscle atrophy in mice. The Journal of clinical investigation *123*, 611-622.

Potocky, T.B., Menon, A.K., and Gellman, S.H. (2003). Cytoplasmic and nuclear delivery of a TAT-derived peptide and a beta-peptide after endocytic uptake into HeLa cells. J Biol Chem *278*, 50188-50194.

Prado, C.L., Pugh-Bernard, A.E., Elghazi, L., Sosa-Pineda, B., and Sussel, L. (2004). Ghrelin cells replace insulin-producing beta cells in two mouse models of pancreas development. Proc Natl Acad Sci U S A *101*, 2924-2929.

Rath, A., Glibowicka, M., Nadeau, V.G., Chen, G., and Deber, C.M. (2009). Detergent binding explains anomalous SDS-PAGE migration of membrane proteins. Proc Natl Acad Sci U S A *106*, 1760-1765.

Resh, M.D. (2012). Targeting protein lipidation in disease. Trends Mol Med *18*, 206-214.

Reya, T., and Clevers, H. (2005). Wnt signalling in stem cells and cancer. Nature *434*, 843-850.

Ritchie, T.K., Grinkova, Y.V., Bayburt, T.H., Denisov, I.G., Zolnerciks, J.K., Atkins, W.M., and Sligar, S.G. (2009). Chapter 11 - Reconstitution of membrane proteins in phospholipid bilayer nanodiscs. Methods in enzymology *464*, 211-231.

Rosenbaum, M., Nicolson, M., Hirsch, J., Heymsfield, S.B., Gallagher, D., Chu, F., and Leibel, R.L. (1996). Effects of gender, body composition, and menopause on plasma concentrations of leptin. The Journal of clinical endocrinology and metabolism *81*, 3424-3427.

Satou, M., Nishi, Y., Yoh, J., Hattori, Y., and Sugimoto, H. (2010). Identification and characterization of acyl-protein thioesterase 1/lysophospholipase I as a ghrelin deacylation/lysophospholipid hydrolyzing enzyme in fetal bovine serum and conditioned medium. Endocrinology *151*, 4765-4775.

Schuck, P. (2000). Size-distribution analysis of macromolecules by sedimentation velocity ultracentrifugation and lamm equation modeling. Biophys J *78*, 1606-1619.

Schwarze, S.R., Ho, A., Vocero-Akbani, A., and Dowdy, S.F. (1999). In vivo protein transduction: delivery of a biologically active protein into the mouse. Science *285*, 1569-1572.

Schwenke, D.O., Tokudome, T., Kishimoto, I., Horio, T., Shirai, M., Cragg, P.A., and Kangawa, K. (2008). Early ghrelin treatment after myocardial infarction prevents an increase in cardiac sympathetic tone and reduces mortality. Endocrinology *149*, 5172-5176.

Sengstag, C. (2000). Using SUC2-HIS4C reporter domain to study topology of membrane proteins in Saccharomyces cerevisiae. Methods in enzymology *327*, 175-190.

Shen, H., and Chou, J.J. (2008). MemBrain: improving the accuracy of predicting transmembrane helices. PLoS One *3*, e2399.

Shindou, H., Eto, M., Morimoto, R., and Shimizu, T. (2009). Identification of membrane O-acyltransferase family motifs. Biochemical and biophysical research communications *383*, 320-325.

Song, W.J., Schreiber, W.E., Zhong, E., Liu, F.F., Kornfeld, B.D., Wondisford, F.E., and Hussain, M.A. (2008). Exendin-4 stimulation of cyclin A2 in beta-cell proliferation. Diabetes *57*, 2371-2381.

Spencer, S.J., Miller, A.A., and Andrews, Z.B. (2013). The role of ghrelin in neuroprotection after ischemic brain injury. Brain sciences *3*, 344-359.

Steculorum, S.M., Collden, G., Coupe, B., Croizier, S., Lockie, S., Andrews, Z.B., Jarosch, F., Klussmann, S., and Bouret, S.G. (2015). Neonatal ghrelin programs development of hypothalamic feeding circuits. The Journal of clinical investigation *125*, 846-858.

Sun, Y., Ahmed, S., and Smith, R.G. (2003). Deletion of ghrelin impairs neither growth nor appetite. Molecular and cellular biology *23*, 7973-7981.

Sun, Y., Asnicar, M., Saha, P.K., Chan, L., and Smith, R.G. (2006). Ablation of ghrelin improves the diabetic but not obese phenotype of ob/ob mice. Cell metabolism *3*, 379-386.

Sun, Y., Wang, P., Zheng, H., and Smith, R.G. (2004). Ghrelin stimulation of growth hormone release and appetite is mediated through the growth hormone secretagogue receptor. Proc Natl Acad Sci U S A *101*, 4679-4684.

Sweet, C.R., Williams, A.H., Karbarz, M.J., Werts, C., Kalb, S.R., Cotter, R.J., and Raetz, C.R. (2004). Enzymatic synthesis of lipid A molecules with four amide-linked acyl chains. LpxA acyltransferases selective for an analog of UDP-N-acetylglucosamine in which an amine replaces the 3"-hydroxyl group. J Biol Chem *279*, 25411-25419.

Swift, A.M., and Machamer, C.E. (1991). A Golgi retention signal in a membrane-spanning domain of coronavirus E1 protein. J Cell Biol *115*, 19-30.

Szewczuk, L.M., Saldanha, S.A., Ganguly, S., Bowers, E.M., Javoroncov, M., Karanam, B., Culhane, J.C., Holbert, M.A., Klein, D.C., Abagyan, R., *et al.* (2007). De novo discovery of serotonin N-acetyltransferase inhibitors. Journal of medicinal chemistry *50*, 5330-5338.

Takada, R., Satomi, Y., Kurata, T., Ueno, N., Norioka, S., Kondoh, H., Takao, T., and Takada, S. (2006). Monounsaturated fatty acid modification of Wnt protein: its role in Wnt secretion. Dev Cell *11*, 791-801.

Takahashi, T., Ida, T., Sato, T., Nakashima, Y., Nakamura, Y., Tsuji, A., and Kojima, M. (2009). Production of n-octanoyl-modified ghrelin in cultured cells requires prohormone processing protease and ghrelin O-acyltransferase, as well as n-octanoic acid. Journal of biochemistry *146*, 675-682.

Tamaki, H., Shimada, A., Ito, Y., Ohya, M., Takase, J., Miyashita, M., Miyagawa, H., Nozaki, H., Nakayama, R., and Kumagai, H. (2007). LPT1 encodes a membrane-bound O-acyltransferase involved in the acylation of lysophospholipids in the yeast Saccharomyces cerevisiae. J Biol Chem *282*, 34288-34298.

Taylor, M.S., Hwang, Y., Hsiao, P.Y., Boeke, J.D., and Cole, P.A. (2012a). Ghrelin O-acyltransferase assays and inhibition. Methods in enzymology *514*, 205-228.

Taylor, M.S., Hwang, Y., Hsiao, P.Y., Boeke, J.D., and Cole, P.A. (2012b). Ghrelin O-acyltransferase assays and inhibition. Methods in enzymology *514*, 205-228.

Taylor, M.S., Ruch, T.R., Hsiao, P.Y., Hwang, Y., Zhang, P., Dai, L., Huang, C.R., Berndsen, C.E., Kim, M.S., Pandey, A., *et al.* (2013). Architectural organization of the metabolic regulatory enzyme ghrelin O-acyltransferase. J Biol Chem *288*, 32211-32228.

Teubner, B.J., Garretson, J.T., Hwang, Y., Cole, P.A., and Bartness, T.J. (2013). Inhibition of ghrelin O-acyltransferase attenuates food deprivation-induced increases in ingestive behavior. Hormones and behavior *63*, 667-673.

Thompson, P.R., Wang, D., Wang, L., Fulco, M., Pediconi, N., Zhang, D., An, W., Ge, Q., Roeder, R.G., Wong, J., *et al.* (2004). Regulation of the p300 HAT domain via a novel activation loop. Nat Struct Mol Biol *11*, 308-315.

Tokudome, T., Kishimoto, I., Miyazato, M., and Kangawa, K. (2014). Ghrelin and the cardiovascular system. Frontiers of hormone research *43*, 125-133.

Tong, J., Prigeon, R.L., Davis, H.W., Bidlingmaier, M., Kahn, S.E., Cummings, D.E., Tschöp, M.H., and D'Alessio, D. (2010). Ghrelin suppresses glucose-stimulated insulin secretion and deteriorates glucose tolerance in healthy humans. Diabetes *59*, 2145-2151.

Trudel, L., Tomasetto, C., Rio, M.C., Bouin, M., Plourde, V., Eberling, P., and Poitras, P. (2002). Ghrelin/motilin-related peptide is a potent prokinetic to reverse gastric postoperative ileus in rat. American journal of physiology Gastrointestinal and liver physiology *282*, G948-952.

Tschöp, M., Smiley, D.L., and Heiman, M.L. (2000). Ghrelin induces adiposity in rodents. Nature *407*, 908-913.

Tschöp, M., Wawarta, R., Riepl, R.L., Friedrich, S., Bidlingmaier, M., Landgraf, R., and Folwaczny, C. (2001). Post-prandial decrease of circulating human ghrelin levels. Journal of endocrinological investigation *24*, RC19-21.

Tusnady, G.E., and Simon, I. (2001). The HMMTOP transmembrane topology prediction server. Bioinformatics *17*, 849-850.

Vetting, M.W., Hegde, S.S., Javid-Majd, F., Blanchard, J.S., and Roderick, S.L. (2002). Aminoglycoside 2'-N-acetyltransferase from Mycobacterium tuberculosis in complex with coenzyme A and aminoglycoside substrates. Nature structural biology *9*, 653-658.

Wang, W., and Malcolm, B.A. (1999). Two-stage PCR protocol allowing introduction of multiple mutations, deletions and insertions using QuikChange Site-Directed Mutagenesis. Biotechniques *26*, 680-682.

Wierup, N., Svensson, H., Mulder, H., and Sundler, F. (2002). The ghrelin cell: a novel developmentally regulated islet cell in the human pancreas. Regul Pept *107*, 63-69.

Willesen, M.G., Kristensen, P., and Romer, J. (1999). Co-localization of growth hormone secretagogue receptor and NPY mRNA in the arcuate nucleus of the rat. Neuroendocrinology *70*, 306-316.

Wortley, K.E., Anderson, K.D., Garcia, K., Murray, J.D., Malinova, L., Liu, R., Moncrieffe, M., Thabet, K., Cox, H.J., Yancopoulos, G.D., *et al.* (2004). Genetic deletion of ghrelin does not decrease food intake but influences metabolic fuel preference. Proc Natl Acad Sci U S A *101*, 8227-8232.

Wortley, K.E., del Rincon, J.P., Murray, J.D., Garcia, K., Iida, K., Thorner, M.O., and Sleeman, M.W. (2005). Absence of ghrelin protects against early-onset obesity. The Journal of clinical investigation *115*, 3573-3578.

Wren, A.M., Seal, L.J., Cohen, M.A., Brynes, A.E., Frost, G.S., Murphy, K.G., Dhillo, W.S., Ghatei, M.A., and Bloom, S.R. (2001a). Ghrelin enhances appetite and increases food intake in humans. The Journal of clinical endocrinology and metabolism *86*, 5992.

Wren, A.M., Small, C.J., Abbott, C.R., Dhillo, W.S., Seal, L.J., Cohen, M.A., Batterham, R.L., Taheri, S., Stanley, S.A., Ghatei, M.A., *et al.* (2001b). Ghrelin causes hyperphagia and obesity in rats. Diabetes *50*, 2540-2547.

Yada, T., Dezaki, K., Sone, H., Koizumi, M., Damdindorj, B., Nakata, M., and Kakei, M. (2008). Ghrelin regulates insulin release and glycemia: physiological role and therapeutic potential. Current diabetes reviews *4*, 18-23.

Yang, J., Brown, M.S., Liang, G., Grishin, N.V., and Goldstein, J.L. (2008a). Identification of the acyltransferase that octanoylates ghrelin, an appetite-stimulating peptide hormone. Cell *132*, 387-396.

Yang, J., Zhao, T.J., Goldstein, J.L., and Brown, M.S. (2008b). Inhibition of ghrelin O-acyltransferase (GOAT) by octanoylated pentapeptides. Proc Natl Acad Sci U S A *105*, 10750-10755.

Yang, J., Zhao, T.J., Goldstein, J.L., and Brown, M.S. (2008c). Inhibition of ghrelin O-acyltransferase (GOAT) by octanoylated pentapeptides. Proc Natl Acad Sci U S A *105*, 10750-10755.

Yi, C.X., Heppner, K.M., Kirchner, H., Tong, J., Bielohuby, M., Gaylinn, B.D., Muller, T.D., Bartley, E., Davis, H.W., Zhao, Y., *et al.* (2012). The GOAT-ghrelin system is not essential for hypoglycemia prevention during prolonged calorie restriction. PLoS One *7*, e32100.

Yon, J., and Fried, M. (1989). Precise gene fusion by PCR. Nucleic acids research *17*, 4895.

Yu, C., Chen, J., Lin, S., Liu, J., Chang, C.C., and Chang, T.Y. (1999). Human acyl-CoA:cholesterol acyltransferase-1 is a homotetrameric enzyme in intact cells and in vitro. J Biol Chem *274*, 36139-36145.

Zhang, C.Y., Baffy, G., Perret, P., Krauss, S., Peroni, O., Grujic, D., Hagen, T., Vidal-Puig, A.J., Boss, O., Kim, Y.B., *et al.* (2001). Uncoupling protein-2 negatively regulates insulin secretion and is a major link between obesity, beta cell dysfunction, and type 2 diabetes. Cell *105*, 745-755.

Zhang, J.H., Chung, T.D., and Oldenburg, K.R. (1999). A Simple Statistical Parameter for Use in Evaluation and Validation of High Throughput Screening Assays. Journal of biomolecular screening *4*, 67-73.

Zhang, W., Chai, B., Li, J.Y., Wang, H., and Mulholland, M.W. (2008). Effect of des-acyl ghrelin on adiposity and glucose metabolism. Endocrinology *149*, 4710-4716.

Zhang, Y., Fang, F., Goldstein, J.L., Brown, M.S., and Zhao, T.J. (2015). Reduced autophagy in livers of fasted, fat-depleted, ghrelin-deficient mice: reversal by growth hormone. Proc Natl Acad Sci U S A *112*, 1226-1231.

Zhao, C., Chen, A., Jamieson, C.H., Fereshteh, M., Abrahamsson, A., Blum, J., Kwon, H.Y., Kim, J., Chute, J.P., Rizzieri, D., *et al.* (2009). Hedgehog signalling is essential for maintenance of cancer stem cells in myeloid leukaemia. Nature *458*, 776-779.

Zhao, T.J., Liang, G., Li, R.L., Xie, X., Sleeman, M.W., Murphy, A.J., Valenzuela, D.M., Yancopoulos, G.D., Goldstein, J.L., and Brown, M.S. (2010a). Ghrelin O-acyltransferase (GOAT) is essential for growth hormone-mediated survival of calorie-restricted mice. Proc Natl Acad Sci U S A *107*, 7467-7472.

Zhao, T.J., Sakata, I., Li, R.L., Liang, G., Richardson, J.A., Brown, M.S., Goldstein, J.L., and Zigman, J.M. (2010b). Ghrelin secretion stimulated by {beta}1-adrenergic receptors in cultured ghrelinoma cells and in fasted mice. Proc Natl Acad Sci U S A *107*, 15868-15873.

Zheng, Y., Mamdani, F., Toptygin, D., Brand, L., Stivers, J.T., and Cole, P.A. (2005). Fluorescence analysis of a dynamic loop in the PCAF/GCN5 histone acetyltransferase. Biochemistry *44*, 10501-10509.

Zhou, A., Webb, G., Zhu, X., and Steiner, D.F. (1999). Proteolytic processing in the secretory pathway. J Biol Chem *274*, 20745-20748.

Zhu, X., Cao, Y., Voogd, K., and Steiner, D.F. (2006). On the processing of proghrelin to ghrelin. J Biol Chem *281*, 38867-38870.

Zigman, J.M., Nakano, Y., Coppari, R., Balthasar, N., Marcus, J.N., Lee, C.E., Jones, J.E., Deysher, A.E., Waxman, A.R., White, R.D., *et al.* (2005). Mice lacking ghrelin receptors resist the development of diet-induced obesity. The Journal of clinical investigation *115*, 3564-3572.

CURRICULUM VITAE

PERSONAL

1983 Born (Baltimore, Maryland, USA)

EDUCATION & TRAINING

2005-2015 **M.D., PhD., The Johns Hopkins University School of Medicine** (Baltimore, MD)
Pharmacology PhD. thesis advisors Philip A. Cole, M.D., Ph.D., and
Jef D. Boeke, Ph.D., D.Sc.

2001-2005 **B.S.E. Princeton University** (Princeton, NJ)
Chemical engineering, *Magna Cum Laude*. Certificates: Computer Science, Spanish.

1989-2001 **Gilman School** (Baltimore, MD)

RESEARCH & TEACHING EXPERIENCE

2014-2015 **Laboratory of Kathleen Burns,** The Johns Hopkins University School of Medicine

2011-2013 **Laboratory of Jef Boeke,** The Johns Hopkins University School of Medicine

2007-2012 **Laboratories of Philip Cole and Jef Boeke,** The Johns Hopkins University School of Medicine

2011-2012 **iGEM Team Mentor,** Johns Hopkins University

2008-2009 **Histology Teaching Assistant,** The Johns Hopkins University School of Medicine

2006 **Laboratory of Solomon Snyder,** The Johns Hopkins University School of Medicine

2006 **Assistant Track Coach,** Gilman School

2004-2005 **Laboratory of Christodoulos Floudas,** Princeton University

2004 **Laboratory of Curt Civin,** The Johns Hopkins University School of Medicine

2003-2005 **Outdoor Action Leader and Instructor,** Princeton Unviersity

2003 **Laboratory of Joáquin Morán,** Universidad de Salamanca ,Salamanca, Spain

SELECTED HONORS & AWARDS

2014	**Ehrlich Award,** The Johns Hopkins University School of Medicine Young Investigators' Day
2013	**The Outstanding Abstract in Basic Research,** Johns Hopkins University Dept. of Pathology Young Investigators' Day
2011	**Outstanding Presentation Prize,** Johns Hopkins University Department of Molecular Biology and Genetics
2005	NIH Medical Scientist Training Program, The Johns Hopkins University School of Medicine
2005	**Magna Cum Laude,** Princeton University
2005	**Merck and Company Outstanding Senior Thesis Award,** Princeton University
2005	**Myers Award,** Princeton Track and Field.
2004-2005	**Tau Beta Pi Member,** First Election, Princeton University
2004	**American Society of Hematology Summer Medical Student Award**
2000-2001	**Cum Laude Society (first election), Alexander Randall, Jr. Prize for Publications, National Merit Scholarship Finalist, AP Scholar with distinction**. Gilman School (Baltimore, MD)

.

POSTER PRESENTATIONS, PODIUM PRESENTATIONS, AND JOURNAL REVIEWS

2014 June 30 **Taylor M.S.,** *"Affinity proteomics reveals human host factors implicated in discrete stages of LINE-1 retrotransposition."* (Podium Presentation), Johns Hopkins Pathology Grand Rounds.

2014 April 17 **Taylor M.S.**, et al**.,** *"Affinity Proteomics Reveals Human Host Factors Implicated in Discrete Stages of LINE-1 Retrotransposition."* (Poster Presentation), Johns Hopkins University Young Investigators Day.

2014 *Ad Hoc* reviewer for Antimicrobial Agents and Chemotherapy

2013 **Taylor M.S.,** *"How Do Vertebrates Make a Fatty Octanoyl PTM? Architecture of the Metabolic Regulatory Enzyme Ghrelin-O-Acyltransferase (GOAT)."* (Podium Presentation), Meeting of The Centers for Networks and Pathways (NIH TCNP, Bethesda, MD).

2012 **Taylor M.S.,** *"The Transposon-Host interactome: Identification of binding partners in LINE-1 RiboNucleoProtein Complex."* (Podium Presentation), National Center for Dynamic Interactome Research Meeting (Institute for Systems Biology, Seattle, WA).

2012 **Taylor M.S.,** *"The Transposon-Host interactome: Identification of binding partners in LINE-1 RiboNucleoProtein Complex."* (Podium Presentation), and **Taylor M.S.**, et al**.,** *"GOAT Topology: Architecture of a Weight Regulatory Peptide Octanoyltransferase,"* (Podium Presentation), Meeting of The Centers for Networks and Pathways (NIH TCNP, Bethesda, MD).

2011 **Taylor M.S.**, et al**.,** *"Glucose and Weight Control in Mice with a Designed Ghrelin O-Acyltransferase (GOAT) Inhibitor and Studies on the Structure and Function of GOAT."* (Poster Presentation), Meeting of The Centers for Networks and Pathways (NIH TCNP, Bethesda, MD).

2011 FASEB Summer Research Conference: Mobile DNA in Mammalian Genomes (Snowmass, CO).

2010 **Taylor M.S.,** *"Glucose and Weight Control in Mice with a Designed Ghrelin O-Acyltransferase Inhibitor"* (Podium Presentation), Johns Hopkins University MD/PhD Program Retreat (Hershey, PA).

PUBLICATIONS & PATENTS

Taylor MS, LaCava J, Dai L, Mita P, Burns KH, Rout MP, Boeke JD, *"Characterization of L1 RNPs"* in: *Transposons and Retrotransposons: Methods and Protocols*, J. L. Garcia Perez, (Ed.) Springer: 2015.

Sharma R, Rodić N, Burns, KH, **Taylor MS**, *"Immuno-Detection of Human LINE-1 expression"* in: *Transposons and Retrotransposons: Methods and Protocols*, J. L. Garcia Perez, (Ed.) Springer: 2015.

LaCava J, Molloy KR, **Taylor MS**, Domanski M, Chait BT, Rout MP, *"Affinity proteomics to study endogenous protein complexes: Pointers, pitfalls, preferences and perspectives."* **Biotechniques**. 2015 Mar 1;58(3):103-19. PMID: 25757543

Prusevich P, Kalin JH, Ming SA, Basso M, Givens J, Li X, Hu J, **Taylor MS**, Cieniewicz AM, Hsiao PY, Huang R, Roberson H, Adejola N, Avery LB, Casero RA Jr, Taverna SD, Qian J, Tackett AJ, Ratan RR, McDonald OG, Feinberg AP, Cole PA, *"A Selective Phenelzine Analogue Inhibitor of Histone Demethylase LSD1."* **ACS Chem Biol.** 20;9(6):1284-93 (2014). PMID: 24707965. PMC4076021.

Dai L, LaCava J, **Taylor MS**, Boeke JD, *"Expression and detection of LINE-1 ORF-encoded proteins."* Mob Genet Elements. 2014 May 22;4:e29319. PMID: 25054082. PMC4091050.

Chiang MJ, Holbert MA, Kalin JH, Ahn YH, Giddens J, Amin MN, **Taylor MS**, Collins SL, Chan-Li Y, Waickman A, Hsiao PY, Bolduc D, Leahy DJ, Horton MR, Wang LX, Powell JD, Cole PA, *"An Fc domain protein-small molecule conjugate as an enhanced immunomodulator."* **J Am Chem Soc**. 136(9):3370-3 (2014). PMID: 24533830. PMC3954559.

Taylor MS*, LaCava J*, Mita P, Molloy KR, Huang CRL, Li D, Adney EM, Jiang H, Burns KH, Chait BT, Rout MP, Boeke JD, Dai L*, "*Affinity proteomics reveals human host factors implicated in discrete stages of LINE-1 retrotransposition.*" **Cell.** 155(5):1034-1048 (2013). **[*Equal contribution shared first authorship].** PMID: 24267889. PMC3904357.

Rodić N, Sharma R, Sharma R, Zampella J, Dai L, **Taylor MS**, Hruban RH, Iacobuzio-Donahue CA, Maitra A, Torbenson MS, Goggins M, Shih LM, Duffield AS, Montgomery EA, Gabrielson E, Netto GJ, Lotan TL, De Marzo AM, Westra W, Binder ZA, Orr BA, Gallia GL, Eberhart CG, Boeke JD, Harris CR, Burns KH, *"Long INterspersed Element-1 Protein Expression is a Hallmark of Many Human Cancers."* **Am J Pathol.** 184(5):1280-6 (2014). PMID: 24607009. PMC4005969.

Taylor MS, Ruch TR, Hsiao PY, Hwang Y, Zhang P, Dai L, Huang CR, Berndsen CE, Kim MS, Pandey A, Wolberger C, Marmorstein R, Machamer C, Boeke JD, Cole PA. *"Architectural Organization of the Metabolic Regulatory Enzyme Ghrelin-O-Acyltransferase."* **J Biol Chem.** 288(45):32211-32228 (2013). PMID: 24045953. PMC3820860.

Smadbeck J, Peterson MB, Khoury GA, **Taylor MS**, Floudas CA. "*Protein WISDOM: A Workbench for In silico De novo Design of BioMolecules.*" **J. Vis. Exp.** (77), e50476, (2013). PMID: 23912941.

Mitchell LM*****, Cai Y*****, **Taylor MS***, Noronha AM, Chuang J, Dai L, Boeke JD. *"Multichange Isothermal Mutagenesis: a new strategy for multiple site-directed mutations in plasmid DNA."* **ACS Synth. Biol**, No. 2(8):473-7(2013) **[*Equal contribution shared first authorship].** PMID: 23654272. PMC4040258.

Taylor MS, Hwang Y, Hsiao PY, Boeke JD, Cole PA. *"Ghrelin O-acyltransferase assays and inhibition."* **Methods Enzymol.** 514:205-28. Review (2012). PMID: 22975055. PMC3763810.

Dai L, **Taylor MS**, O'Donnell KA, Boeke JD. *"Poly(A) binding protein C1 is essential for efficient L1 retrotransposition and affects L1 RNP formation."* **Mol Cell Biol**. 32(21):4323-36 (2012). PMID: 22907758. PMC3486150.

Barnett BP*****, Hwang Y*****, **Taylor MS***, Kirchner H, Pfluger PT, Bernard V, Lin YY, Bowers EM, Mukherjee C, Song WJ, Longo PA, Leahy DJ, Hussain MA, Tschöp MH, Boeke JD, Cole PA. "*Glucose and weight control in mice with a designed ghrelin O-acyltransferase inhibitor*." **Science** No. 330(6011):1689-92 (2010). **[*Equal contribution shared first authorship].** PMID: 21097901. PMC3068526.

Bellows ML*****, **Taylor MS***, Cole PA, Shen L, Siliciano RF, Fung HK, Floudas CA. "*Discovery of entry inhibitors for HIV-1 via a new de novo protein design framework.*" **Biophysical Journal** No. 99(10):3445-53 (2010). **[*Equal contribution shared first authorship].** PMID: 21081094. PMC2980751.

Bellows ML, Fung HK, **Taylor MS**, Floudas CA, López de Victoria A, Morikis D. "*New compstatin variants through two de novo protein design frameworks.*" **Biophysical Journal**. No. 98 (10):2337-46 (2010). PMID: 20483343. PMC2872270.

Taylor MS, Fung HK, Rajgaria R, Filizola M, Weinstein H, and Floudas CA. "*Mutations Affecting the Oligomerization Interface of G-Protein Coupled Receptors Revealed by a Novel De-novo Protein Design Framework.*" **Biophysical Journal** No. 94(7):2470-81 (2008). PMID: 18178645. PMC2267121.

Floudas C.A, Fung H.K., Morikis D., **Taylor MS.**, and L. Zhang, "*Overcoming the Key Challenges in De Novo Protein Design: Enhancing Computational Efficiency and Incorporating True Backbone Flexibility",* **Proceedings of BIOMAT VI**, Ed. R. Mondaini, Springer, 102, 133-183 (2008).

Fung, HK, **Taylor MS**, Floudas CA, Zhang L, and Morikis D. *"Towards Full-Sequence De Novo Protein Design with Flexible Templates for Human Beta-Defensin-2."* **Biophysical Journal** No. 94(2):584-99 (2008). PMID: 17827237. PMC2157230.

Fung, HK, **Taylor MS**, and Floudas CA, *"Novel Formulations for the Sequence Selection Problem in de Novo Protein Design with Flexible Templates."* **Optimization Methods and Software** Vol. 22, No. 1 51-71 (2007).

Janak SL, **Taylor MS**, Floudas CA, Burka M, and Mountziaris TJ. *"Novel and Effective Integer Optimization Approach for the NSF Panel-Assignment Problem: A Multiresource and Preference-Constrained Generalized Assignment Problem."* **Industrial and Engineering Chemistry Research** No. 45, pp 258-265 (2006).

Janak SL, **Taylor MS**, Floudas CA, Burka M and Mountziaris TJ, "A Novel and Effective Integer Optimization Approach for the NSF Panel Assignment Problem: A Mutli-Resource and Preference-Constrained Generalized Assignment Problem", (US Patent Appl September 2005).